



HAL
open science

The Great Versatility of Supercritical Fluids in Industrial Processes: A Focus on Chemical, Agri-Food and Energy Applications

Manita Kamjam, Somkiat Ngamprasertsith, Ruengwit Sawangkeaw, Manop Charoenchaitrakool, Romain Privat, Jean-Noël Jaubert, Michel Molière

► To cite this version:

Manita Kamjam, Somkiat Ngamprasertsith, Ruengwit Sawangkeaw, Manop Charoenchaitrakool, Romain Privat, et al.. The Great Versatility of Supercritical Fluids in Industrial Processes: A Focus on Chemical, Agri-Food and Energy Applications. *Processes*, 2024, 12 (11), pp.2402. 10.3390/pr12112402 . hal-04762979

HAL Id: hal-04762979

<https://hal.univ-lorraine.fr/hal-04762979v1>

Submitted on 1 Nov 2024

HAL is a multi-disciplinary open access archive for the deposit and dissemination of scientific research documents, whether they are published or not. The documents may come from teaching and research institutions in France or abroad, or from public or private research centers.

L'archive ouverte pluridisciplinaire **HAL**, est destinée au dépôt et à la diffusion de documents scientifiques de niveau recherche, publiés ou non, émanant des établissements d'enseignement et de recherche français ou étrangers, des laboratoires publics ou privés.



Distributed under a Creative Commons Attribution 4.0 International License

Review

The Great Versatility of Supercritical Fluids in Industrial Processes: A Focus on Chemical, Agri-Food and Energy Applications

Manita Kamjam ¹, Somkiat Ngamprasertsith ^{1,*}, Ruengwit Sawangkeaw ², Manop Charoenchaitrakool ³, Romain Privat ⁴, Jean-Noël Jaubert ⁴ and Michel Molière ^{4,5,*}

¹ Department of Chemical Technology, Faculty of Science, Chulalongkorn University, Bangkok 10330, Thailand; manitakamjam@hotmail.com

² Center of Excellence in Bioconversion and Bioseparation for Platform Chemical Production, Institute of Biotechnology and Genetic Engineering, Chulalongkorn University, Bangkok 10330, Thailand; rueangwit.s@chula.ac.th

³ Department of Chemical Engineering, Faculty of Engineering, Kasetsart University, Bangkok 10900, Thailand; fengmnc@ku.ac.th

⁴ Laboratoire Réactions et Génie des Procédés, Université de Lorraine, 54000 Nancy, France; romain.privat@univ-lorraine.fr (R.P.); jean-noel.jaubert@univ-lorraine.fr (J.-N.J.)

⁵ Institut Carnot de Bourgogne-Université de Technologie de Belfort Montbéliard (ICB-UTBM), 90000 Belfort, France

* Correspondence: somkiat.n@chula.ac.th (S.N.); michel.molier@utbm.fr (M.M.)

Abstract: Long a thermodynamic curiosity, supercritical fluids (SCFs) have gradually gained ground in today's life, generating an increasing number of new, efficient processes in diverse industrial sectors and fueling active R&D programs. Indeed, the versatility of SCFs allows them to serve a wide variety of applications. The list includes not only food processing, biofuel production, extraction of biomolecules marketable as medicines, cosmetics and nutraceuticals, but also emerging technologies for the production of electrical power, based on supercritical or transcritical thermodynamic cycles. This jointly authored article will provide a review of important applications covered by our laboratories in the agri-food, chemical and energy sectors. We will then try to detect recent trends and outline future prospects.

Keywords: supercritical fluid; supercritical CO₂; supercritical water; extraction; synthesis; biodiesel; agri-food; electrical power



Citation: Kamjam, M.;

Ngamprasertsith, S.; Sawangkeaw, R.;

Charoenchaitrakool, M.; Privat, R.;

Jaubert, J.-N.; Molière, M. The Great

Versatility of Supercritical Fluids in

Industrial Processes: A Focus on

Chemical, Agri-Food and Energy

Applications. *Processes* **2024**, *12*, 2402.

<https://doi.org/10.3390/pr12112402>

Academic Editor: Ádina L. Santana

Received: 13 September 2024

Revised: 21 October 2024

Accepted: 28 October 2024

Published: 31 October 2024



Copyright: © 2024 by the authors.

Licensee MDPI, Basel, Switzerland.

This article is an open access article

distributed under the terms and

conditions of the Creative Commons

Attribution (CC BY) license ([https://creativecommons.org/licenses/by/](https://creativecommons.org/licenses/by/4.0/)

[https://creativecommons.org/licenses/by/](https://creativecommons.org/licenses/by/4.0/)

[4.0/](https://creativecommons.org/licenses/by/4.0/)).

1. Introduction

Supercritical fluids (SCFs) have long remained an object of curiosity, even mystery, for generations of students tackling the rigorous science of thermodynamics.

However, for several decades, they have given rise to numerous and innovative applications, generating dynamic R&D activities. Indeed, the uses of SCFs have grown considerably and to date cover multiple processes in fields as diverse as chemical syntheses [1], food ingredients [2], primary energy conversion [3], polymers [4], pharmaceuticals [5], cosmetics [6], biomaterials [7], microelectronics [8], waste management [9], soil decontamination, cleaning of various material substrates, and recently, in electric power generation [10].

In this very broad set of applications, SCFs fulfill different roles: as solvents in extractions, as reaction media or reagents in synthesis and as working fluids in energetic cycles. We will focus primarily on three important classes of processes that are studied in our laboratories: extraction, synthesis and thermal energy conversion, the corresponding industry sectors being agri-food, chemistry and energy. Supercritical CO₂ will be the main SCF covered but other fluids, especially water, will be discussed as well.

The primary objective of this jointly written article is to explore the wide operational spectrum of SCF processes and, based on our respective laboratory experiences, to review achievements and prospects in quite distinct applications. In this regard, bringing together in the same article topics as dissimilar as chemical and electrical processes seemed a priori an unusual undertaking. However, this is not illogical because, in both areas, the unique performances of these processes are due to the distinctive physical and chemical behavior of SCFs and are underpinned by similar properties, especially density.

As a first approach to the subject, we will provide a brief historical and bibliographic summary, propose a classification of applications and outline some key theoretical considerations. Indeed, a historical summary will be useful to see how SCF processes have gradually emerged and to properly contextualize current R&D. A classification will help us establish the most comprehensive list of mature and new applications. Finally, recalling some basic notions and highlighting important theoretical points will reveal the key factors underlying process performance; we will also show that, despite their differences, the numerous applications enabled by SCFs have common theoretical foundations.

Finally, from a forward-looking perspective, we will discuss recent trends in the development of SCF-based processes, both at the industrial and R&D levels, and attempt to anticipate possible future evolutions and R&D directions.

In this article, we will use the following notations: the adjectives “supercritical” and “subcritical” will be abbreviated to “SC” and “sbc” respectively; SCF will be the acronym for supercritical fluid; supercritical water will be designated as SCW or SC-H₂O and SFE, SFCs, SFS and SFAs will designate respectively the following classes of process: extractions; general chemical processes; syntheses and analytic applications.

The simulations of SC thermodynamic cycles were performed using ProSimPlus3[®], a steady-state simulation and optimization software from Fives ProSim (Labège, France).

2. Brief History and Bibliography of SCFs

At the beginning of the 19th century, Charles Cagniard de la Tour discovered by chance the existence of the critical point (“CP”) by observing that the splashing noise, caused by a flint rolling in a sealed gun barrel partly filled with a liquid, disappeared above a certain temperature. Then further studies by Thomas Andrews, Michael Faraday, Johannes Natterer and others [11,12], led to a preliminary interpretation of the CP as the point above which a gas can be no longer be liquefied. However, one will have to wait for the 20th century to see concrete applications.

In the early 1900s, chemist Vladimir Ipatiev designed a dedicated high-pressure vessel and investigated a wide selection of SFCs, including: SC-C₂H₄, SC-CCl₄, SC-NH₃ etc. He was nicknamed “the father of catalysis” [13].

In the 1940s, Charles and Georges Friedel used SC-H₂O to synthesize high purity quartz crystals from a solution of alkaline silicates. In the mid-1950s, Zhuze proposed the first series of SCF applications for the processing of coal, petroleum and wool [13].

In 1962, E. Klesper and A. H. Corwin invented the supercritical chromatography [14], after observing that, when used as mobile phases, SCFs enable ultrafast and highly efficient separations thanks to their high diffusivity and solvation strength. Developments initially focused on chiral molecules, then on the separation of complex and chemically closed substances present in nutrients, drugs, biomass, biological and environmental extracts, which still require long and tedious HPLC analytical protocols [15].

In 1966, H. C. Stevens filed US. Patent 3,248,415 in which he applied SC conditions to copolymerize CO₂ and ethylene oxide into polycarbonates [12].

In the years 1970–1980, Kurt Zosel invented decaffeination of coffee beans with SC-CO₂, the first green SFE process which saw massive development and allowed for the gradual banning of toxic chlorinated solvents. In one of his numerous patents, he described as many as 84 possible SFE applications, in which he used SC-CO₂, SC-C₂H₄, SC-N₂O and SC-NH₃ to produce extracts as diverse as petroleum paraffins, dairy fats, chlorophyll extracts (from spinach), etc. [16,17].

The end of the 1960s had seen the discovery of SC-CO₂ as a possible thermodynamic fluid to produce electrical energy thanks to a few inspired researchers, namely: G. Angelino in Italy [18–20], E. G. Feher in the United States [21,22], D.P. Gokhshtein and G. P. Verkhivker in the former USSR [23]. These thermodynamicists predicted that this novel technology would procure strong efficiency gains and significant reductions in component sizes. However, due to the radical novelty of that technology and technical difficulties inherent to closed, high-pressure circuits, developments really began in the 2000s [24].

In the 1970s, SC-H₂O (or “supercritical steam”) was introduced as a working fluid in SC boilers to produce electrical power, resulting in important increases in efficiency [25].

The Allam thermodynamic cycle based on SC-CO₂ was introduced in the 2010s; it promises a major step forward towards decarbonized electricity production along with efficient energy conversion [26–30].

The year 2000 saw the development of SFCs and SFRs in multiple areas: (i) production of biofuels, including green syntheses of biodiesel with SC-MeOH [31–33]; (ii) extractive recovery of non-edible sugars to synthesize second generation ethanol [34]; (iii) advances in polymer manufacturing using SC-CO₂ [35]; (iv) production of nanoparticles of inorganic materials and drugs [36] and (v) various thermodynamic cycle configurations for the production of electricity [37].

Today, there are many other SCF processes, mature, under development or still speculative.

Among mature ones, SC-CO₂ is currently used in various applications: for EOR (enhanced oil recovery) and within refrigeration cycles. Among developing ones, there are namely: sterilization [38] and dry cleaning of sensitive mechanical parts [39], namely electronic wafers [40].

SC-H₂O (or “SCW”) also lends itself to multiple processes, which are extensively reviewed in the reference [41]:

- Inorganic syntheses (SFS) that yield high value products (namely nano electronic components [42]).
- Water electrolysis under SC conditions, to directly produce compressed dihydrogen: this process would be advantageous for feeding future H₂ energy chains, but it is energetically costly due to the elevated T_c and P_c data of SC-H₂O (374 °C; 221 bar) [43].
- The processing of fossil fuels (crude oil; coal; kerogen; sand oil) or biomass [44].
- Supercritical water oxidation (SCWO), which is a clean, green process to decompose toxic wastes [45].

Although this article will mainly focus on SC-CO₂, we will briefly discuss SCW processes in Section 3.

- Supercritical combustion is a rather futurist concept in which a fuel or a propellant (hydrocarbon or cryogenic fluid) would be used in its SC state to power diesel or rocket engines, decreasing ignition delays and accelerating combustion, resulting in less fuel consumption and less NO_x emissions [46].

Table 1 shows a list and classification of the many SCF-based processes in use or under investigation to date. It only provides high level information: the few references cited are essentially to introduce the different subjects. It will be supplemented by more precise data in Sections 4–6.

Table 1. Preliminary list of outstanding SCF processes.

Application Area	SCF	Process Name	Objective	Result (Product or Installation)	Refs.
Physics	CO ₂	Extraction	Recover valuable molecules	Flavors and fragrances; drugs; nutraceuticals	[47–50]
	CO ₂ ; H ₂ O	Purification	Remove impurities	Detoxicated products	[51–53]
	CO ₂	Impregnation Dyeing	Change texture/color	Finish textile fabrics	[45–55]
Chemistry	CO ₂	Synthesis	Improve syntheses	Polymers; nanoparticles	[56–60]
				Pharmaceuticals	[61]
	H ₂ O	Synthesis	Make inorg. (nano)objects	Ceramics; nanoelectronics	[62]
	CO ₂ -ROH	Transesterification	React alcohol with triglycerides	Biodiesel	Cf Section 5.1.1
	RCOOMe(Et)	Interesterification	React ester with triglycerides	Biodiesel	Cf Section 5
	H ₂ O	Hydrolysis/Pyrolysis/Oxidation (SCWO)	Reform hydrocarbons	CH ₃ OH from CH ₄	[63,64]
			Recover	Monomers from plastics	[65,66]
Decompose			Detoxicate solvent wastes or hazardous substances	[45,67,68]	
Biology	CO ₂	Sterilization	Disinfect	Safe medical tools	[69,70]
Oil and Gas industry	CO ₂	Enhanced Oil Recovery	Recover fossil products	More Petroleum	[71]
Environment	CO ₂	CCS	Sequester CO ₂ in SC state	Decarbonized processes	[72]
Laboratory	CO ₂ —C _n H _m	Chromatography	Separate/identify/quantify	Substance analysis	[73]
Heat-to-Power	Water, CO ₂	Electrical power generation	Convert heat into electric power	Power plants	[18–30] Cf Section 6
Fuel-to-power	Fossil fuel	Combustion in SC cond.	Produce mech. power	Engine car, rockets	[46]
Power-to-Gas	Water	Electrolysis	Split water into H ₂ and O ₂	Hydrogen	[43]
Thermal Conditioning	CO ₂ , C ₃ H ₈	Heating	Generate calories	Heat pumps	[74]
		Refrigeration	Generate frigories	Refrigerators; air condition	[75]

3. Technical Keys

This section will first give a simplified description of supercritical fluids and analyze why the specifics of this physical state open a wide range of original applications with advantageous performances.

3.1. Definition and Specificities of the Supercritical State

3.1.1. Definition and Properties of SCFs

According to its usual definition, the critical point (CP) of a fluid is the thermodynamic state in which the densities of the gas and liquid phases become equal, and their interface disappears. The critical pressure (P_c) and temperature (T_c) data of the two most used SCFs are: (31 °C—73.8 bar) for CO₂ and (374 °C—221 bar) for H₂O.

For $T > T_c$ and $P > P_c$, the fluid is said to be supercritical (“SC”).

3.1.2. Specificities of SCFs

The viscosity of an SCF is close to that of a gas. Its density is close to that of a liquid. Surface tension is a property that applies to liquid/gas contacts: it is zero for any SCF which is therefore completely miscible with gases. Its interfacial tension, a property that applies to liquid/solid contacts, is very small.

The different physical states of a compound can be schematically differentiated by comparing the values of (i) the kinetic energy of molecules (which increases with temperature) and (ii) their potential energy (which comes from structural bonds, H-bonds and Van der Waals forces). The latter are attractive dipolar interactions that change in function of intermolecular distances.

Figure 1 schematizes the structures of the different phases of carbon dioxide. In a solid, the constitutive elements (atoms, molecules or ions) form rigid networks and do not move. In liquids, molecules move stochastically but tend to associate to form short-lived “clusters”: this increases viscosity and surface tension, thereby decreasing general diffusivity [76]. The transition to the supercritical state by increasing temperature causes an expansion and increases the kinetic energy of the molecules, which tends to break most of these clusters. This reduces viscosity and increases both diffusivity and interfacial tension, resulting in better “wetting” and easier penetration into exogenous particles or drops.

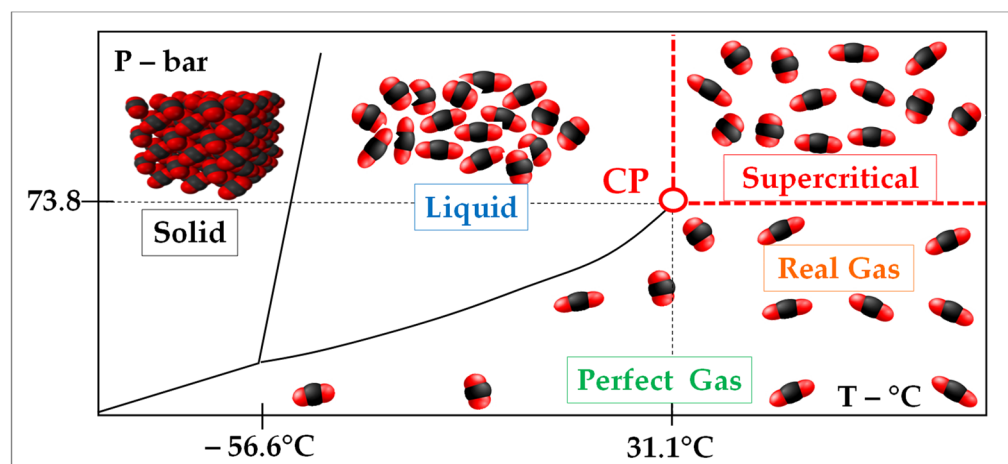


Figure 1. Schematic representation of molecular density of a fluid in different states.

However, as shown by Monte Carlo and Molecular Dynamics simulations, SCF molecules nevertheless tend to form some clusters around solutes, which promotes solvation [76,77]. During extraction processes, a high molecular density (achieved by high pressures), is necessary to keep the solute and solvent molecules in contact and ensure the solvation effect. In fact, as shown below, high pressures increase the density of the SCFs and enhance their solvation power.

Finally, the miscibility of SCFs with gases turns some heterogeneous reactions into homogenous ones, thus eliminating interphase transport resistance and accelerating kinetics.

3.1.3. The Versatility of SCFs in Processes

Two factors contribute to making SCFs versatile process fluids.

The first is their ability to perform a plurality of functions in distinct applications:

- As a solvent in extraction or purification processes;
- As a reaction medium in chemical syntheses (during which external substances react together);
- As a reagent, the SCF being itself engaged and consumed in chemical reactions;
- As working fluid in thermodynamic cycles: for refrigeration or to produce mechanical/electric power.

The second is linked with their unique properties, some relating to mass and heat transfer, others to the ability to solubilize a number of solid or liquid substrates in variable concentrations.

To delve deeper into these important aspects, we will examine the key roles played by the most important of these physicochemical properties in different processes. For this, we will take SC-CO₂ as a paradigm but will see that the conclusions drawn generalize to all SCFs, namely to SC-H₂O.

Among these properties, density is very important and will be discussed first.

3.2. Why Does Density Play a Key Role in All SCF Applications?

3.2.1. Density Is a Key Factor in Solubilization Processes

A useful solubility indicator was introduced in 1936 by Joel Hildebrand for subcritical liquids and solids. This is the “Hildebrand solubility parameter” (HSP, also noted “ δ ”), which is defined as [78]:

$$\delta = \left(\frac{\Delta U}{Vm} \right)^{0.5} \approx \left(\frac{\Delta H_v - RT}{Vm} \right)^{0.5} \quad (1)$$

This definition involves the latent heat of vaporization (ΔH_v , expressed as a molar enthalpy) and the molar volume (Vm), the numerator being the “cohesive energy density” (ΔU) which is the energy that would be necessary if one wanted to extract a unit volume of molecules from the bulk of a given compound (solute or solvent) and transfer it to an ideal gas state. In most of the databases reporting thermodynamic properties, the solubility parameter is given at the reference temperature of 25 °C. To overcome the interactions of neighboring molecules inside this bulk, this virtual operation would require supplying some energy which equals the heat of vaporization of the compound divided by its molar volume in the condensed state. Interestingly, HSP data have the dimension of P^{1/2} and are expressed in MPa^{1/2}. For e.g., for a solute (“su”) to be soluble in a solvent (“sv”), it is necessary that equivalent interactions are created between the su and sv molecules. Therefore, substances having similar δ values (e.g., δ_{sv} and δ_{su} differing by less than 2 MPa^{1/2}) should be compatible with each other; in other terms: “like dissolves like” [79]. This compatibility criterion governs different physical processes: (i) solvation (solute in solvent); (ii) miscibility (liquid with liquid); (iii) swelling (polymer in solvent). The HSP is therefore a useful but merely qualitative solubility indicator, especially for nonpolar materials, i.e., organics and polymers.

In their development of very high-pressure chromatography, Giddings et al., extended this concept to SCFs used as solvents. Based on theoretical considerations and the dimension [MPa^{1/2}] of HSP parameters, they established a relationship between the δ_{SCF} on one hand, and the critical pressure and density (ρ_{cr}) on the other hand [79,80]:

$$\delta_{SCF} = K \cdot \left(\frac{P_c^{1/2}}{\rho_{cr}} \right) \cdot \rho \quad (2)$$

where K is a constant that they determined using experimental data. It is worth mentioning that we owe this fundamental equation to researchers who, in the 1960s, pioneered supercritical chromatography [80].

To highlight the relevance of Equation (2), Figure 2 shows the iso-density lines of SC-CO₂ in a P-T diagram. It indicates that the density and, correlatively, the HSP decrease as T increases. However, very importantly, both density and solvation power increase as P increases: this effect constitutes a distinctive property that allows SCFs to compete with organic solvents in extractive applications, when brought to high pressures. This point will be prevalent throughout this article.

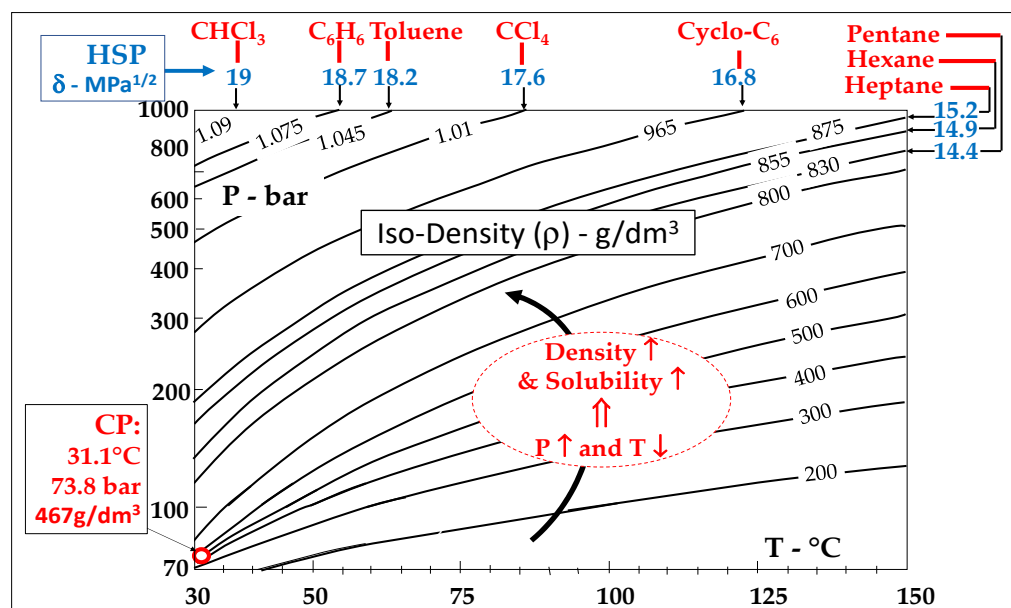


Figure 2. Density of SC-CO₂ as a function of P and T with correspondences between SC-CO₂ and selected organic solvents, in terms of HSP.

As an illustration, Figure 2 shows the correspondence, at high pressures, with some selected organic solvents in terms of HSP data (Equation (1) was used for organic solvents while Equation (2) was used for SCFs). However, it must be mentioned that usual SCF processes are in fact conducted at much more moderate pressures (typically 80–200 bar) and, to compensate for the limited solvation strength of CO₂ in this pressure range, it is usual to add limited amounts of a cosolvent (often ethanol or methanol) which acts as a “polarity modifier. Nevertheless, it will be shown in Section 4 (Table 2) that pressures of up to 300 bar (30 MPa) are now used on an industrial scale.

Table 2. Commercialized SC-CO₂ extraction plants operating nowadays.

Business Type	Company	Country	Raw Material	Year	Extractor Capacity
Decaffeination plant	SKW/Degussa	Germany	Tea	1986	3 × 8 m ³
Decaffeination plant	Lavazza	Italy	Coffee	1992	3 × 20 m ³
Multipurpose extraction plant	Suprex/Trumpf	Czech Republic	Spices and herbs	1993	1 × 200 L (55 MPa)
Rice treatment	Five King Cereals	Taiwan	Rice	1997	3 × 6 m ³
Extraction plant	Extract Solutions	New Zealand	Hops, herbs and nutraceuticals	2001	3 × 850 L (55 MPa)
Oil extraction plant	U-max	Korea	Sesame oil	2003	2 × 2600 L (55 MPa)
Purification plant	Sabaté/Diamant	France/Spain	Cork	2004	3 × 8500 L
Purification plant	Diam-Bouchage	Spain	Cork	2010	3 × 9000 L
Purification plant	Diam-France	France	Cork	2015	3 × 20,000 L
Extraction plant for spices and herbs	Plant Lipids Private Limited	India	Spices and herbs	2017	3 × 300 L
Extraction plant for natural substances	Curtin University	Malaysia	Frankincense, dabai, gaharu, black pepper	2017	2 × 10 L (100 MPa)
World’s largest hops extraction plant	Hopfenveredlung St. Johann GmbH	Germany	Hops extract	2021	8 × 4200 L

Another limitation of the HSP concept is that it has a mere thermodynamic basis (Equation (1)) and does not take into account some processes which precede solubilization, especially the collapse of the structure in the case of a solid solute. This point will be covered in Section 3.5.

In summary, the HSP of a given SCF solvent is determined either by its density ρ or by its pressure P as there is a tight correlation between both properties: it has actually become customary to plot SCF properties as a function of temperature and density instead of temperature and pressure.

Tables of HSP values exist for many industrial compounds, including feedstocks for polymer syntheses (monomers) [81]. Other more complex solubility parameters have been proposed. For example, the model designed by Hansen involves three parameters δ_i ascribed to three molecular effects: molecular attraction, dispersion forces and hydrogen bonds, respectively [82]. It is often considered more precise than the Hildebrand system but is considerably more complex to use.

3.2.2. Density Is Also Key to Efficiency in Thermal Power Production

Interestingly, density also plays a key role in the energy balance of power cycles used to produce electricity and is a major factor determining their efficiency.

Figure 3 shows a supercritical Brayton cycle using SC-CO₂ as the working fluid in a P-T diagram similar to that of Figure 2, along with plots of the iso-density lines [83].

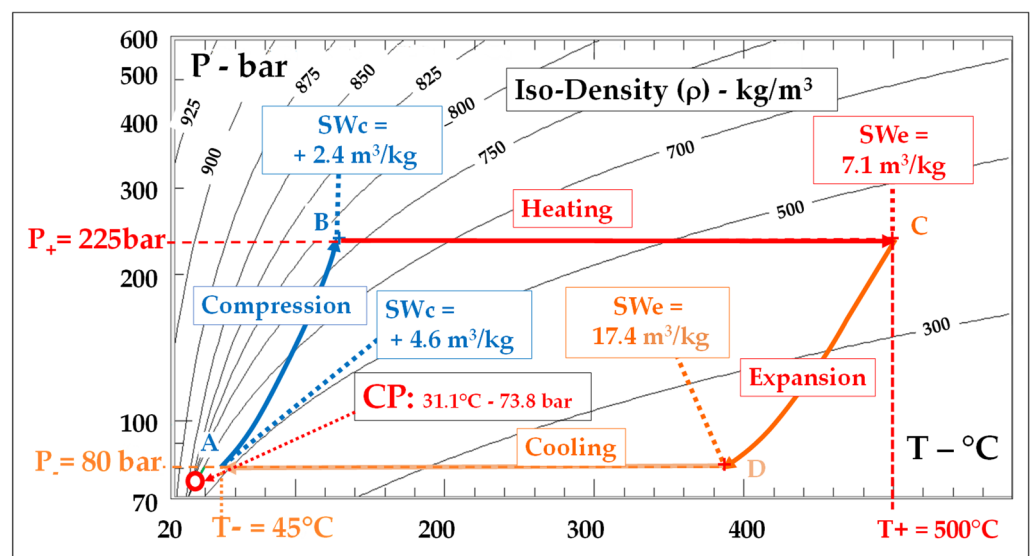


Figure 3. Pressure–temperature diagram of a SC-CO₂ Brayton cycle with the values of the specific mechanical energies involved during the expansion (SWe) and compression (SWc) stages.

In this cycle, we took $(T-, P-) = (45\text{ °C}, 75\text{ bar})$ and $(T+, P+) = (500\text{ °C}, 225\text{ bar})$: the notations $P-$ and $P+$ (respectively, $T-$ and $T+$) designate the low and high pressure/temperature levels of the Brayton cycle. This cycle is truly supercritical since all its stages take place above the CP and there is consequently no condensation stage.

The importance of density comes from Equation (3), which expresses the mechanical energy “SW” consumed (respectively produced) when reversibly compressing (respectively expanding) 1 kg of the working fluid by one unit of pressure [30]:

$$SW = \left(\frac{\delta W}{dP} \right) = 1/\rho \quad (3)$$

“SW” stands for Specific Work per unit of pressure (in m³/kg. i.e., the reversal of density) and δw is the specific mechanical energy (in J/kg) exchanged by the system with its environment, per kg of fluid, when the pressure changes by one unit.

As per usual thermodynamic conventions, δw is counted positively for a compression and negatively for an expansion, so that SW is positive, both during compressions (“ SW_c ”) and expansions (“ SW_e ”).

Equation (3) is therefore essential in any thermodynamic cycle as it determines its energy balance: when the density increases, the corresponding work decreases and vice versa. This key role played by density in the efficiency of power cycles is a point rarely mentioned.

Figure 3 (which refers to a supercritical Brayton cycle) can be interpreted as follows:

- Compression consumes fewer work because ρ is high, so that SW_c is low: in average $3.5 \text{ m}^3/\text{kg}$ in the present example.
- Expansion produces much more energy because ρ is low, so that SW_e is high: in average $12.3 \text{ m}^3/\text{kg}$.

Overall, in such a supercritical cycle, the expansion stage produces about 3.5 times more energy than the compression consumes. In comparison, this factor is only two for contemporary Brayton which uses air as the working fluid and operates in subcritical conditions; yet, these cycles are driven by the most modern gas turbines which are fired above $1350 \text{ }^\circ\text{C}$, a temperature level much higher than that of $500 \text{ }^\circ\text{C}$ taken for the Brayton SC- CO_2 cycles under consideration.

Other remarkable features of supercritical power cycles will be discussed in Section 6. We will see that this technology, although still in development, is important as it has the potential to (i) reduce the carbon footprint of the electrical sector and (ii) enable faster electrification worldwide thanks to reduced installation costs.

3.3. How Do Other SCF Characteristics Influence SCF Processes?

In addition to density, other properties have significant impacts on the speed of mass and heat transfers as well as on the kinetics of the different steps of extractions and chemical reactions.

To provide a comprehensive view, Figure 4 schematizes the progress of any extraction process which proceeds in four steps whatever the type of solvent. The latter is either a chemical solvent or SC- CO_2 in contact with a porous substrate which is, for example, a piece of solid biomass containing an extractable substance.

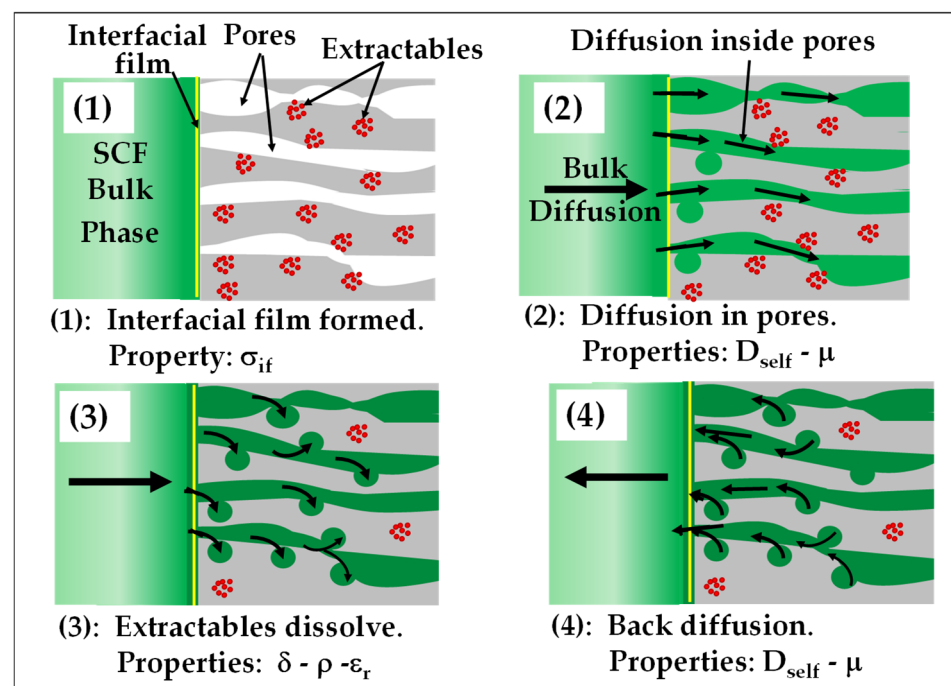


Figure 4. The four steps of an extraction process. The arrows represent solvent migrations.

- The first step is the wetting of the solid: an interfacial film of SCF molecules forms along its surface, the corresponding property being the SCF/solid interfacial tension, noted " σ_{if} ".
- Then, the SCF begins to diffuse into the pores, the relevant properties being its self-diffusion coefficient (D_{self}) and its dynamic viscosity (μ). This phenomenon involves Fick diffusion, in which SCF molecules collide with each other and possibly Knudsen diffusion, in which the same molecules collide with the walls of the pores, when the latter are extremely narrow.
- In the third step, the SCF reaches the extractables and dissolves them. . . or not. Indeed, as it will be explained in Section 3.5, for solubilization to occur, it is necessary that the solid network of the solute collapses, which depends on the value of the dielectric constant (ϵ_r) of the SCF, i.e., its polarity. Once the solid is destabilized and collapses, the degree of solubilization will depend on the match between the values of its own solubility parameter (its HSP) and that of the SCF, as explained above.
- In the fourth and final step, the extractable dissolved in the SCF diffuses back to the bulk SCF phase; here, the important properties are as follows: (i) the mutual diffusion of the extractable in the SCF (D_{mut}), (ii) the viscosity (μ) of the SCF and (iii) its self-diffusion (back to the bulk volume: D_{self}).

Finally, when the process is a chemical reaction, the thermal conductivity (κ) will be relevant for the removal of the heat of reaction.

Therefore, to assess how SCFs compete with organic solvents, we will compare the respective values of all these properties. We will start with those relating to mass and heat transfers, taking again SC-CO₂ as a paradigm.

The effect of the solubility parameter has been already discussed in Section 3.2.1 and the role of the dielectric constant (ϵ_r) will be covered later, when dealing with SC water (Section 3.5).

3.3.1. Surface and Interfacial Tension Data

It is first important to distinguish two notions: *surface tension* (ST, also noted " σ_s ") applies to a contact between a liquid and a gaseous phase (usually: air) while *interfacial tension* (IFT; notation " σ_{if} ") refers to the contact between any two substances: liquid–liquid, liquid–solid; solid–gas ("surface energy" being here a synonym). Although, incorrectly, "surface tension" is often the only designation used; this distinction is necessary when dealing with SCFs as their ST values are zero, a point which is supported by computations of the σ_s of CO₂ (Figure 5). This figure also shows that usual organic solvents have much higher ST data, confirming the superiority of SC-CO₂.

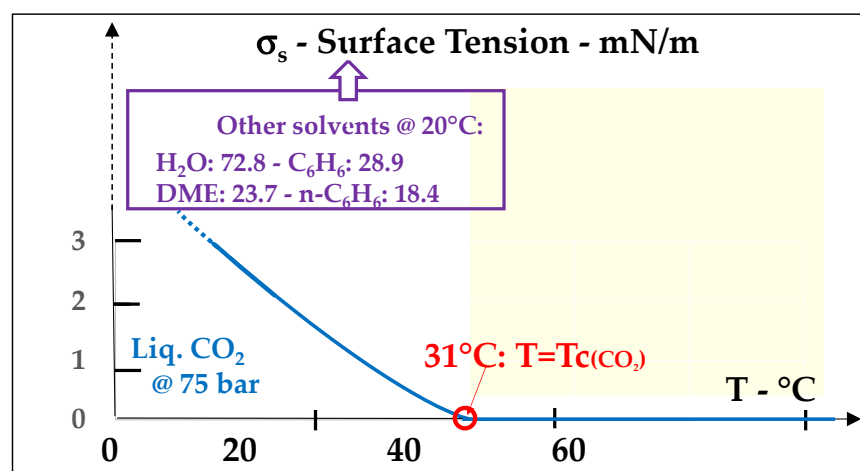


Figure 5. Surface tension data of CO₂ and comparison with some solvents.

In SCF applications, it is therefore the IFT which is important as it determines the ability to wet any given substrate involved in the form of solid particles or drops of immiscible or poorly soluble liquid. The lower the IFT, the better the wetting effect.

Unfortunately, IFT data for solids are rare in the literature devoted to SCF processes. Nevertheless, studies relating to EOR (enhanced oil recovery) in the oil and gas sector and to CCS (Carbon Capture and Sequestration) processes have generated some data for SC-CO₂ in contact with certain minerals (quartz; clays; granite; coals, etc.) (Figure 6). This allows us to note the significant decrease in IFT near the CP [84].

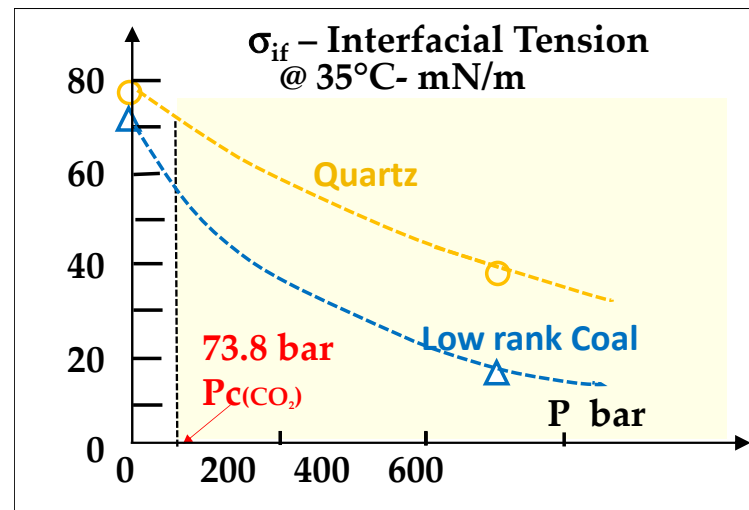


Figure 6. Interfacial tensions between C and quartz and low rank coal.

In the different figures below, the yellow areas correspond to the supercritical regions.

As an example of the wetting power of SC-CO₂, Figure 7 shows that the IFT of SC-CO₂ in contact with dodecane is about five times lower than that of liquid water in contact with the same hydrocarbon [85].

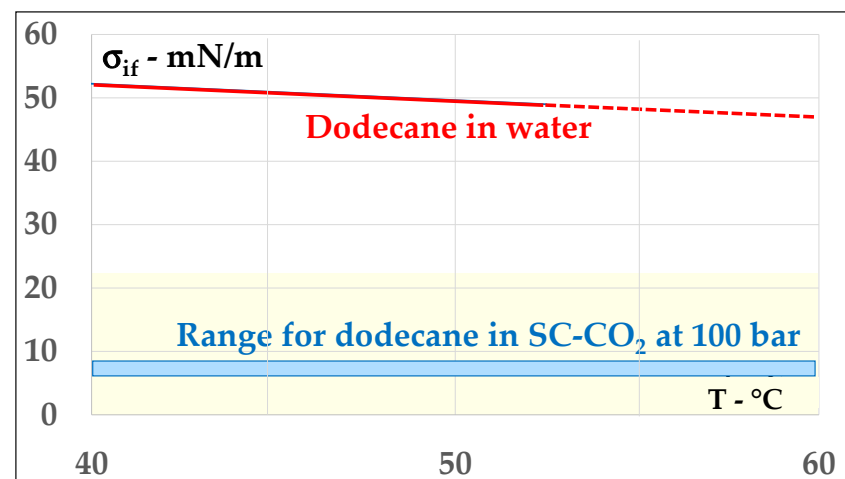


Figure 7. Compared IFT data of the pairs (dodecane/SC-CO₂) and (dodecane/water)].

3.3.2. Diffusivity

Here also, we must distinguish two notions: self-diffusion is the transport of a single chemical species caused by an existing concentration gradient, while mutual diffusion relates to the mixing of two different species. In SCF applications, we will consider the Fick-type (or “bulk”) diffusion which is an unhindered migration that prevails when the width (w_p) of the path (here the pore radius of a solid substrate) is much greater than the

mean free path of the SCF molecules: this occurs in practice when $w_p > 1 \mu\text{m}$. For a pore radius of less than $0.01 \mu\text{m}$, Knudsen diffusion prevails and when w_p is in between, both Fick and Knudsen diffusion coexist [86].

Figure 8a shows that the self-diffusion coefficients of SC-CO₂ are several orders of magnitude greater than that of conventional organic solvents [86,87]. In addition, Figure 8b indicates that the mutual diffusion coefficients (at 33 °C and at infinite dilutions) of methanol and ethanol are three to four times greater in SC-CO₂ [88] than in toluene [89] (**note**: in the case of toluene, a correction was made from the values at 25 °C, using the Arrhenius law and an activation energy of -40 kJ/mol).

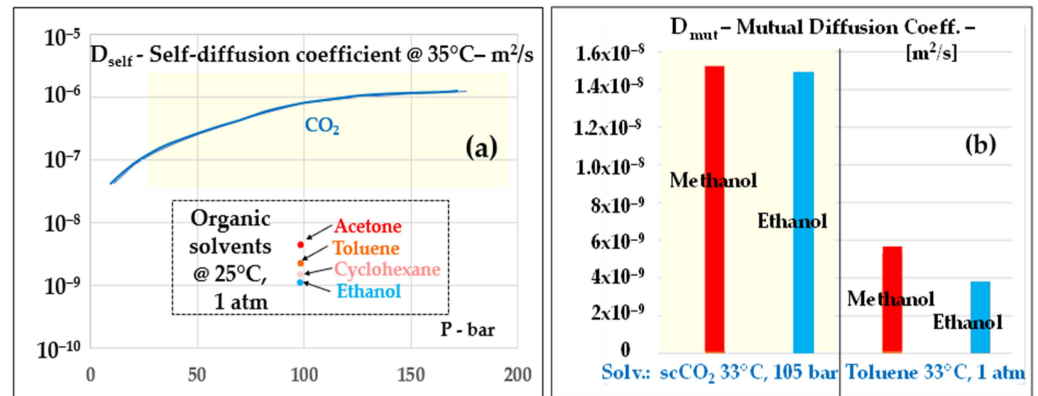


Figure 8. Compared diffusion coefficients: (a) D_{self} of CO₂ versus D_{self} of various solvents; (b) D_{mut} of methanol and ethanol in SC-CO₂ versus in toluene.

3.3.3. Viscosity

Figure 9a shows a plot of the dynamic viscosity of SC-CO₂ at three values of pressure: 73.8 bar (the critical pressure), 125 and 175 bar. Viscosity is particularly small at low pressures, so the use of low or moderate pressures is favorable when dealing with diffusion-controlled reactions. Figure 9b indicates that SC-CO₂ is more than six times less viscous than toluene at 1 atm. Its viscosity increases with pressure but stays far below that of toluene. Calculations were performed using the NIST-REFPROP-10.0 software [83].

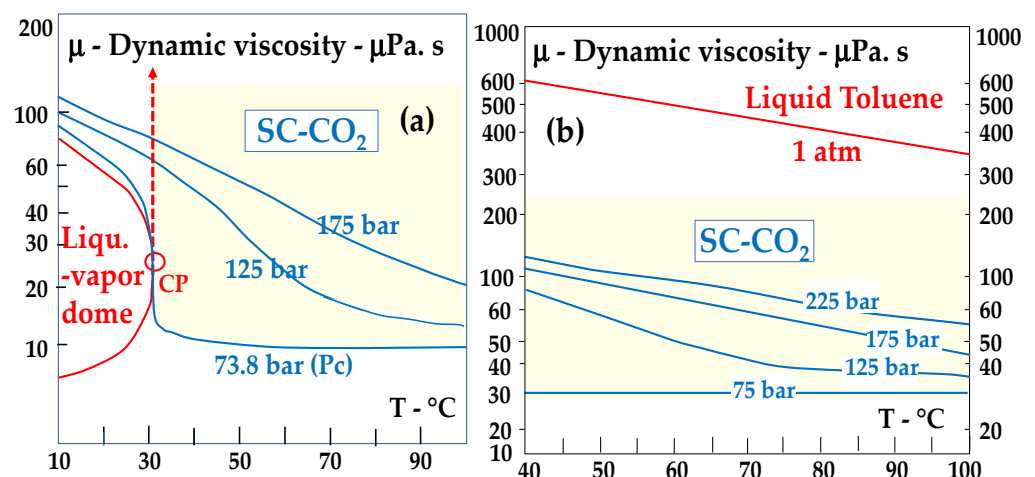


Figure 9. (a) Plots of SC-CO₂ viscosity; (b) comparison with toluene [83].

3.3.4. Thermal Conductivity

Besides the properties governing mass transfers, thermal conductivity (κ) is another important property which conditions heat transfers. Figure 10 shows a chart of the thermal conductivity of SC-CO₂. It increases with pressure and marks a steep increase at the

critical point, but this is a very local peak which practically does not influence overall heat exchanges.

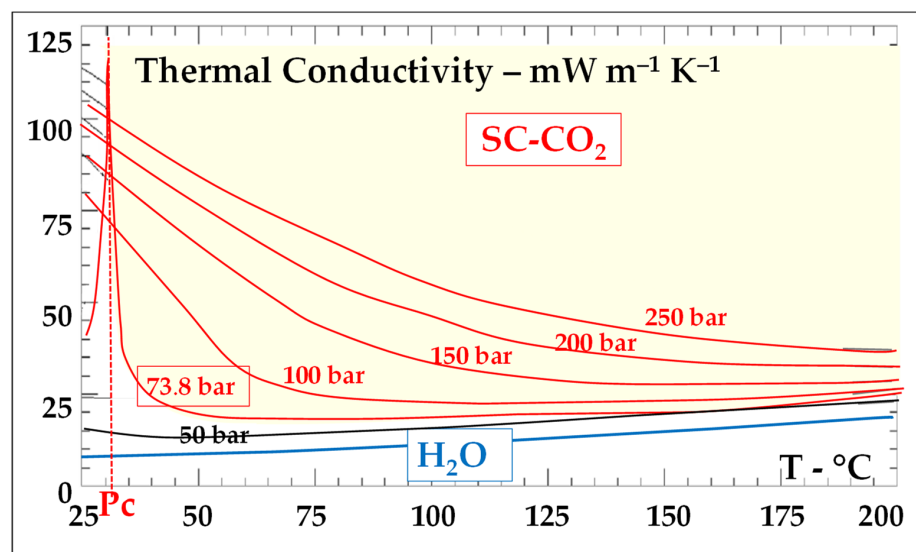


Figure 10. Compared thermal conductivity data of SC-CO₂ and liquid water at 1 atm; computed with [83].

Above the critical pressure, κ is higher than that of liquid water which is practically unaffected by pressure.

3.4. Brief Review of Supercritical Water Properties (SCW)

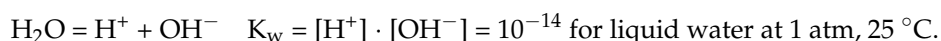
The trends highlighted above regarding the characteristic properties of SC-CO₂ apply to other SCFs, in particular to SCW. The main focus of this article being SC-CO₂, we have placed the data for water at the end of this article (Appendix A). The variations in density, viscosity, and thermal conductivity prove to be quite similar to those of CO₂, albeit at much higher temperatures and pressures (Figures A1–A3).

3.5. Particular Properties Conditioning the Solubilization Step

Two characteristics of SCF need to be considered separately because they do not have an impact on mass or heat transfer but are a prerequisite for the solubilization process of a solid. Indeed, as mentioned in Section 3.2.1, while solubility parameters (e.g., the HSP) determine the possible extent of solvation, they do not specify whether the solid structure will collapse in the presence of the solvent. Here the relevant data are (i) the dielectric constant (ϵ_r) which depends on the polarity of the solvent and, to a lesser extent (ii) the ionic product (K_w), which refers to protonic dissociations and applies especially to water.

3.5.1. Ionic Product

The notion of ionic product (K_w) is defined for protic liquids which, like water, can dissociate into ions and act as Brønsted acids. This is mainly the case for water as other dissociable protic SCFs (organic or inorganic acid) are not used in practice. Water develops hydrogen bonds ($H^{\delta+}-OH^{\delta-}$) which are strong enough to cause a partial dissociation:



This dissociation being endothermic, K_w increases with temperature and is multiplied by 1000 between 25 °C ($K_w = 10^{-14}$) and 300 °C ($K_w = 10^{-11}$). Then, it decreases as the hydrogen bonds become deactivated above the T_c [90]. The consequence is that water becomes more likely to enter into radical reactions (i.e., with organic compounds) rather than acid–base reactions (i.e., with inorganic compounds).

3.5.2. Dielectric Constant (or “Relative Permittivity”)

The dielectric constant ϵ_r of a material is defined as the ratio between its electrical permittivity (ϵ) and that of a vacuum (ϵ_0); it is always greater than one.

Let us consider a solvent in contact with a solid potentially soluble in it (e.g., an extractable). This solid is the site of an electric field due to the charged species it contains. These can be ions, or permanently/instantly polarized molecules, which carry opposite electric charges q_+ and q_- . This electric field is periodic at the scale of a crystal cell. Since the dielectric constant of any solvent is higher than 1, any solid in contact with a solvent sees a decrease in the intensity of its internal electric field due to the reduction in the attraction forces between the charged species it contains, this being expressed by Equation (4) [91]:

$$F_{coul} = \frac{1}{4\pi\epsilon_0\epsilon_r} \frac{q_+q_-}{r^2} \quad (4)$$

This tends to separate the oppositely charged species of the solute from each other and thus destabilize and potentially collapse the structure of the solute, which is the first step for its solubilization by the solvent. Three cases can be distinguished: (i) when the solute is ionic (e.g., a salt like Na^+ , Cl^-), the charged species are cation/anion pairs; (ii) when it is a polar protic solute (e.g., methanol: $\text{CH}_3^{\delta+}\text{-OH}^{\delta-}$), the charged species are permanent dipoles and, (iii) when the solute is an apolar molecule (e.g., CO_2 ; C_6H_6 or CCl_4), the charges come from instantaneous dipoles that appear due to mutual electric influence and whose charges change depending on the relative instant positions of the molecules during their natural thermal agitation [91]. The more polar the solute, the more difficult it is to separate the charges, to collapse the structure and start the dissolution of the solid. However, reciprocally, the more polar the solvent (here the SCF), the higher its dielectric constant and its destabilizing potential are. Since the coulombian forces are maximal in the case of ion pairs, strong ϵ_r values are necessary to dissolve ionic salts.

3.5.3. Dielectric Constant Determines Application Profiles

-SC- H_2O alone constitutes a particular class of SCF due to its protic character and its strong hydrogen bonds. Consequently, its dielectric constant is very high at 25 °C (about 80), exceeded only by those a few “superacids” (120 for fluorosulfuric acid and 84 for hydrofluoric acid) that are however not suitable SCFs [92]. It increases with pressure.

Figure 11 shows a plot of the electrical constant of water at 250 bar. Due to the progressive disappearance of hydrogen bonds [93], it decreases when temperature increases, which causes a loss of solubilization of ionic salts and the precipitation of metal hydroxides, allowing their reaction to form new chemical compounds [94]. Figure 11 confirms the more pronounced decrease in ϵ_r upon passage to the critical state ($T > 374$ °C).

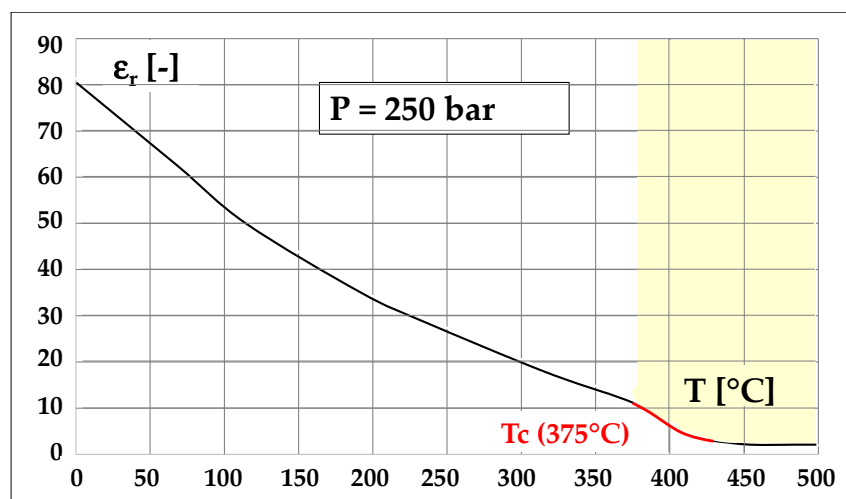


Figure 11. Plot of dielectric constant of H_2O versus temperature (calculated at 250 bar).

Therefore, as a solvent, water favors reactions involving polar and strongly ionic salts. For instance, SCW is a suitable medium for the synthesis of Eu-doped yttrium-aluminum garnets (YAGs) with formula $(Y,Eu)_3Al_5O_{12}$ (Figure 12a), which feature better performances as solid-state lasers than those prepared with conventional solid-state methods. These YAGs are also used as LED phosphors [95]. A wide variety of similar syntheses in SCW are possible [96].

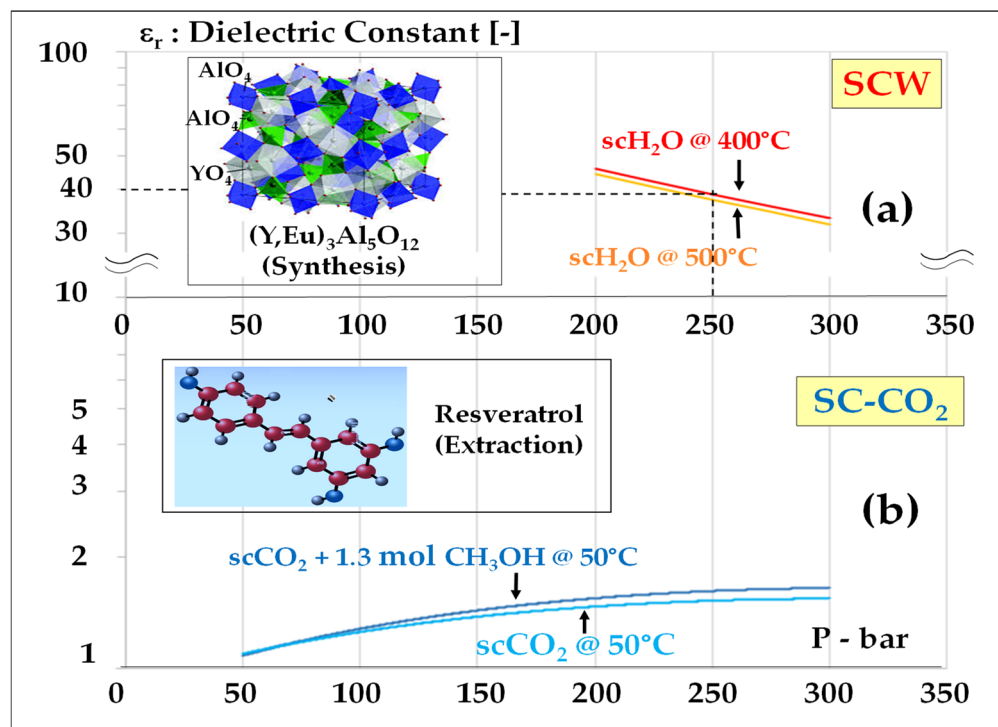


Figure 12. Dielectric constants of SC-H₂O and SC-CO₂ and corresponding application examples (a,b).

-CO₂ is, in contrast, an aprotic, symmetrical and apolar molecule. It has a low dielectric constant, between 1 and 1.5, i.e., approximately ten times smaller than that of SCW [97]. Since it is unable to destabilize the lattices of ionic compounds, it cannot dissolve them but can dissolve apolar or, to some extent, polar aprotic solutes.

For example, it is used to isolate resveratrol by extraction, an apolar biomolecule which is namely present in grapes and tree bark [98] (Figure 12b). This substance is a polyphenol belonging to the class of stilbenoids (i.e., derivatives of stilbene). It has a complex formula (E-5-(4-hydroxystyryl)benzene-1,3-diol) and acts as phytoalexin, i.e., a substance produced by plants to defend themselves against attacks by pathogens, including insects, bacteria and fungi. It is also attributed with multiple therapeutic virtues, including inhibition of platelet aggregation, possible cancer chemopreventive activity and antibacterial/antifungal protection. In recent years it has been produced, marketed and is now widely available as a nutraceutical substance [99–101].

3.6. Summary of SCF Properties—Their Roles in SCF Applications

In conclusion, there is a convergent set of properties, namely: density; interfacial tension; viscosity; diffusivity and thermal conductivity, which help enhance both the mass and heat transfer capabilities of SCFs and make them efficient media for extractions and chemical reactions. Therefore, it must be emphasized—if necessary—that the supercritical state is indeed a specific state and that SCFs are by essence different from gases brought to high pressures.

In addition, it is possible to optimize process efficiency by playing on one or several of the following parameters:

- At first, according to the ionic/polar character of the feedstock and targeted products, one will use an SCF having the appropriate dielectric constant.
- Then, to achieve the solubility match between feedstock and SCF, one will adjust the solubility parameter of the latter either by increasing pressure (and density) and/or by adding a cosolvent.

3.7. Practical SCF Selection Guidelines

In the history of SCFs, besides SC-CO₂ and SC-H₂O, a relatively long list of SCFs have been investigated, including SC-C₂H₄; SC-C₄H₁₀; SC-N₂O; SC-NH₃; SC-CCl₄; SC-SF₆; etc., as we saw in Section 2 [13–17]. However, progress in “green chemistry”, initiated in the 1990s namely by the EPA’s Pollution Prevention Act [102], have induced more environmentally conscious practices. The “twelve principles” of green chemistry were theorized in 2004 by E. J. Beckman [103]. This new philosophy has led to the gradual banning of species that are toxic or harmful to the environment, particularly organics which contain halogens and/or are gaseous at room temperature as they could escape into the environment when isolating the end-product. Alcohols (methanol; ethanol) are liquid and are free from this ban.

3.7.1. Usages of SC-CO₂ for Organic Extractions and Reaction Processes

In practice, due to its multiple advantages, CO₂ is the most popular SCF, at least for extractions and organic reactions, thanks to multiple favorable aspects:

- It is an environmentally benign, weakly toxic and relatively cheap commodity;
- The CO₂ molecule is thermally and chemically stable, therefore “neutral” in many reactions and usable in power cycles;
- Its volatility at ambient pressure renders the recovery of extraction or reaction products easy and eliminates the risk of contaminating them;
- It has favorable interfacial tension, viscosity, diffusivity and thermal conductivity as set out above;
- It is aprotic and not prone to react in acid–base reactions;
- It is resistant to free radical attacks;
- Its full miscibility with gases (as an SCF) starts as soon as 31 °C;
- As a non-polar substance, it is miscible with many organic compounds;
- Finally, SC-CO₂ is compatible with some fluorinated surfactants that increase its miscibility with water by forming microemulsions, opening the door to broader chemistry [104]; however, this aspect deviates from green chemistry principles.

Its main drawbacks are the following:

- CO₂ is a weak solvent in terms of solubility parameter, as mentioned above, which leads to the use of polar cosolvents;
- Dense (high-pressure) CO₂ reacts with water producing carbonic acid and a pH down to 2.8;
- As a Lewis acid, it reacts with organic bases (amines).

3.7.2. Usages of SCW for More Energetic Processes (Syntheses and Decompositions)

SC-H₂O (or SCW) is a powerful SCF when one wishes to carry out organic and inorganic reactions, in particular syntheses:

- It boasts a zero toxicity and environmental impact and is ubiquitously accessible;
- Among SCFs, it has both the highest solubility parameter (48 MPa^{1/2} in the HSP scale [78]) and highest dielectric constant (Figure 11); therefore, it lends itself to many syntheses requiring polar or even ionic media [95,96];
- When used at high temperatures, it allows for the performance of a wide series of processes [31], namely:
- Oxidation reactions (SWO), including the possible break-down of toxic or hazardous wastes and their transformation into innocuous CO₂ and inorganic chloride efflu-

ents [105]. For example, a dual reactor system performing first hydrolysis and then oxidation has been designed [106].

- Reforming of biomass to produce “bio-oils” (or “bio-crudes”) [107].
- Conversion of polymers by liquefaction to recover monomers: water acting as a reagent, solvent and as a source of free radicals and hydrogen during this process [108].
- Conversion of biomass by gasification [109].
- Catalytic conversion of glycerol into hydrogen, a process which would allow for the valorization of significant surpluses of glycerol generated by the production of biodiesel [110].

However, the reforming of hydrocarbons does not seem to be within the reach of SC-H₂O technology, due to the very high level of free energy change involved.

4. Uses of SC-CO₂ for Greener Chemistry

Supercritical fluids, and especially SC-CO₂, align with green chemistry principles stated above, by reducing the usage of hazardous organic solvents and increasing energy efficiency. Because of their abundant, non-toxic and non-flammable nature, water and carbon dioxide are the ideal substances for SCF extractions. In this section, we will elaborate on SCF applications that are studied in our laboratories; they are mainly based on SC-CO₂, SC alcohols and esters which are reactants in biofuel syntheses.

4.1. Extractions of Valuable Food and Pharmaceutical Products

4.1.1. Industrial Development Status

By searching the SCOPUS database over the period 2014–2024, we found 414 research articles, seven of which were review papers. SC-CO₂ has been effectively used for extracting bioactive compounds sourced from plants, e.g., fruit and vegetables, spices, coffee, tea and microalgae [111,112], with major applications in food formulations.

From an industrial standpoint, based on the reference list provided by the NATEX database published by Prozesstechnologie GmbH (Ternitz, Austria) [113], the SC-CO₂ extraction plants currently in operation and devoted to food processing are gathered in Table 2.

This table reveals that commercial SC-CO₂ extraction plants have existed since 1986 and confirms that the use of SC-CO₂ is effective on an industrial scale, especially for food and pharmaceutical processing. Unfortunately, the plants installed in other world regions, such as China and North and South America are not compiled in the NATEX database. Yet, in these world regions, there are many companies providing SC-CO₂ extractors. For example, COFCO (China National Cereals, Oils, and Foodstuffs Corporation, Beijing, China) is one of the largest state-owned Chinese enterprises that employs SC-CO₂ in various extractive applications. In Colorado, USA, Mile High Labs is a producer of cannabinoids (a useful medicine during cancer chemotherapies) that also uses SC-CO₂ extraction. Unfortunately, the details of these companies' processes are confidential.

4.1.2. Outstanding Advances in Extractions

Introducing new raw materials, especially some which are rarely found in common markets, is a way to bring novelty by widening the application spectrum, with experiments starting at the laboratory scale. However, the limited availability of such raw materials may prevent production on an industrial scale. Notable examples of such new raw materials extracted with SC-CO₂ are summarized in Table 3.

Table 3. Extractions by SC-CO₂ of value substances from selected raw materials: operational conditions and yields (papers published within 2014–2024).

Raw Material	Extraction Conditions			Yield (%)	Value Substance	Ref.
	MPa	°C	min			
Lemon basil straw	30	60	180	1.09	Caryophyllene oxide	[114]
Chinese agarwood	29	60–65	150	0.12	Sesquiterpenic alcohol	[115]
Amaranth flour	19.7–29.6	40–60	N/R	5.3–7.7	PUFAs *, squalene, high protein flour	[116]
Lemon basil seed	27.5–29.0	60	180	10	Omega-3 oils, defatted fiber, protein powder	[117]
Annatto seed	20	40	N/R	1.69–2.14	Bixin	[118]
Annatto seed	25.0	60	45	1.40	Bixin, tocotrienols, tocopherols	[119]
Annatto seed	10, 20 ^a	60, 40 ^a	N/R	0.92–2.62	Geranylgeraniol, tocots	[120]
Field pumpkin seed waste	10, 22, 38 ^a	35, 45, 50 ^a	45	11.5	Free fatty acid, Δ ⁷ -sterols	[121]
Black cumin seed	35	35	90	37	Tocopherols, phytosterols, and polyphenols	[122]
Black cumin seed	30	50	60	35	Thymoquinone, <i>p</i> -cymene, hexanal	[123]
Chestnut ^b	20	45	180	2.5	Antioxidant oil	[124]
Rice bran ^b	40	40	80	9.4	Phenolics, flavonoids, γ-oryzanols, and tocopherols	[125]

* PUFAs is for polyunsaturated fatty acids. ^a Sequential extraction process. ^b Co-solvent is 10% ethanol.

All these studies deserve separate discussions:

- Lemon basil (*Ocimum citriodorum* Vis.) straw was found as an alternative feedstock for extracting caryophyllene oxide [114]. This anticancer substance is found in other plants such as basil (*Ocimum* spp.), salvia (*Salvia* spp.) and elsholtzia (*Elsholtzia* spp.). However, experimental results showed that lemon basil straw was a prime source of caryophyllene oxide which can be efficiently extracted using SC-CO₂ or via a hydrodistillation method.
- Recently, a new sesquiterpenic alcohol, 14β,15β-dimethyl-7αH-eremophila-9,11-dien-8β-ol, was discovered from Chinese agarwood (*Aquilaria sinensis*) and extracted with SC-CO₂ [115]. The main products are the classical agarwood chromones along with sesquiterpenic constituents typically found in agarwood essential oils as described in the literature.
- By applying the zero-waste concept, a production method for defatted amaranth (*Amaranthus tricolor*) flour with SC-CO₂ has been designed [116]. The defatted flour had outstanding techno-functional properties such as a high protein content, water adsorption and water swelling capacity, as well as oil absorption capacity. The highest oil extraction yield (7.7%) was obtained at 29.6 MPa and 50 °C. In addition, high squalene content is an additional benefit [117].
- To confirm the profitability of the SC-CO₂ extraction option, some researchers reported an economic analysis of defatted fiber produced from lemon basil (*Ocimum citriodorum* Vis.) seeds [118]. Three products, defatted fibers, an omega-3 rich oil and a protein powder made this process viable. The minimum size of SC-CO₂ extractor for profitable plant was found to be 50 L. The project feasibility was partially conditioned by the price of basil seed.
- Economic studies relating to annatto (*Bixa orellana*) seed extraction were also reported. Integrating an SC-CO₂ extraction with a sugarcane biorefinery was a promising approach to ensure profitability [119].
- Obtaining multiple products such as bixin, tocotrienols and tocopherols from annatto seeds was another approach to improving profit [120]. A two-step sequential extraction with SC-CO₂ was applied to annatto seeds to increase the concentration of bioactive compounds, geranylgeraniol and tocots [120]. In the first step, the extraction was performed at 60 °C and 10 MPa to recover the geranylgeraniol-rich fraction and

was conducted at 40 °C and 20 MPa in the second step to recover the tocotrienols-rich fraction.

- A three-step sequential SC-CO₂ extraction was described to recover free fatty acid and Δ⁷-sterols from field pumpkin (*Cucurbita pepo* L.) seed wastes. It was found that this sequential process enhanced the extractable yield up to 8% [121].
- Recently, a comparative study relating to the production of black cumin (*Nigella sativa* L.) seed oils using either SC-CO₂ extractions or conventional methods (i.e., Soxhlet and mechanical separation) was reported [122]. Antioxidant activities of extracted oils were measured by ABTS [2,2'-azinobis (3-ethyl-benzothiazoline-6-sulfonate)] and DPPH [2,2-Diphenyl-1-picrylhydrazyl]. It was concluded that the SC-CO₂ pathway promotes antioxidant activity of the recovered oil.
- Our research group has reported about the effects of temperature and pressure on volatile compounds, namely thymoquinone, *p*-cymene and hexanal contained in China-cultivated black cumin seeds when it was extracted with SC-CO₂ [123]. The maximum thymoquinone content was obtained at 50 °C and 30 MPa. The results of this work revealed that volatile compounds contained in black cumin seed oil are more sensitive to temperature than pressure.
- Chestnut (*Castanea sativa*) burs were treated with SC-CO₂ and the antioxidant activities of the extracted oil was evaluated through ABTS and DPPH radical scavenging assays [124]. It was found that adding 10% of ethanol is suitable to confer elevated antioxidant activity to the extracted compounds.
- Another study showed that the antioxidant activity of rice bran oil evaluated through ABTS radical scavenging assay was improved when adding 10% ethanol to the extracting SC-CO₂ [125]. In the rice bran oil, phenolics, flavonoids, γ-oryzanols and tocopherols dominate in the antioxidant activity. Under constant pressure, increasing temperature from 40 °C to 60 °C sharply declined the amounts of those compounds and the antioxidant activity.

Regarding the trends and prospects of SCF processes, a general discussion will be offered in Section 7.

4.2. Polymer Processing: Towards More Bio-Sourced Products

SC-CO₂ is a prominent candidate as a green solvent in polymer synthesis, alongside ionic liquids and water. Its plasticizing effect on polymeric structures, which enhances chain mobility, makes it an ideal medium for polymer synthesis and processing [126]. Using the advanced query TITLE-ABS-KEY (supercritical AND CO₂ AND polymer) for the period between 2013 and 2024, 1131 documents were found in the SCOPUS database. According to the outstanding review article written by Kiran and titled Supercritical Fluids and Polymers—The Year in Review—2014, 10 applications in this field were identified [127]. These applications were (i) polymer solutions and phase behavior, (ii) polymerizations, (iii) particle formation/micronization for drug delivery systems, (iv) films, (v) fibers, (vi) membranes, (vii) nanocomposites, (viii) porous materials-foams/scaffolds, (ix) organogels and (x) lignocellulosic polymers.

4.2.1. Advances in Polymer Science

Regarding polymer solutions and their phase behavior, it must be noticed that the solubility of polymers in SC-CO₂ differs from that of small non-polar molecules, due to different molecular weight. The sorption of SC-CO₂ into a polymer occurs before the polymer chain unfolds into the SC-CO₂ matrix. Therefore, modeling the phase behavior between SC-CO₂ and polymers requires new types of systems. For the solubility of small molecules in SC-CO₂, a cubic equation of state (EOS), such as the Peng–Robinson or Redlich–Kwong EOS, is typically used [128,129]. For the solubility of polymers, other EOS models, mostly lattice-based ones like the Sanchez–Lacombe Equation of State (S–L EOS) or the Statistical Associating Fluid Theory (SAFT), work well [130]. Studies of phase behaviors are commonly conducted in a high-pressure view cell. Recently, measurements

relating to the phase behavior of biopolymers such as poly(L-lactic acid) [131] and poly(ϵ -caprolactone) [132] in SC-CO₂ have been reported. The focus of studies devoted to polymer solutions and phase behavior is gradually shifting from petroleum-based polymers to bio-based polymers, in line with the bio-circular economy.

Due to the difficult solubilization of polymers in SC-CO₂, dissolving monomers in SC-CO₂ and then polymerizing them is an alternative approach. Such polymerization reactions, including polycondensation, radical polymerization, emulsion and suspension polymerization, precipitation polymerization, dispersion polymerization and ring-opening polymerization, are feasible [133]. These reactions can generate new materials, including aerogels, composites, films, foams, fibers and porous materials. However, controlling the molecular weight distribution is challenging due to the high reactivity in SC-CO₂. The techniques of Controlled Radical Polymerization (CRP) or Reversible-Deactivation Radical Polymerization (RDRP) were developed to terminate polymer chain growth through multiple reversible radical deactivation steps. RAFT (Reversible Addition-Fragmentation chain Transfer) polymerization and other methods [134] have also been introduced as alternative approaches to control the molecular weight of polymers synthesized in SC-CO₂. Trends in SC-CO₂ polymerization are towards biodegradable polymers for use in biomedical and pharmaceutical applications [135].

4.2.2. Novel Polymeric Structures

Particle Shaping

Particle formation is a key topic when processing polymers in SC-CO₂ for the production of drug delivery packages, adsorbents and catalyst supports [136]. RESS (Rapid Expansion of Supercritical Solutions) was the first technique applied in this research area. Briefly, a polymer-SC-CO₂ solution is rapidly depressurized through a nozzle or atomizer to form fine particles. While RESS is simple, it is limited by the solute's solubility and possible nozzle blockages. The PGSS technique (Particles from Gas-Saturated Solutions/Suspensions) involves extracting an emulsion or suspension solution using SC-CO₂, followed by expansion through a nozzle or atomizer, which consumes less SC-CO₂ than RESS. The SAS (Supercritical Anti-Solvent) technology includes GAS (Gas Anti-Solvent), ASES (Aerosol Solvent Extraction System) and SEDS (Solution Enhanced Dispersion by Supercritical Fluids). SAS processes start with a polymer dissolved in organic solvents such as ethanol or dichloromethane. In GAS, SC-CO₂ flows through the solution, expanding the organic solvent and forming fine particles in the precipitation chamber. In ASES, the solution is sprayed into an SC-CO₂ chamber to produce particles of adjustable size. In SEDS, the supersaturated solution and SC-CO₂ are atomized together in a coaxial nozzle.

In SAS processes, the addition of drugs or active compounds to the solution for encapsulation or co-precipitation has been widely explored. Besides these classical techniques, other advanced methods have been reviewed elsewhere [137,138]. From an industrial perspective, particle formation using SC-CO₂ is particularly suitable for applications in medical sciences, especially nanomedicine [139].

Regarding the optimum drug delivery effect, several comprehensive reviews on the advancements in supercritical fluid technology for polymer processing in pharmaceutical applications have been periodically compiled and updated [135,140–143]. Through the use of SC-CO₂ technology, polymer/drug composites are developed for various purposes, the primary challenge being the effective modification of the dissolution kinetics of active compounds to achieve optimal therapeutic outcomes. The required drug release kinetics can vary based on the specific medical application. Selecting the appropriate polymeric carrier is crucial for ensuring that the drug is released at the desired rate and/or that the specific site of action is accessed. PVP is currently the most widely used polymer and is regarded as one of the top carriers, as it frequently enables the production of uniform and spherical composite particles. Following PVP, PLA and PLLA are also commonly used as suitable carriers. Additionally, pH-sensitive polymers like Eudragit have gained interest for targeted drug release. Eudragit L100-55, which is soluble at a pH above 5.5, corresponding

to the duodenum in the small intestine, protects the active compound from the acidic gastric environment while also avoiding side effects on the gastric tract. It has been effective in achieving controlled release of NSAIDs, antibiotics and bronchodilator drugs from SAS microspheres. Other types of polymers, such as PEG, poly(lactide-co-glycolide) (PLGA), ethyl cellulose and zein, as well as cyclic oligosaccharides like β -cyclodextrin (β -CD) and its derivatives, have also been used in particle formation with SC-CO₂. The current challenge in forming drug/polymer composites with SC-CO₂ is finding new polymeric carriers that are compatible with the process technology and can achieve the desired dissolution kinetics. The use of polymeric blends combining hydrophobic and hydrophilic polymers has not yet been explored in detail [140].

Polymeric Films and Membranes

From a research point of view, surface modification of thin films or membranes using SC-CO₂ has been reported as an alternative method to modify their specific properties, such as electrochemical properties [144], apparent contact angle [145], gas permeability and selectivity [146]. For example, SC-CO₂ led to the reorganization of ionic channels in Nafion membranes under high pressure [144]. Diluting polyoxaperfluorobutyl bromide in SC-CO₂ before coating it onto the polymer matrix significantly reduced the apparent contact angle hysteresis of the resulting gel thin films [145]. However, thin films obtained with SC-CO₂ showed no significant difference in gas permeability compared to ethanol-treated thin films [146]. SC-CO₂-assisted electrospinning is widely employed to fabricate nanofibers [147]. Although it is considered a greener electrospinning method, SC-CO₂-assisted electrospinning is more complex than conventional electrospinning due to the high-pressure operation. In surface modification and electrospinning applications, SC-CO₂ acts as a solvent to reduce viscosity and improve the flow properties of polymer solutions. On an industrial scale, when materials are used in non-food industries, organic solvents are generally more convenient than SC-CO₂, except for issues related to flammability.

Foaming and Porous Products

The synthesis of porous materials, foams, and scaffolds using SC-CO₂ is a vibrant area of research [148], as important as studies devoted to polymer solutions and phase behavior, polymerization and particle formation.

Industrial foaming technologies, including extrusion foaming, bead foaming and injection molding foaming, rely on pressurizing a polymer/gas solution, mixing, and then depressurizing to initiate bubble nucleation and growth. Foaming with SC-CO₂ involves three steps: dissolving SC-CO₂ into the polymer/gas medium, generating cell (bubble) nucleation and growing the cells (bubbles) or expanding the polymer. SC-CO₂ acts as a physical foaming agent, and its properties are adjustable by temperature and pressure. Polymer properties, such as the glass transition temperature, melting temperature and viscosity, also play an important role in foaming processes. Batch foaming with SC-CO₂ is suitable for lab-scale research due to its simplicity and repeatability. On the other hand, industrial production prefers extrusion foaming because of its continuous operation and scalability. Sustainable foams, biodegradable foams and biofoams are among current research trends in polymer foaming with SC-CO₂ [149]. Biodegradable foams include biosourced polymers (starch and poly(hydroxyalkanoate)), as well as synthetic polymers, such as poly(L,D-lactic acid) and poly(ϵ -caprolactone) [150,151].

Polymer foaming with supercritical carbon dioxide (SC-CO₂) presents several key benefits. As an environmentally friendly choice, SC-CO₂ is non-toxic, non-flammable and serves as a greener alternative to conventional chemical blowing agents that are often harmful to the environment. The use of SC-CO₂ also provides precise control over the foaming process, allowing for adjustments in pressure, temperature and CO₂ concentration to produce foams with specific cell sizes and densities. Furthermore, polymers foamed with SC-CO₂ tend to have superior mechanical properties, including enhanced impact resistance and thermal insulation, owing to the uniformity and consistent size of the foam cells.

Additionally, the plasticizing effect of SC-CO₂ reduces the required processing temperature for foaming, making it particularly advantageous for temperature-sensitive polymers and contributing to potential energy savings.

By integrating particle leaching with supercritical foaming methods, the challenges of pore size adjustment and the production of scaffolds with precise pore structures and high porosity can be overcome. This approach holds significant potential in the field of tissue engineering. Various studies have investigated the fabrication of highly interconnected biodegradable polymer scaffolds using SC-CO₂ foaming and particle leaching techniques. For example, Zhang et al. [132] fabricated highly connected porous poly(ϵ -caprolactone) (PCL) scaffolds by blending PCL with water-soluble poly(ethylene oxide) (PEO) as a sacrificial material. The addition of PEO not only aided in foaming PCL by enhancing its viscosity, but also significantly improved the porosity and interconnectivity of the PCL scaffolds after leaching. The porosity increased by as much as 93.5%, and the open pore content rose to 90.9% for the PCL50 blend (containing 50% PCL by weight). Similarly, Reignier and Huneault [152] prepared highly porous PCL scaffolds with highly interconnected pores using PCL, PEO and salt particulate leaching. Xin et al. [153] fabricated bimodal porous PLGA scaffolds using SC-CO₂ foaming and different sizes of NaCl particles as porogens. Bimodal porous scaffolds with macro- and micropore structures were produced by adjusting the foaming temperature, pressure and the different sizes and mass fractions of the NaCl porogen. Salerno et al. [154] demonstrated that bimodal porous scaffolds for bone regeneration could be successfully prepared using SC-CO₂ foaming and the porogen leaching technique. Poly(ϵ -caprolactone) (PCL) was blended with thermoplastic zein (TZ), which acted as a porogen, and hydroxyapatite (HA). The resulting PCL/TZ and PCL/TZ-HA scaffolds exhibited a macroporosity with a mean pore size of $134 \pm 80 \mu\text{m}$ and $121 \pm 49 \mu\text{m}$, respectively, and micropores in the range of 1–10 μm . Both bimodal porous scaffolds also promoted the adhesion, colonization and proliferation of osteoblast cells for up to 28 days *in vitro*.

In addition to using particle leaching with SC-CO₂ foaming, some researchers have incorporated reinforcing agents with SC-CO₂ foaming to enhance the mechanical characteristics of polymeric bone scaffolds. Carrascosa et al. [155] employed high-pressure CO₂ foaming to produce PLGA-based foams with added reinforcement agents, such as Mg(OH)₂, hydroxyapatite (HA) and Mg, to achieve foams with improved mechanical properties. The resulting foams were rigid, non-sticky and stable over time, exhibiting high porosity. The compressive stresses achieved—1.85 MPa for Mg(OH)₂ and 3.81 MPa for HA—were comparable to the 4.2 MPa compression resistance for trabecular bovine bone as reported in the literature.

Although the supercritical foaming technique offers a wide range of applications, its use comes with several challenges. A major issue is the substantial initial cost associated with acquiring specialized high-pressure equipment. Additionally, the process is technically demanding and requires precise optimization of processing parameters, including temperature, pressure and CO₂ concentration, to achieve consistent and reproducible foam structures. Controlling the size, shape and distribution of scaffold pores using the SC-CO₂ foaming technique continues to be a critical challenge in scaffold production [156].

4.3. Challenges and Limitations of SC-CO₂ in Green Chemistry

While SC-CO₂ offers substantial advantages, there are challenges and limitations associated with its use.

These include technical and economical obstacles such as high investment costs, limited extraction of polar compounds, low solubility of polar monomers in SC-CO₂ and limitations to the practical use of SC-CO₂ as a reaction medium. Further research is needed to overcome the obstacles related to the correct use of SC-CO₂ which represents the most efficient green media in chemical industries [157]. Then, because SC-CO₂ equipment is relatively expensive compared to conventional units, the extracted compounds must be of enough high value, such as functional ingredients, to ensure the profitability of the overall

processes. In addition, the valorization of solid by-products discharged from the SC-CO₂ extractors also plays an important economic role. For example, not only decaffeinated tea and coffee but also caffeine itself are the high-value products that can be obtained from SC-CO₂ extraction of tea leaves and coffee beans. This is a good example for the rationale and profitable implementation of SC-CO₂ extraction processes capable of reaching industrial scale.

High investment cost issue of SC-CO₂ extraction could be simply justified by conducting a techno-economic analysis (TEA). Extracting high value compounds from industrial wastes or by-products is an appropriate strategy. For example, extractions of bioactive compounds from fruit and vegetable wastes [158] and seafood by-products [149] were recently reviewed. Seed and kernel discharge from fruit processing plants are potential sources of unconventional lipids. Besides, peel and pomace are promising sources of bioactive compounds, e.g., phenolics, tocopherol and phytosterol compounds. Omega-3 and omega-6 fatty acids could be recovered from fish and shellfish cut offs such as the head, liver, bone and skin [159]. Economic analysis of SC-SCO₂ extraction of antioxidants from fruit residues, including mango peel, yellow passion fruit seed, raspberry seeds, orange and mandarin peel and açai berry exhausted pulp was recently reported. Material and energy balances were conducted in a computer simulation using Aspen plus and Aspen Process Economic Analyzer software. The economic indicators showed that yellow passion fruit has the highest potential for use as raw materials for SC-CO₂ extraction because of the mild operating conditions and high value of the extracts [160].

Utilization of spent materials discharged from SC-CO₂ extractor, for example as feedstock for a biorefinery, could amplify the margin of the extraction process. Blackberry pomace was introduced as a raw material for producing PUFAs and water-soluble antioxidants via SC-CO₂ and pressurized liquid extractions (PLE), respectively [161]. Solid residue discharged from the SC-CO₂ extractor was subsequently extracted by PLE. The SC-CO₂ extraction at 54.8 MPa, 64 °C and 171 min provided a PUFA-rich fraction containing 64.1% of linoleic acid and 12.9% α -linolenic acid. Furthermore, PLE generated extracts containing several phenolic acids, flavonoids and anthocyanins that conferred an excellent antioxidant activity. In our research group, the sequential extraction of rambutan seed waste to produce unconventional lipids and polysaccharides by SC-CO₂-ethanol and subcritical water extractions was recently demonstrated [162]. The results showed that SC-CO₂-ethanol extraction was able to reduce the optimal conditions of subcritical water extraction without effects on monosaccharide content and molecular weight of extracted polysaccharides [163].

Life-cycle assessment (LCA) is a tool for evaluating the environmental impact of the SC-CO₂ extraction processes. LCA of SC-CO₂ extraction of caffeine from coffee beans to produce caffeine and decaffeinated coffee was reported [164]. When using products or wastes from the coffee industry as feedstock, the environmental impact generated by the agricultural and transportation stage became significantly higher than that created by the SC-CO₂ extraction, especially regarding climate change (CC), ozone depletion (OD), terrestrial acidification (TA), marine eutrophication (ME), human toxicity (HT), photochemical oxidant formation (POF), particulate matter formation (PMF), natural land transformation (NLT), water depletion (WD) and mineral resource depletion (MRD). To emphasize the environmental impacts of SC-CO₂ extraction, the agricultural and transportation stages were excluded in our previous LCA of crude peptides extraction from defatted defective green coffee beans using SC-CO₂, as these beans were considered waste, with their environmental burdens attributed to primary coffee production and outside the gate-to-gate boundaries focused solely on the processing stages [165]. The results showed that the most significant environmental impacts came from SC-CO₂-EtOH extraction, spray drying encapsulation of caffeine and evaporation. To reduce the environmental impacts, CO₂ and ethanol must be recovered and reused in subsequent operations.

In recent research on SC-CO₂ extraction, LCA was performed along with TEA to estimate the environmental and economic aspects, respectively [166]. For example, the TEA and LCA of volatile oil extracted from raw biomass and resin of Agarwood (*Aquilaria*

sinensis) using SC-CO₂ was reported [167]. Unquestionably, TEA indicated that this process is profitable because volatile oil of Agarwood is very expensive (USD 12.5–25 thousand per kg). Fixed capital (FCI) and total capital (TCI) investments were estimated to be USD 6.18 million and USD 7.11 million, respectively for a production capacity of 5280 kg oil per year. Return of investment (ROI) was 12.05% and 19.16% for raw biomass and resin extractions, respectively. Regarding the LCA, the highest environmental impact was generated by the SC-CO₂ extraction process because of the electricity consumption. Because coal and natural gas are the major primary energies used to produce electricity production in Malaysia, the main impact was in terms of global warming potential.

The limited extraction of polar substances and the low solubility of polar monomers can be solved by adding a co-solvent, known as modifier or entrainer. The co-solvent can be involved within a static or dynamic mode. In static mode, the substrate is soaked in the co-solvent for the desired time before SC-CO₂ extraction is performed. In dynamic mode, the co-solvent and SC-CO₂ are mixed and fed through the packed substrate in the extraction chamber. Ethanol is the most widely used co-solvent in SC-CO₂ extractions and preferably bioethanol owing to its renewability and low-toxicity. By searching the SCOPUS database in August 2024 over the period 2014–2024 (www.scopus.com, accessed on 18 August 2024), we found 197 research articles that involved SC-CO₂ extraction using ethanol as a co-solvent. It is certain that increasing ethanol concentration significantly enhances the solubility of polar compounds. However, to prevent shifting from SC-CO₂ extraction to ethanolic extraction, it should be kept below 20%, preferably 10% based on SC-CO₂ consumption. Besides other conventional polar solvents such as acetone and methanol, the green solvents, e.g., ethyl lactate and ethyl acetate, were demonstrated as suitable co-solvents to maintain the environmental benefit of SC-CO₂ extraction [168]. It was found that adding ethyl lactate provides the highest caffeine yields in both static and dynamic modes at 70 °C and 30.0 MPa, respectively. Ethyl lactate and ethyl acetate, when introduced as co-solvents for polycaprolactone and polycaprolactone-hydroxyapatite composites, foamed with SC-CO₂ [169]. It was indicated that both co-solvents enhance the low temperature foaming of the composite polymers.

The use of SC-CO₂ as a reaction medium for chemical synthesis with or without using heterogeneous catalysts have been implemented at industrial scale, especially in the pharmaceutical industry because SC-CO₂ slightly impacts on catalyst properties [170]. On the other hand, the effects of biocatalysts such as microbial whole-cells and isolated enzymes, including lipases, are limited because they interfere with properties of SC-CO₂, particularly by altering its solubility and diffusivity characteristics. Regarding microbial whole-cells biocatalysts, substrate and product both diffused through cell membranes leading the cell disruption. Moreover, SC-CO₂ has the effects of conformational changes of enzyme active site that causes their deactivation. Operating temperature and pressure influenced enzyme activity and stability as well [171]. Since biocatalyzed reactions proceed favorably in aqueous media, this poses another major obstacle to the alternative use of SC-CO₂ with biocatalysts.

Overall, adding co-solvents actually improves the solubility of polar compounds in SC-CO₂ extraction but increases the complexity and toxicity of the reaction system.

5. Syntheses of Biofuels: Towards Greener Mobility and Electricity

Biodiesel and bioethanol stand out as the most popular biofuels [172].

In this review, we will focus on biodiesel syntheses using supercritical fluid technology, which is a main research activity in our laboratory.

Biodiesel is one of the most used biofuels for mobility applications (diesel cars) and potentially for electricity production. It represents a sustainable and green substitute for conventional, non-renewable fossil fuels [172]. It offers benefits such as biodegradability, reduced toxicity and decreased greenhouse gas emissions [173]. Supercritical fluid technology, an alternative synthesis route, enables non-catalytic and clean biodiesel production using supercritical alcohols as a reactant.

Synthesis under SC conditions is well-suited to produce biodiesel from various feedstocks, including low-cost ones containing high levels of free fatty acids (FFAs), which pose challenges within conventional catalytic processes. SC conditions allow high reaction rates and short reaction times [174,175]. Because no catalyst is needed, unlike in conventional catalytic reactions, the production process is more environmentally friendly, as it generates no wastewater and yields clean glycerol as a by-product. Additionally, it avoids the high cost and potential inactivation of enzymes, which are common challenges in enzyme-catalyzed methanolysis during biocatalytic reactions [174,176].

5.1. History of Biodiesel Processes Using SCFs

Based on a Scopus database search in August 2024 (www.scopus.com, accessed on 18 August 2024) using the keywords “biodiesel” and “supercritical”, the number of research publications related to non-catalytic supercritical processes for biodiesel production reveals a clear growing trend with 531 documents published from 2014 to 2024, compared to 389 documents from 2003 to 2013. This highlights a rising interest of researchers to explore catalyst-free biodiesel production.

During the development of biodiesel syntheses, two pathways were successively explored: trans- and interesterification (Figure 13).

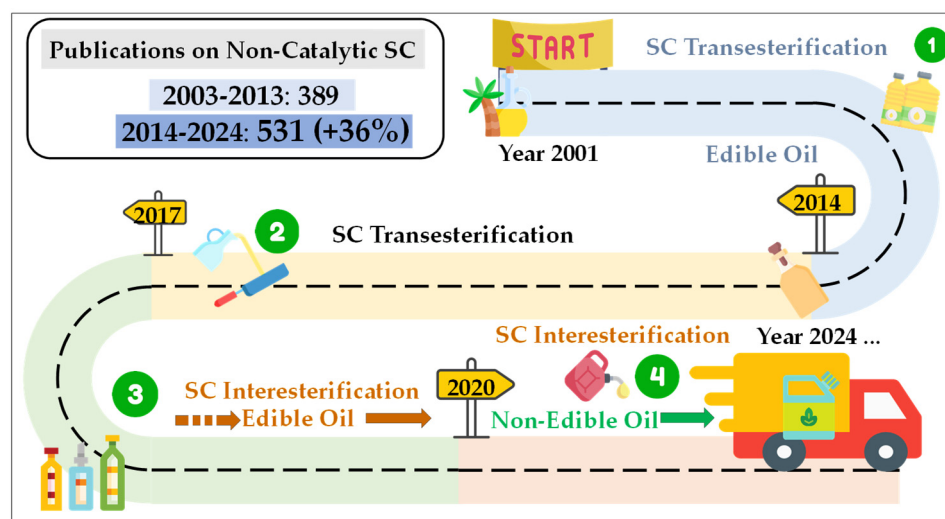


Figure 13. A brief history of the biodiesel development using SCFs.

The corresponding reactions are shown in Table 4.

Table 4. Main trans- and interesterification reactions involved in biodiesel SC syntheses.

Solvent	Reaction	Critical Temp. (°C)	Critical Pressure (MPa)	Ref.
Methanol	Transesterification: $\text{Triglyceride} + 3 \text{ MeOH} \leftrightarrow 3 \text{ FAME} + \text{Glycerol}$	239.0	8.1	[177,178]
Ethanol	Transesterification: $\text{Triglyceride} + 3 \text{ EtOH} \leftrightarrow 3 \text{FAEE} + \text{Glycerol}$	243.0	6.3	[178,179]
Methyl acetate	Interesterification: $\text{Triglyceride} + 3 \text{ MeOAc} \leftrightarrow 3 \text{ FAME} + \text{TA}$	233.8	4.7	[178,180]
Ethyl acetate	Interesterification: $\text{Triglyceride} + 3 \text{ EtOAc} \leftrightarrow 3 \text{FAEE} + \text{TA}$	250.0	3.8	[178,181]

MeOH = Methanol; FAMEs = Fatty acid methyl esters; EtOH = Ethanol; FAEEs = Fatty acid ethyl esters; EtOAc = Ethyl acetate; MeOAc = Methyl acetate; TA = Triacetin.

5.1.1. First Pathway: Transesterification

The first research on biodiesel production under supercritical conditions was published in 2001 by Saka and Kusdiana, who produced rapeseed oil-based biodiesel using supercritical methanol [182]. The process typically involves the transesterification of triglycerides, which are natural oils, with short-chain alcohols like methanol or ethanol at supercritical temperature and pressure. The main reaction product is a biodiesel which is either a FAME (fatty acid methyl ester) or a FAEE (fatty acid ethyl ester), along with glycerol as a by-product (Table 4). Under SC conditions, the triglyceride and the alcohol (an acyl acceptor) form a homogeneous phase, allowing for rapid transesterification. This homogeneity is achieved since high temperatures and pressures improve the solubility of non-polar triglycerides and reduce the dielectric constant of alcohol, resulting in a single phase of oil/alcohol mixture [176]. However, during transesterification using supercritical alcohols, a post-reaction treatment is required to separate the purified ester product from glycerol [178]. Table 5 summarizes examples of transesterification reactions performed with SC-MeOH and SC-EtOH and using various TG feedstocks, including edible oils such as rapeseed [182], palm [183] and soybean oil [184], non-edible oils such as neem and mahua oil [185], crude castor oil [186], sura honne oil [187], third generation feedstock such as microalgae (*Chlorella protothecoides*) oil [188] and waste oils such as spent coffee grounds [189] and waste palm oils [183].

This table includes studies conducted both in our laboratory and by other researchers. The experiments were carried out at temperatures of 275 °C to 425 °C, pressures of 15.0 to 45.0 MPa and with reactant-to-oil molar ratios from 12:1 to 50:1.

5.1.2. Second Pathway: Interesterification

Because the transesterification process requires the removal of the unwanted glycerol by-product whose price has plummeted [190], there is a growing interest in developing a class of glycerol-free processes, called interesterification, to avoid surpluses of crude glycerol. Interesterification involved converting triglycerides with light SC carboxylate esters into FAMES or FAAEs and producing triacetin as a by-product (Table 4) [191]. Carboxylate esters have, therefore, been employed as an alternative to conventional alcohols [192]. Saka and Isayama published the first research on noncatalytic interesterification with carboxylate esters in 2009. They produced rapeseed oil-based biodiesel using supercritical methyl acetate [193] at the optimal conditions of 350 °C, 20 MPa, with a methyl acetate to oil molar ratio of 42:1; they obtained a FAME yield of 97.0%. Triacetin, a by-product, has shown outstanding qualities as a fuel additive. Eliminating the necessity for triacetin separation from biodiesel contributes to a cleaner and more sustainable process [194]. However, a previous study showed that the triacetin concentration should not exceed 10% (w/w) to avoid the degradation of fuel properties [195]. In 2012, Goembira et al. [196] first compared various carboxylate esters as reagents for the SC production of biodiesel. They found that supercritical methyl acetate gave the highest yield, followed by ethyl acetate. Consequently, this review focuses on supercritical methyl acetate and ethyl acetate.

5.2. Overview of Main Trans- and Interesterification Processes

Table 5 gives typical examples of interesterification reactions using SC methyl acetate (MeOAc) or ethyl acetate (EtOAc) and various feedstocks, including edible oils (e.g., rapeseed [183], palm oil [171]), non-edible oils (e.g., crambe seed oil [197]) and waste oils (e.g., spent coffee grounds oil [198]).

Table 5. Trans- and interesterification processes involving various feedstocks and SC conditions.

Feedstock	Reactant	Molar Ratio (Oil: Reactant)	Temp./Pressure/Reaction Time (°C/MPa/min)	Esters (wt%)	Process/Reactor Type	Ref.
<i>Supercritical transesterification</i>						
Edible oil:						
Rapeseed oil	Methanol	42:1	350.0/45.0/4.0	95.0	Batch reactor with stirrer	[182]
Refined palm olein oil	Methanol	12:1	400.0/15.0/20.0	90.0	Continuous tubular reactor	[183]
Canola oil	Methanol	40:1	350.0/20.0/10.0	100.0	Continuous spiral reactor	[199]
Refined palm olein oil	Ethanol	30:1	300.0/30.0/60.0	80.1	Continuous tubular reactor	[200]
Canola oil	Ethanol	40:1	350.0/20.0/30.0	100.0	Continuous spiral reactor	[199]
Soybean oil	Ethanol	15:1	320.0/20.0/50.0	62.5	Continuous reactor	[184]
Non-edible/waste oil:						
Neem oil	Methanol	50:1	425.0/30.0/15.0	83.0	Batch reactor	[185]
Mahua oil	Methanol	50:1	425.0/30.0/10.0	99.0	Batch reactor	[185]
Crude castor oil	Methanol	43:1	300.0/21.0/90.0	96.5	Batch-shaken tank reactor	[186]
Sura honne oil (<i>Calophyllum inophyllum</i> oil)	Methanol	40:1	400.0/30.0/30.0	80.0	SS-316 stainless steel batch reactor	[187]
Used palm olein oil	Ethanol	30:1	300.0/30.0/60.0	73.4	Continuous tubular reactor	[200]
Used palm olein oil	Methanol	12:1	400.0/15.0/20.0	80.0	Continuous tubular reactor	[183]
Spent coffee grounds	Ethanol	30:1	275.0/15.0/40.0 (Batch) 325.0/15.0/29.4 (Continuous)	88.4 (Batch) 83.4 (Continuous)	Batch tube reactor and continuous tubular reactor	[189]
<i>Chlorella protothecoides</i> oil	Methanol	19:1	320.0/15.2/31.0	90.8 (RSM)	Continuous flow tubular reactor	[188]
<i>Chlorella protothecoides</i> oil	Ethanol	33:1	340.0/17.0/35.0	87.7 (RSM)	Continuous flow tubular reactor	[188]
<i>Supercritical interesterification</i>						
Edible oil:						
Rapeseed oil	Methyl acetate	42:1	350.0/20.0/45.0	97.0	Flow-type reactor	[193]
Rapeseed oil	Methyl acetate	40:1	305.0/20.0/30.0	97.2 (RSM)	Continuous plug flow reactor	[201]
Palm oil	Ethyl acetate	30:1	380.0/16.0/42.4	90.9	Continuous tubular reactor	[181]
Palm oil	Ethyl acetate	30:1	380.0/20.0/45.0	~75.0	Fixed-bed reactor	[202]
Non-edible/waste oil:						
Crambe seed oil	Methyl acetate	NS	375.0/20.0/15.0	66.5	Continuous tubular reactor	[197]
Spent coffee grounds	Ethyl acetate	30:1	325.0/15.0/50.0 (Batch) 350.0/15.0/25.2 (Continuous)	91.8 (Batch) 86.4 (Continuous)	Batch tube reactor and continuous tubular reactor	[198]

NS: not specified.

Most of the interesterification studies have been carried out at 305 °C to 380 °C and under 15.0–20.0 MPa, with reactant-to-oil molar ratios ranging from 30:1 to 40:1.

Campanelli et al. [203] reacted various oils with supercritical methyl acetate and observed that biofuel yields were not affected when reacting different feedstock oils, including edible and non-edible.

5.3. Influence of Process Parameters

The reactions involved in SC biodiesel production are performed at temperatures and pressures well above the critical points of the reacting alcohols and carboxylate esters, as

detailed in Table 5 [178]. Figure 14 summarizes the main factors influencing the reactions in SC biodiesel production.

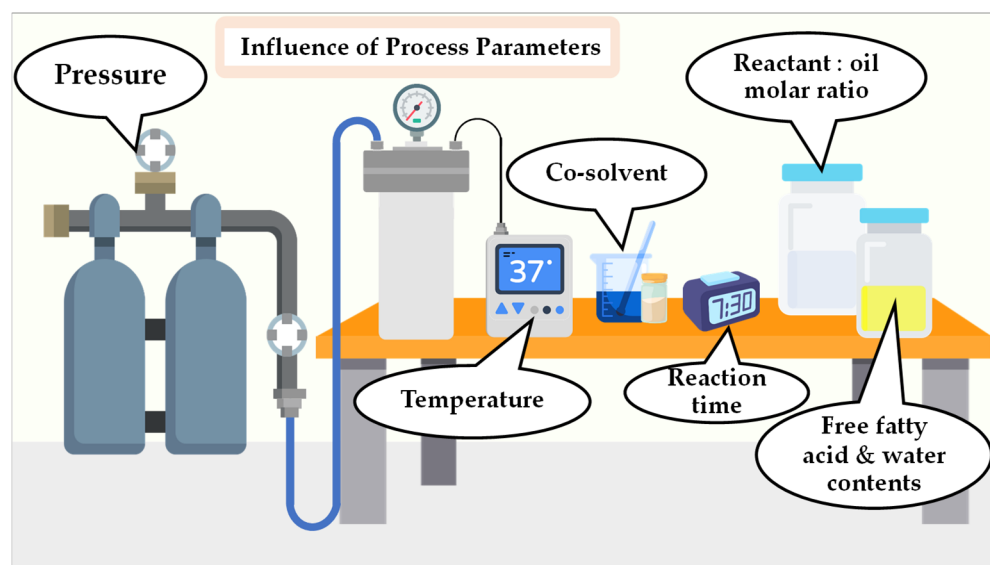


Figure 14. Influence of process parameters on SC biodiesel production.

Effect of temperature: An increase in temperature speeds up the reaction rate, enhances the yields of FAMEs and FAEEs and generally reduces reaction time by improving mass transfer [178,198,202]. However, excessively high temperatures can also cause the thermal decomposition of esters into low-molecular-weight compounds like hydrocarbons [204,205].

Ngamprasertsith et al. [200] found that temperatures above 300 °C degrade unsaturated fatty acids (UFAs) of palm oil, thus reducing the ester content. Due to higher UFA levels, used palm oil has lower reactivity than refined palm oil. In addition, batch reactors exhibited noticeable thermal degradation due to prolonged contact with hot reactor walls. In contrast, continuous reactors needed higher temperatures for optimal yield due to flow dynamics, mixing efficiency and heat transfer [189,206].

Effect of pressure: A higher pressure level improves density and solubility, increasing the reaction rate between reactants [204,207,208]. Previous research showed that pressure improves the yield up to a specific limit, beyond which its effect either became adverse or had no impact on yield [181,204].

Reactant/oil molar ratio: A higher reactant/oil molar ratio enhances conversion by shifting the reaction towards the targeted products. However, excess alcohol can also decrease the reaction mixture's density and temperature, reducing biodiesel yield [200,204]. Furthermore, high alcohol contents may decrease process effectiveness due to the significant energy required for preheating and recovering the alcohol [209]. Therefore, some studies suggest that it is better to use higher temperatures to complete the conversion rather than high molar ratios [183,205].

Reaction time: As reaction time increases, the yield of fatty acid alkyl esters rises until it reaches a maximum, after which the production rate remains constant [174]. Prolonged reaction times can lead to decreased biodiesel yields due to its incipient decomposition [178,204].

Free fatty acid and water content: The presence of water slightly boosts the biodiesel yield by facilitating triglyceride hydrolysis. In contrast, it was found that the content of free fatty acids either had no substantial impact [210] or increased ester yield owing to their esterification by alcohols, raising the fatty acid alkyl ester production [174,205].

Addition of co-solvent or heterogeneous catalysts: Co-solvents such as acetone, tetrahydrofuran (THF) and *iso*-propanol have been reported to improve the homogeneity of the reaction

mixture, thereby increasing the transesterification reaction rate [211]. Akkarawatkhoosith et al. [211] found that a higher 80.0% fatty acid ester was achieved with the 20 wt% addition co-solvent under 350 °C, alcohol-to-oil molar ratio of 23:1 and 3.5 min. In comparison, 65.6% of ester was obtained with an absent co-solvent. Additionally, using SC-CO₂ as a co-solvent can reduce the high pressure, temperature and alcohol-to-oil ratio requirements [212]. Han et al. obtained a FAME yield of 98.0% under mild conditions of 280 °C, 14.3 MPa a methanol-to-oil molar ratio of 24:1, 10 min and a CO₂-to-methanol ratio of 0.1 [212].

Furthermore, adding heterogeneous catalysts, such as ZnO, CaO, MnO₂, CuO, Al₂O₃ and MgO, boosts efficiency, allowing for milder reaction conditions and increasing economic viability and environmental sustainability [213].

5.4. Challenges and Limitations of Biodiesel Supercritical Syntheses

First, because unsaturated fatty acids can degrade at high temperatures, achieving the 96.5% biodiesel yield mandated, for example, by the EN14214 standard proves challenging [200]. However, such minimum yield is not specified in the standards of several countries, such as Brazil and India, where biodiesel containing less than 96.5% ester can be blended with petrodiesel fuel for automobile uses [214]. Process modifications, such as adding co-solvents [211] and implementing two-step protocols [215] could be applied to increase the FAEE content. In addition, further studies involving genetic modifications of non-edible and waste feedstocks may generate cheaper and readily available feedstocks to enhance biodiesel yield [186].

Next, the high temperatures and pressures required by the process raise costs due to the need for high-grade reactor materials. On another hand, using a high alcohol-to-oil molar ratio can lead to excessive energy consumption and environmental loads [174,209]. Choosing a suitable solvent for the process is also essential.

Although methanol exhibits the highest activity, it is toxic and its tendency to absorb water increases the risks of corroding reactor equipment. Bioethanol is an alternative reagent owing to its renewable nature and ecologically beneficial properties, thereby addressing environmental concerns [207].

Until now, the production of SC biodiesel has not been implemented at neither industrial nor pilot scale. However, substantial work has been carried out on the techno-economic feasibility of the SC biodiesel route, using feedstocks such as jatropha, palm and waste cooking oil, and with plant capacities ranging from 10,000 to 40,000 tons per year. This work is summarized in Table 6 [216–220]. However, the choice of feedstocks significantly impacts production costs. It was reported that feedstock prices represent more than 50% of it, methanol price being also an important factor [218]. Several scenarios demonstrate promising economic viability, with positive net present values and acceptable payback durations.

Overall, the findings indicate that biodiesel production under SC conditions is technologically and economically viable: it offers lower production costs than conventional methods, notably because it produces premium biodiesel and glycerol and eliminates any additional post-processing. In addition, this would bring progress in terms of the environment.

However, a recent evolution in the political context of the biodiesel sector affects these positive economic prospects: many countries have recently limited the fraction of vegetable oil production eligible for biodiesel production due to the food-versus-fuel competition debate, so that producers of vegetable oils are less tempted to face significant investments in new installations.

Future work should prioritize further economic analysis of various raw materials, process optimization, long-term feasibility studies and life cycle assessments, in order to further justify both profitability and environmental sustainability.

Table 6. Economic analyses of SC biodiesel production from various oil feedstocks (figures are in USD millions).

Item	Yusuf and Kamarudin [216]	Martinovic et al. [217]	Sakdasri et al. [218]	Gutiérrez and de Santa-Ana [219]	Tipsri and Lersbamrungsuk [220]
Plant capacity (tons/y)	40,000	15,000	30,000	40,000	10,000
Feedstocks	<i>Jatropha</i>	Waste cooking oil	Palm oil	Waste cooking oil	NS
Equipment cost	1.25	2.60	2.92	0.93	0.85
Fixed capital cost	7.52	5.39	6.86	6.26	NS
Working capital	1.13	1.02	1.90	0.94	NS
Total capital investment	9.41	6.42	8.76	7.19	2.65
Raw material cost (yr ⁻¹)	15.25	US\$ 6.70/ton	US\$ 6.70/ton	24.85	NS
Direct manufacturing cost (yr ⁻¹)	24.25	US\$ 815.96/ton	US\$ 769.84/ton	31.30	NS
Indirect manufacturing cost (yr ⁻¹)	1.76	NS	NS	NS	NS
Total fixed costs (yr ⁻¹)	NS	US\$ 82.36/ton	US\$ 49.42/ton	1.01	0.32
Total operating cost (yr ⁻¹)	46.43	NS	NS	NS	4.41/year
Total general manufacturing expenses costs (yr ⁻¹)	NS	US\$ 12.08/ton	US\$ 6.59/ton	4.97	NS
Total production cost (yr ⁻¹)	31.20	US\$ 936.76/ton	US\$ 851.10/ton	37.28	NS
Unit production cost (kg ⁻¹)	0.78 US\$	US\$ 863.19/ton	US\$ 777.53/ton	NS	NS
Break-even prices	NS	NS	NS	US\$ 840.68/ton	US\$ 0.53/Kg
Internal rate of return (%)	NS	NS	NS	31.61% (20 yrs.)	NS
Net annual profit	NS	NS	NS	9.57	NS
Payback period (y)	NS	NS	NS	2.39	NS
Net Present Value (20 y)	NS	NS	NS	45.48	NS

NS = Not specified.

5.5. Biodiesel as a Green, Efficient Gas Turbine Fuel

Gas turbines are turbomachines which convert the chemical energy contained in fuels, such as natural gas or petroleum distillates, into mechanical energy, which is either used for propulsion in jet engines or converted into electricity in land-based gas turbines coupled to electric generators. They can operate on most gaseous and liquid fuels, which makes them highly flexible prime-movers for electric power production [221]. However, burning fossil fuels results in a high carbon footprint of the thermal electric sector [222].

Many studies and field tests show that biodiesel is a possible alternative fuel for gas turbines and can contribute to energy decarbonization [221,223,224]. We performed a Scopus database search from 2014 to 2024 using the keywords “gas turbine” and “biodiesel” and found 157 research publications related to this area, compared to 134 for the 2003–2013 period, which demonstrates a growing interest for alternative primary bioenergies to reduce fossil fuel reliance.

A General Electric team studied the combustion and the emissions of biodiesel produced from rapeseed oil in a Frame 6B (40 MWe) power generation gas turbine [224]. They found that the combustion of biodiesel is very clean, resulting in extremely low emissions of carbon monoxide, unburned hydrocarbons, polycyclic aromatic hydrocarbons and aldehydes. This is mainly due to the linearity of the carbon chains of FAMES, which can be easily oxidized by oxygen, resulting in complete combustion, alongside their good

biodegradability in the environment. Sulfur oxide (SO_x) emissions were found to be very low (<1 ppm). Regarding nitrogen oxide (NO_x) emissions, due to (i) its oxygen content which results in lower adiabatic stoichiometric combustion temperature (“ $T_{ad,st}$ ”) and (ii) the absence of FBN (Fuel-Bound Nitrogen), biodiesel was found to emit less NO_x than diesel oils. This result was then confirmed by computations of the $T_{ad,st}$ data made on many classes of bio- and petrodiesel fuels, which showed systematically lower NO_x values for biodiesels [225]. In contrast, Altaher et al. [226] found that NO_x emissions increased with increasing biodiesel concentration and attributed it to biodiesel’s higher oxygen content and modified delay times in the atomization process. The NO_x levels emitted by biodiesel depend mainly on the $T_{ad,st}$ data which increase with machine load, the fuel-to-air ratio and, to a lesser extent, on the composition of the biodiesel, i.e., the vegetable oils.

When comparing the performance of biodiesel to Jet A aviation fuel in aero-gas turbines, the findings revealed that gas turbines operate similarly with both [223]. Biodiesel has superior lubricating properties compared to other fuel types, improving the operation of mechanical fuel components. On another hand, the cetane number and flash point of biodiesel are higher, thereby improving general safety against fire and explosions in all applications [227].

However, some significant challenges must be addressed in aviation applications, including performance at low-temperature, slightly lower energy content and material compatibility. Combining biodiesel with petroleum-based fuel and selecting biodiesel feedstocks that produce fuels with higher heating values can solve these issues. Utilizing compatible seals like Viton or Teflon and using elastomers with higher acrylonitrile content can solve the swelling problem caused by biodiesel in fuel circuits [213]. Additionally, the risk of a slow phase separation between biodiesel and diesel oil and the higher susceptibility of biodiesel to bacterial degradation are factors to consider during storage [224].

6. Applications in Electric Power Generation

Not surprisingly, H₂O and CO₂ are also the two SCFs that can be used as working fluids to generate thermal power, that is, to convert heat into electricity within condensation (Rankine) or non-condensation (Brayton) cycles. This is because the circuits of power cycles always experience leaks and both fluids are not only widely available but also have zero impact (H₂O) and relatively benign impact (CO₂) on the environment.

6.1. Supercritical Steam Cycles

All power cycles using H₂O as a fluid are of the Rankine type, i.e., they include a vaporization stage (production of steam by heating in a boiler) and a condensation stage (by cooling in a condenser) [228]. They are traditionally called “steam cycles” [229].

H₂O has its critical point (CP) at 374 °C—221 bar.

Figure 15a represents the temperature–entropy (T-S) diagrams of two steam Rankine cycles: (1) a subcritical (“sbc”) cycle, drawn in green color and (2) a supercritical (“SC”) one, drawn in red, in which the superheated steam (leaving the boiler furnace) is above 221 bar and generally above 540 °C.

Figure 15b highlights, in purple, the critical H₂O isobar (221 bar), which separates the sbc zone (located to its right and drawn in green) from the SC zone (to its left and in pink). In fact, the SC-H₂O cycles should be called “transcritical” rather than supercritical, since the portion STUPQ of their contour is below the critical isobar.

In both the SC and sbc cycles, the hottest point is the “superheat” peak: points E and R, respectively. After a first expansion in the High-Pressure (HP) steam turbine (lines EF and RS), the steam goes back to the boiler where it is “reheated” (lines FG and ST); it is then re-expanded in the Medium-Pressure (MP) turbine and finally in the Low-Pressure (LP) turbine (lines GH and TU) to recover maximum power. Steam is then condensed (lines HA and UP) and re-pumped into the boiler (small segments AB and PQ).

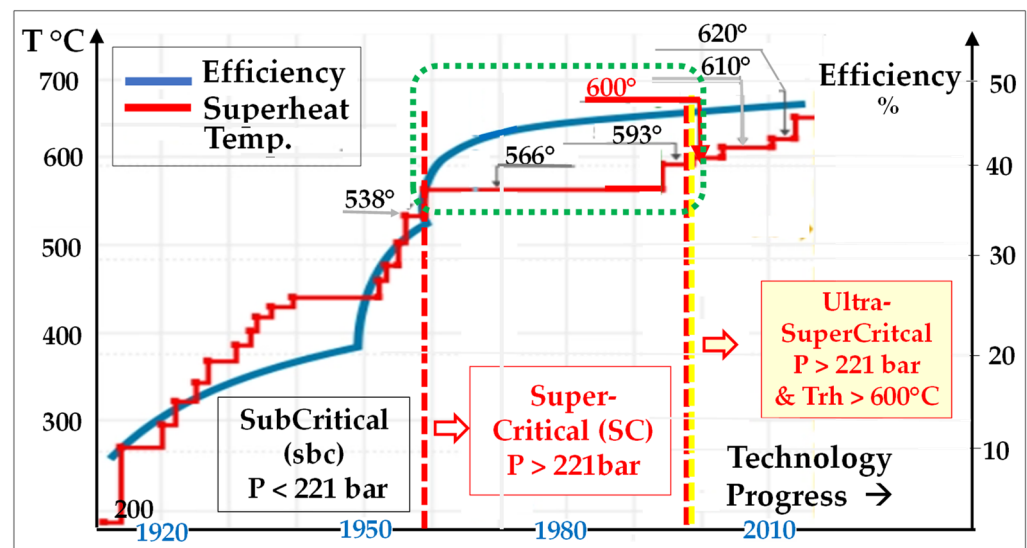


Figure 16. Evolution of superheat temperature and efficiency of steam cycle; according to [230].

For example, the Block No 8 of the Rheinhafen–Dampfkraftwerk (Karlsruhe, Germany), commissioned in 2013, is a USC cycle of 912 MWe that has a baseline efficiency greater than 46% and can reach 47.5%; the steam has a superheat temperature of 600–620 °C at the inlet of the HP turbine which must have, therefore, a rotor made in highly-alloyed austenitic steel (25% chromium) [231].

Concerning the most advanced prospects, steam pressures and temperatures of up to 415 bars and 700 °C are considered, which would yield an efficiency level of up to 50%. However, such advanced steam cycles would require major changes in the structural alloys, especially those of the superheater heat exchangers, resulting in high CAPEX in addition to long and costly programs of development and qualification [232].

6.2. Supercritical CO₂ Cycles

As an important preliminary remark and as already mentioned (Section 3.2.2), the density of the working fluid plays a key role in power generation cycles. This effect explains the superiority of SC Brayton cycles since SCFs are much denser than the gases or vapors used in classical sbc Rankine and Brayton cycles. This technology offers other important advantages [233], including the reduction in the dimensions of mechanical components, particularly those of turbomachines, which provide a substantial economic benefit.

We will illustrate these effects in the case of a Concentrated Solar Power (CSP) plant [PF].

6.2.1. The High Efficiency Potential of SC-CO₂ Cycles in Solar Energy Conversion

Today CSP plants are driven by conventional sbc steam cycles [234]. A typical example is shown schematically in Figure 17a [235].

Solar energy is reflected and concentrated by a field of heliostats towards a receiving tower which constitutes the heat source. The heat is extracted by a flow of molten salt stored in a hot tank; it feeds a steam generator, which, in turn, powers a Rankine cycle and is then collected in a “cold” tank from where it returns to the receiving tower.

Figure 17b displays a possible transposition of this installation into a SC-CO₂ Brayton cycle which was previously schematized (diagram of Figure 3) and in which the steam generator is replaced by a heat exchanger between the molten salt and CO₂ [236]. This particular powertrain configuration comprises a compressor, a turbine and a heat recuperator; the latter recovers the heat that is still contained in the CO₂ leaving the turbine. This unit has no condenser because it is entirely supercritical and therefore without any condensation stage, like in all Brayton cycles.

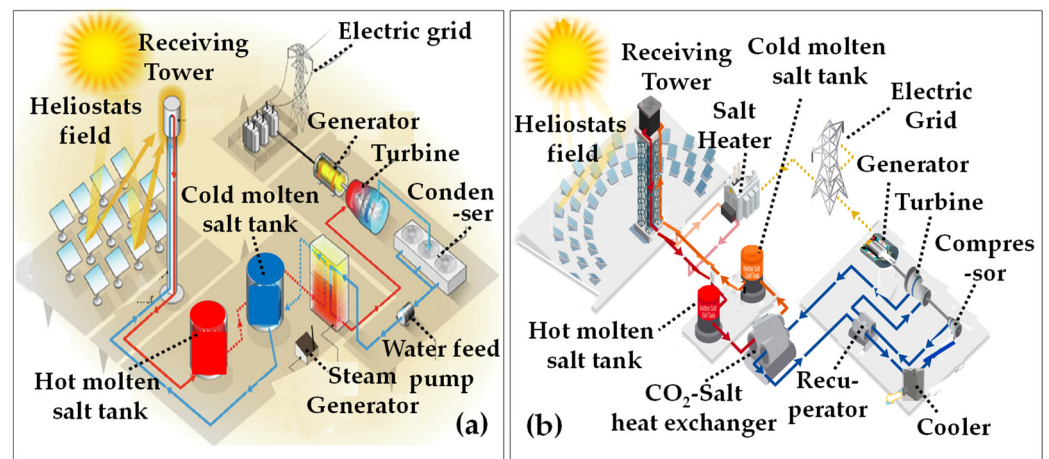


Figure 17. Sketches of CSP power units based on (a) a sbc steam Rankine cycle, according to [235]; (b) a SC-CO₂ Brayton cycle, according to [236].

Using ProSimPlus[®], we have compared the electric performances of the two configurations, in which (i) the sbc Rankine steam cycle featured both a superheating (176 bar—552 °C) stage and a reheating (46 bar—551 °C) stage and (ii) the SC-CO₂ cycle had double heat recuperation and recompression stages [233]. In both cases, the molten salt entered the receiving tower at 565 °C and transferred 270 MWth to the working fluid (steam and CO₂ respectively).

We assumed zero irreversibility losses, which led to optimistic energy performances but provided a common basis for comparing the two configurations. Our calculations showed the superiority of the SC-CO₂ option [237]; indeed, compared with the steam cycle, the SC-CO₂ produces 9.2% more power (129 versus 119 MWe) and boasts four additional points of efficiency (48.1% versus 44.1%), which represents a real breakthrough.

It should be noted, however, that, unlike SC-CO₂ cycles, Rankine cycles are a very mature technology.

6.2.2. Overall Benefits Inherent to SC-CO₂ Power Cycles

A. Free choice of the heat sink

Since Brayton SC-CO₂ cycles have no condensation stage (Figure 3), the heat sink can have a temperature above the T_c of CO₂ (31.1 °C). In the context of climate change, this is an advantage over steam cycles which requires a heat sink (a river or, better, a sea) below the condensation temperature of the steam. Incidentally, this explains why new nuclear plants, based on steam cycles, are now preferably installed by the sea, to avoid the “thermal pollution” of rivers. SC-CO₂ Brayton cycles are free of this constraint.

B. Reduction in the size of turbomachines

In a previous article, we also showed how the high density of SC-CO₂ makes most powertrain components smaller in size than corresponding ones in steam cycles [20]. Indeed, for aerodynamic reasons, the cross-sectional areas of a turbomachine must be dimensioned inversely proportional to the density of the working fluid passing through it. Consequently, SC-CO₂ machines exhibit reduced diameters. This point is qualitatively illustrated by Figure 18a [238]. In addition, the pressure ratios of SC-CO₂ cycles are much lower than those of steam cycles, which also reduces the number of stages and consequently machine lengths (Figure 18b) [239].

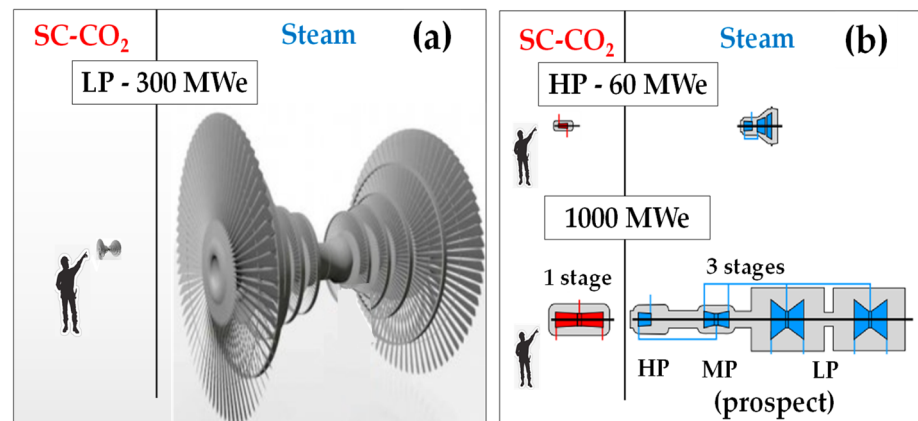


Figure 18. Comparisons between the sizes of a steam and a SC-CO₂ turbine: (a) reduction in diameter; (b) reduction in shaft length (after [238] and [239] respectively).

Overall, the machines are smaller, reducing the footprint of the overall powertrain and minimizing capital expenditure.

C. Towards zero CO₂ emission power plants: Allam cycles

Recently introduced SC-CO₂ cycle concepts offer the prospect of decarbonizing the electricity sector. In these designs, heat is supplied to the SC-CO₂ cycle by burning natural gas not with air but with pure oxygen, a process known as “oxy-combustion” [26,27,240]. Therefore, the combustion step introduces only H₂O and some additional CO₂ (but no N₂) into the cycle. Since the working fluid must remain pure CO₂, H₂O is first removed from the cycle and then the additional CO₂ is extracted in supercritical conditions, allowing it to be directly sequestered.

The most advanced concept is represented by the Allam cycle, a diagram of which is shown in Figure 19 [26,27].

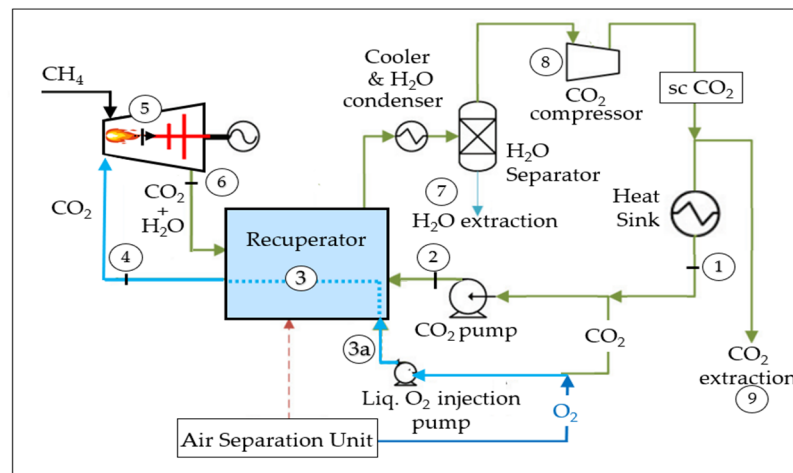


Figure 19. Simplified sketch of the Allam cycle; after [26]. For meaning of circled numbers, see text.

Natural gas, which can be assimilated to pure methane, is introduced into the combustion chamber of the turbine (mark 5) and burned with pure O₂ that has been previously admixed into the SC-CO₂ circuit (mark 3a). This “oxycombustion” process generates water and additional carbon dioxide, in the absence of nitrogen, through the very simple reaction: $\text{CH}_4 + 2 \text{O}_2 \rightarrow \text{CO}_2 + 2 \text{H}_2\text{O}$.

Expansion in the turbine generates electrical power. Then: (i) the resulting supercritical stream (6) passes through a special heat recuperator (3), (ii) water is condensed and removed from the cycle (7), (iii) the SC-CO₂ stream is then expanded (8) and (iv) the excess CO₂

produced by combustion is extracted (9). The remaining SC-CO₂ stream is cooled at the heat sink (1), goes through the compressor (which, for SCFs, is similar to a pump: (2)) and through the recuperator (3) before being reinjected into the turbine (4).

In addition to the possibility to capture CO₂, this process is likely to yield high power generation efficiencies; it would also give the possibility to recover the combustion water for any other use.

All these qualities perfectly match the portrait of the power plant of the future: *high efficiency* (low fuel consumption); *CCS-readiness* and virtuous *recovery of zero-cost water*.

Several power plants of this type have been commissioned but the version involving continuous CO₂ capture is still in development [241,242].

6.3. General Status of SC Power Technologies

The common advantage of SC power cycles lies in their superior efficiencies, which allow a reduction in the carbon footprint of the electricity sector.

- A. Concerning SC-H₂O cycles (i.e., SC steam cycles), there are currently about 400 power plants which operate based on this type of cycle [243].
- B. Concerning SC-CO₂ Brayton cycles, an additional benefit lies in the reduction in size of mechanical equipment: by decreasing the cost of power plants, this makes it possible to accelerate electrification around the world, knowing that more than 760 million people are still without access to electricity [244].

However, for the efficiency of SC-CO₂ cycles to exceed that of steam Rankine cycles, significant R&D work must still be carried out on turbomachines (compressors and turbines), whose isentropic efficiencies strongly condition the efficiency of SC Brayton cycles. Suitable structural material should also be used to cope with the high temperature and important mechanical stresses undergone by turbine rotors [233,237].

- C. Allam SC-CO₂ cycles could take a big step towards carbon-free electricity. As mentioned above, several power plants of this type have been commissioned but without continuous CO₂ capture.

Overall, the benefits of SC power cycles justify the hopes placed in this technology to significantly reduce the carbon footprint and allow for more effective use of fuels in the electrical sector.

7. Foreseeable Trends and Prospects

When trying to anticipate trends and possible prospects, it is useful to distinguish the short term from the middle/long term.

7.1. Short Term

The analyses presented in Sections 4–6 can inspire short-term activities, for example:

- A. Carry out comparative studies between the available techniques, as well as economic analyses;
- B. Study/implement strategies to approach the zero-waste concept;
- C. Develop sequential SC extractions and combine them with other techniques such as mechanical and subcritical water extraction;
- D. Focus on TEAs (techno-economic analyses) and LCAs (life-cycle assessments) to determine both profitability and environmental compliance when envisaging industrial applications;
- E. Regarding supercritical power technology, development efforts should focus on maximizing the efficiency and reliability of compressors and turbines and qualifying appropriate structural materials: these tasks are classic, but not necessarily easy.

7.2. Middle-Long Term

When it comes to middle-long term trends and prospects, many possible industrial developments and research directions are likely to gain momentum. However, general

experience with the emergence of new technologies teaches us that industrial applications often occur quite late after the corresponding discoveries. Indeed, the inventiveness of researchers generally goes faster than the pace of industrial development: for example, as noted in Section 2, pioneering work on SC-CO₂ power technology dates back to the 1960s, but real R&D only began in the 2000s. Additionally, as long as they are profitable, old technologies often resist changes because new ones require upfront investments that delay the decision for such changes.

For these reasons, it will not be surprising to find references to somewhat dated research below.

7.2.1. Recovery of High-Value Biomolecules

The following directions seem worth exploring:

- A. Identify new raw materials that are potential sources of already known molecules of interest. A possible option is the extraction of valued substances from “fatal” process wastes [245,246]. A possible example is tree bark which represents a massive, mostly unexploited forestry waste that contains substantial amounts of tannins, terpenoids and polyphenols (namely resveratrol and astringine) as secondary tree metabolites [247].
- B. Alternatively, search for other interesting molecules likely to create new market opportunities, particularly in the fields of fast-developing markets, which includes cosmetics, nutraceuticals and pharmaceutical products. This requires, however, long-term collaborative research with the corresponding industry branches.

Other possible applications exist, an example being the production of bio-sourced Liquid Organic Hydrogen Carriers (LOHC) [248].

7.2.2. Alternative Sterilization Processes

The increasing complexity of biomedical equipment in terms of geometry and fragility (e.g., biological tissues, technical textiles) lead to substitute “gentle” but efficient sterilization alternatives for classical, often harsh treatments (ethylene oxide, dry or autoclave heating, radioactive exposure). SC-CO₂ sterilization under low temperatures and pressures is an open option [249,250].

7.2.3. Cleaning of High-Value Products

As future electronic devices will probably have nanoscale dimensions, the high interfacial tension of liquid water will prevent its use as a cleaning agent. This is a field where SCFs can become instrumental [76,251].

7.2.4. Fabrication of Nano Electronic Components

Due again to their nano dimensions, future semiconductor devices will require new methods for patterning them and for depositing functional layers featuring complex morphologies. Here also, SCFs can be an option for syntheses and further processing [252,253]. This also includes the fabrication of supercapacitors, which requires complex coating and deposition steps [96,254]. The SAS (Supercritical Anti-Solvent) technique, already described in Particle Shaping Section, consists of precipitating a targeted substance from a solution using SC-CO₂. It is a promising technique which enables preparing not only micrometric superconducting particles but also pharmaceutical products, dyes, explosives, polymers and biopolymers [255–257].

7.2.5. Recovery of High-Value Metals from Spent Catalysts and WEEE

The ores of precious metals are overexploited and become short to meet the increasing global demand, e.g., for automobile depollution systems. Likewise, the demand for rare earths from the electronic industry is increasing exponentially. In this context, their recovery from end-of-life products, e.g., from spent catalysts and WEEE (*Waste from Electrical and Electronic Equipment*) becomes a serious alternative [258]. Recovery via pyrolysis is a harsh,

polluting process. The use of SC-CO₂ along with CO₂-soluble copolymers grafted with complexing groups, allow to extract palladium from spent catalysts [259]. An oxidative, two-stage process using SCW in the presence of oxygen was developed by Johnson-Matthey to remove carbonaceous compounds and then recover precious metals, as oxides, from spent catalysts [260].

7.2.6. Possible Advances in the Energy Sector

In the field of energy, SCFs can be involved in the reprocessing of spent nuclear fuels. For example, a novel, SC-CO₂-based process (called Super-DIREX, for “Supercritical Fluid Direct Extraction”) had been studied in Japan to potentially replace the traditional PUREX process (for “Plutonium, Uranium, Reduction, Extraction”) that uses extraction cascades of U and Pu by solutions of tributylphosphate (TBP) in dodecane. This new process involves mixtures of SC-CO₂ with specific complexing agents at 40–60 °C and 100–200 bar [261].

Another catalyzed SCW-based process could also be developed to dispose of low-activity nuclear wastes [262].

Finally, an interesting source of novelty would lie in using SCFs to directly convert biomass energy into heat and then into electricity within CCS-ready concepts.

8. Conclusions

This jointly authored article aimed to offer a global vision of the broad spectrum of processes based on supercritical fluids, highlighting some large commonalities between them, taking stock of current achievements and attempting to anticipate future developments.

To introduce the subject, we started with a brief history of SCFs to show their emergence as process fluids and the gradual expansion of their application portfolio for which we presented a preliminary list and classification. This high-level list revealed a very broad range of applications that crosses multiple sectors of the global economy.

From a theoretical point of view, the challenge of bringing together, in this article, applications pertaining to sectors as distinct as food, chemistry and electrical power has proven to be fruitful since, in all these areas, the distinctive performances achieved by these processes are due to common physical behaviors of SCFs and can be explained by similar physicochemical properties.

From an industrial standpoint, the review of SCF processes already implemented or under development in the agri-food and biomass conversion sectors led to two important statements. First, a considerable number of industrial facilities are already operational, the oldest dating back to 1986 and the latest one being a large hops extraction plant commissioned in 2017; moreover, the currently accessible list of industrial plants is limited to the EU. Second, there is a growing R&D activity around the world in the branches of nutraceuticals, pharmaceuticals and new food products, most of them focusing on new specialties or new approaches to producing existing specialties. The challenges in pursuing industrialization projects are in terms of CAPEX for the acquisition of high-pressure equipment, operating costs for fluid compression and scalability to industrial standards. This is why a current trend is to carry out technical-economic analyses (TEA) and life cycle analyses (LCA) to test the viability of projects upstream.

Examination of electrical applications reveals a growing fleet of supercritical power plants which use supercritical water (called “supercritical steam” in this branch of activity). They gradually supplant conventional subcritical steam power plants. It also shows promising prospects for applications of supercritical CO₂ cycles despite serious challenges related to the disruptive characteristics of this technology.

These reviews were supplemented by original results developed in our laboratories which confirm the observed trends.

A major driver for future developments of SCF processes lies in their distinctive, pressure-tunable solvation properties, which represent a unique tool enabling the development of greener processes capable of reducing the use of chemical solvents. Concerning the electricity production sector, the strong assets of SCF technologies are (i) their uncommon

capacity to reduce the carbon footprint of this sector and (ii) the potential to enable faster electrification thanks to substantial reductions in installation costs.

Finally, we tried to provide a perspective of future extensions of this process portfolio by widening the scope of applications as much as possible. Here again, the prospects are numerous and brilliant for exploiting the useful singularities of SCF properties that we endeavored to highlight in this article.

Author Contributions: Conceptualization, S.N. and M.M.; methodology, R.P., M.M., J.-N.J. and S.N.; software (at LRGP), R.P.; validation, J.-N.J.; formal analysis, M.M. and S.N.; investigation, M.M. and S.N.; resources, M.M. and S.N.; data curation, R.P., J.-N.J. and S.N.; writing—original draft preparation, M.M., R.S., M.K. and M.C.; writing—review and editing, J.-N.J., R.P. and S.N.; visualization, M.M. and S.N.; supervision, R.P., J.-N.J. and S.N.; project administration, R.P. and J.-N.J.; funding acquisition, S.N. (no funding on LRGP activities). All authors have read and agreed to the published version of the manuscript.

Funding: The research conducted at LRGP received no external funding. The research at Chulalongkorn University is supported by Ratchadapisek Somphot Fund for Postdoctoral Fellowship, Chulalongkorn University.

Data Availability Statement: Data supporting reported results can be obtained from authors through an email request addressed to the corresponding authors.

Conflicts of Interest: The authors declare no conflicts of interest.

Appendix A. Mass and Heat Transfer Properties of H₂O

The characteristics highlighted in Section 3, concerning the specific properties of SC-CO₂, apply to all other SCFs and in particular to SC-H₂O which has its critical point at 374 °C, 220.6 bar. Figure A1 that shows the iso-density lines, confirms the general shape observed for CO₂ (Figure 2) with a monotonic increase in density with pressure at constant temperature.

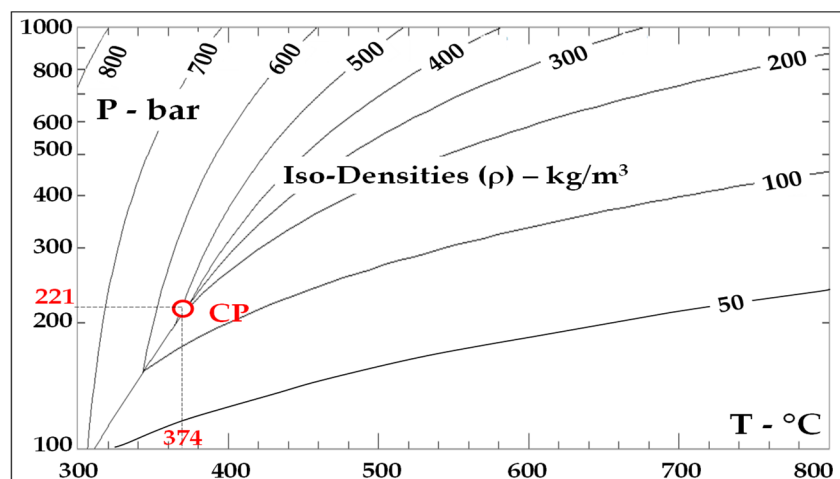


Figure A1. Iso-density lines of H₂O [73].

The chart of dynamic viscosity (Figure A2) shows that, like for CO₂ (Figure 9a): (i) there is, at constant pressure, a strong decrease in viscosity above T_c and (ii) at constant temperature, an increase with pressure [73]. Finally, Figure A3 shows the very high values (above 100 mW·m⁻¹·K⁻¹) of the thermal conductivity of SC-H₂O. As in the case of SC-CO₂, it increases with pressure and marks a steep jump at the critical point but, here too, it is a very local peak which practically does not influence overall heat exchanges. At 400 °C, 300 bar, it is 10 times greater than that of liquid water at 80 °C, 1 atm.

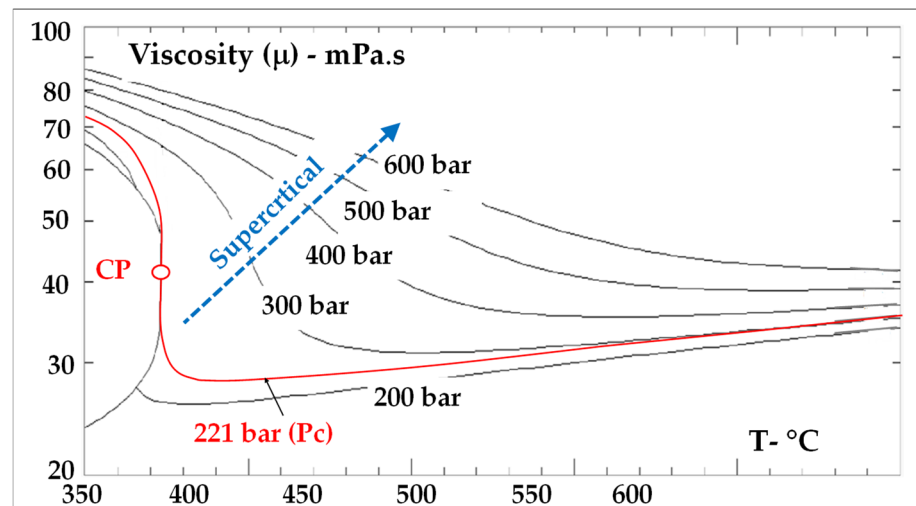


Figure A2. Viscosity chart of water [73].

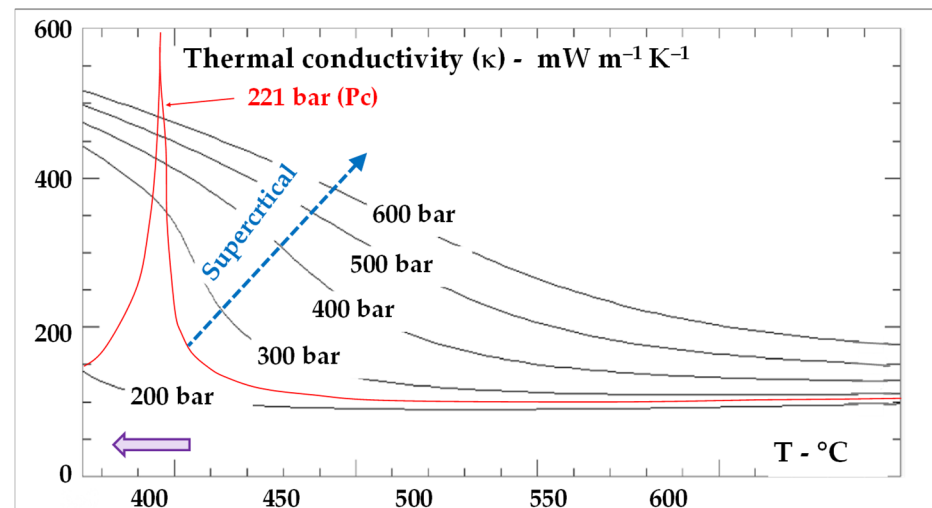


Figure A3. Thermal conductivity [73].

References

1. Su, W.; Zhang, H.; Xing, Y.; Li, X.; Wang, J.; Cai, C.A. Bibliometric analysis and review of supercritical fluids for the synthesis of nanomaterials. *Nanomaterials* **2021**, *11*, 336. [[CrossRef](#)] [[PubMed](#)]
2. Mara, E.M.; Braga, M.E.; Gaspar, M.C.; de Sousa, H.C. Supercritical fluid technology for agrifood materials processing. *Curr. Opin. Food Sci.* **2023**, *50*, 100983.
3. Guo, Y.; Wang, S.Z.; Xu, D.H.; Gong, Y.M.; Ma, H.H.; Tang, X.Y. Review of catalytic supercritical water gasification for hydrogen production from biomass. *Renew. Sust. Energ. Rev.* **2010**, *14*, 334–343. [[CrossRef](#)]
4. Tutek, K.; Masek, A.; Kosmalka, A.; Cichosz, S. Application of fluids in supercritical conditions in the polymer industry. *Polymers* **2021**, *13*, 729. [[CrossRef](#)]
5. Pasquali, I.; Bettini, R.; Giordano, F. Supercritical fluid technologies: An innovative approach for manipulating the solid-state of pharmaceuticals. *Adv. Drug Deliv. Rev.* **2008**, *60*, 399–410. [[CrossRef](#)]
6. Zorić, M.; Banožić, M.; Aladić, K.; Vladimir-Knežević, S.; Jokić, S. Supercritical CO₂ extracts in cosmetic industry: Current status and future perspectives. *Sustain. Chem. Pharm.* **2022**, *27*, 100688. [[CrossRef](#)]
7. Salerno, A.; Pascual, C.D. Bio-based polymers, supercritical fluids and tissue engineering. *Process Biochem.* **2015**, *50*, 826–838. [[CrossRef](#)]
8. Weibel, G.L.; Ober, C.K. An overview of supercritical CO₂ applications in 2 microelectronics processing. *Microelectron. Eng.* **2003**, *65*, 145–152. [[CrossRef](#)]
9. Li, K.; Xu, Z. A review of current progress of supercritical fluid technologies for e-waste treatment. *J. Clean. Prod.* **2019**, *227*, 794–809. [[CrossRef](#)]
10. Zhu, Q. Innovative power generation systems using supercritical CO₂ cycles. *Clean Energy* **2017**, *1*, 68–79. [[CrossRef](#)]

11. Berche, B.; Henkel, M.; Kenna, R. Critical Phenomena: 150 Years Since Cagniard de la Tour. Available online: <https://arxiv.org/pdf/0905.1886> (accessed on 27 July 2024).
12. Jessop, P.G.; Leitner, W. Supercritical fluids as media for chemical reactions. In *Chemical Synthesis Using Supercritical Fluids*; Wiley: New York, NY, USA, 1999; pp. 1–36.
13. Nicholas, C.P. Dehydration, dienes, high octane, and high pressures: Contributions from Vladimir Nikolaevich Ipatieff, a Father of catalysis. *ACS Catal.* **2018**, *8*, 8531–8539. [[CrossRef](#)]
14. Klesper, K.; Corwin, A.H.; Turner, D.A. High pressure gas chromatography above critical temperatures. *J. Org. Chem.* **1962**, *27*, 700–701.
15. Si-Hung, L.; Bamba, T. Current state and future perspectives of supercritical fluid chromatography. *TrAC Trends Anal. Chem.* **2022**, *149*, 116550. [[CrossRef](#)]
16. Zosel, K. Process for the Separation of Mixtures of Substances. U.S. Patent 3,969,196, 13 July 1976.
17. Zosel, K. Process for the Decaffeination of Coffee. U.S. Patent 4,260,639 45, 7 April 1981.
18. Angelino, G. Perspectives for the liquid phase compression gas turbine. *J. Eng. Power* **1967**, *89*, 229–236. [[CrossRef](#)]
19. Angelino, G. Carbon dioxide condensation cycles for power production. *J. Eng. Power* **1968**, *90*, 287–295. [[CrossRef](#)]
20. Angelino, G. Real gas effects carbon dioxide cycles. In Proceedings of the ASME 1969 Gas Turbine Conference and Products Show, Cleveland, OH, USA, 9–13 March 1969. paper No 69GT.103.
21. Feher, E.G. The supercritical thermodynamic power cycle. *Energy Convers.* **1968**, *8*, 85–90. [[CrossRef](#)]
22. Hoffmann, J.R.; Feher, E.G. 150 kWe Supercritical Closed Cycle System. *J. Eng. Power* **1971**, *93*, 70–80. [[CrossRef](#)]
23. Gokhshtein, D.P.; Verkhivker, G.P. Use of carbon dioxide as a heat carrier and working substance in atomic power stations. *Sov. At. Energy* **1969**, *26*, 430–432. [[CrossRef](#)]
24. Dostal, V.; Driscoll, M.J.; Hejzlar, P.; Todreas, N.E. A Supercritical CO₂ gas turbine power cycle for next-generation nuclear reactors. In Proceedings of the 10th International Conference on Nuclear Engineering, Arlington, VA, USA, 14–18 April 2002.
25. Salazar-Pereyra, M.; Lugo-Leyte, R.; Bonilla-Blancas, A.E.; Lugo-Méndez, H.D. Thermodynamic analysis of supercritical and subcritical Rankine cycles. In Proceedings of the ASME Turbo Expo 2016, Seoul, Republic of Korea, 13–17 June 2016. article GT2016-57814.
26. Allam, R.; Martin, S.; Forrest, B.; Fetvedt, J.; Lu, X.; Freed, D.; Brown, G.W.; Sasaki, T.; Itoh, M.; Manning, J. Demonstration of the allam cycle: An update on the development status of a high efficiency supercritical carbon dioxide power process employing full carbon capture. *Energy Procedia* **2017**, *114*, 5948–5966. [[CrossRef](#)]
27. Allam, R.J.; Martin, S.; Forrest, B.A.; Fetvedt, J.; Lu, X.; Freed, D.; Nomoto, H.; Itoh, M.; Okita, N.; Jones, C. High efficiency and low cost of electricity generation from fossil fuels while eliminating atmospheric emissions, including carbon dioxide. *Energy Procedia* **2013**, *37*, 1135–1149. [[CrossRef](#)]
28. Colleoni, L.; Sindoni, A.; Ravelli, S. Comprehensive thermodynamic evaluation of the natural gas-fired allam cycle at full load. *Energies* **2023**, *16*, 2597. [[CrossRef](#)]
29. White, M.T.; Bianchi, G.; Chai, L.; Tassou, S.A.; Sayma, A.I. Review of supercritical CO₂ technologies and systems for power generation. *Appl. Therm. Eng.* **2021**, *185*, 116447. [[CrossRef](#)]
30. Molière, M.; Geiger, F.; Privat, R.; Jaubert, J.N. Emerging Thermodynamic Cycles and Thermal Power Generation. In Proceedings of the ECOS 2022—The 35th International Conference on Efficiency, Cost, Optimization, Simulation and Environmental Impact of Energy Systems, Copenhagen, Denmark, 3–7 July 2022. Available online: https://www.researchgate.net/publication/382625003_Emerging_Thermodynamic_Cycles_and_Thermal_Power_Generation#fullTextFileContent (accessed on 11 August 2024).
31. Bunyakiat, K.; Makmee, S.; Sawangkeaw, R.; Ngamprasertsith, S. Continuous production of biodiesel via transesterification from vegetable oils in supercritical methanol. *Energy Fuels* **2006**, *20*, 812–817. [[CrossRef](#)]
32. Sakdasri, W.; Sawangkeaw, R.; Ngamprasertsith, S. An entirely renewable biofuel production from used palm oil with supercritical ethanol and low molar ratio. *Braz. J. Chem. Eng.* **2017**, *34*, 1023–1034. [[CrossRef](#)]
33. Rathore, V.; Madras, G. Synthesis of biodiesel from edible and non-edible oils in supercritical alcohols and enzymatic synthesis in supercritical carbon dioxide. *Fuel* **2007**, *86*, 2650–2659. [[CrossRef](#)]
34. Prado, J.M.; Lachos-Perez, D.; Forster-Carneiro, T.; Rostagno, M.A. Sub- and supercritical water hydrolysis of agricultural and food industry residues for the production of fermentable sugars: A review. *Food Bioprod. Process.* **2016**, *98*, 95–123. [[CrossRef](#)]
35. Kazarian, S.G. Polymer Processing with Supercritical Fluids. *Polym. Sci. Ser. C* **2000**, *42*, 78–101.
36. Sodeifian, G.; Behvand-Usefi, M.M. Solubility, extraction, and nanoparticles production in supercritical carbon dioxide: A mini-review. *ChemBioEng Rev.* **2023**, *10*, 133–166. [[CrossRef](#)]
37. Guo, J.Q.; Li, M.J.; He, Y.L.; Jiang, T.; Ma, T.; Xu, J.L.; Cao, F. A systematic review of supercritical carbon dioxide (S-CO₂) power cycle for energy industries. *Energy Convers. Manag.* **2022**, *258*, 115437. [[CrossRef](#)]
38. Badens, E.; Spilimbergo, S.; Calvo, J. Special issue on sterilization with supercritical carbon dioxide. *J. Supercrit. Fluids* **2022**, *190*, 105716. [[CrossRef](#)]
39. Sutanto, S.; van Roosmalen, M.J.E.; Witkamp, G.J. Mechanical action in CO₂ dry cleaning. *J. Supercrit. Fluids* **2014**, *93*, 138–143. [[CrossRef](#)]
40. Saga, K. Wafer cleaning using supercritical CO₂ in semiconductor and nanoelectronic device fabrication. *Solid State Phenom.* **2007**, *134*, 97–103. [[CrossRef](#)]

41. Brunner, G. Hydrothermal and supercritical water processes. In *Supercritical Fluid Science and Technologies Series*; Kiran, E., Ed.; Elsevier: Amsterdam, The Netherlands, 2014; Volume 5.
42. Reverchon, E.; Adami, R. Nanomaterials and supercritical fluids? *J. Supercrit. Fluids* **2006**, *37*, 1–22. [[CrossRef](#)]
43. Borsboom-Hanson, T.; Holm, T.; Mérida, W. Techno-economics of sub- and supercritical water electrolysis. *Energy Convers. Manag.* **2022**, *265*, 115741. [[CrossRef](#)]
44. Nasyrova, Z.R.; Kayukova, G.P.; Vakhin, A.V.; Djimasbe, R.; Chemodanov, A.E. Heavy oil hydrocarbons and kerogen destruction of carbonate–siliceous domanic shale rock in sub- and supercritical Water. *Processes* **2020**, *8*, 800. [[CrossRef](#)]
45. Thomason, T.B.; Modell, M. Supercritical water destruction of aqueous wastes. *Hazard. Waste* **1984**, *4*, 453–467. [[CrossRef](#)]
46. Yang, V. Modeling of supercritical vaporization, mixing and combustion in liquid-fuels propulsion systems. *Proc. Combust. Inst.* **2000**, *28*, 925–942. [[CrossRef](#)]
47. Sahena, F.; Zaidul, I.S.M.; Jinap, S.; Karim, A.A.; Abbas, K.A.; Norulaini, N.A.N.; Omar, A.K.M. Application of supercritical CO₂ in lipid extraction—A review. *J. Food Eng.* **2009**, *95*, 240–253. [[CrossRef](#)]
48. De Aguiar, A.C.; Vardanega, R.; Viganó, J.; Silva, E.K. Supercritical Carbon Dioxide Technology for Recovering Valuable Phytochemicals from Cannabis sativa L. and Valorization of Its Biomass for Food Applications. *Molecules* **2023**, *28*, 3849. [[CrossRef](#)]
49. Herrero, M.; Cifuentes, A.; Ibanez, E. Sub- and supercritical fluid extraction of functional ingredients from different natural source: Plants, food-byproducts, algae and microalgae: A review. *Food Chem.* **2006**, *98*, 136–148. [[CrossRef](#)]
50. Aydi, A.; Wüst Zibetti, A.; Al-Khazaal, A.Z.; Eladeb, A.; Adberraba, M.; Barth, D. Supercritical CO₂ extraction of extracted oil from *Pistacia lentiscus* L.: Mathematical modeling, economic evaluation and scale-up. *Molecules* **2020**, *25*, 199. [[CrossRef](#)] [[PubMed](#)]
51. Zosel, K. Separation with supercritical gases: Practical applications. *Angew. Chem. Int. Ed.* **1978**, *17*, 702–709. [[CrossRef](#)]
52. Reverchon, E. Supercritical fluid extraction and fractionation of essential oils and related products. *J. Supercrit. Fluids* **1997**, *10*, 1–37. [[CrossRef](#)]
53. Manjare, S.D.; Dhingra, K. Supercritical fluids in separation and purification: A review. *Mater. Sci. Energy Technol.* **2019**, *2*, 463–484. [[CrossRef](#)]
54. Machado, D.; Mosquera, J.E.; Martini, R.E.; Goni, M.L.; Ganan, N.A. Supercritical CO₂-assisted impregnation/deposition of polymeric materials with pharmaceutical, nutraceutical, and biomedical applications: A review (2015–2021). *J. Supercrit. Fluids* **2002**, *191*, 105763. [[CrossRef](#)]
55. Hassabo, A.G.; Zayed, M.; Bakr, M.; Abd-Elaziz, M.; Othman, H.A. Applications of supercritical carbon dioxide in textile finishing: A review. *J. Text. Color. Polym. Sci.* **2022**, *19*, 179–187. [[CrossRef](#)]
56. Zhang, X.; Heinonen, S.; Levanen, E. Applications of supercritical carbon dioxide in materials processing and synthesis. *RSC Adv.* **2014**, *4*, 61137–61152. [[CrossRef](#)]
57. Cooper, A.I. Polymer synthesis and processing using supercritical carbon dioxide. *J. Mater. Chem.* **2000**, *10*, 207–234. [[CrossRef](#)]
58. Pascu, O.; Cacciuttolo, B.; Marre, S.; Pucheault, M.; Aymonier, C. ScCO₂ assisted preparation of supported metal NPs. Application to catalyst design. *J. Supercrit. Fluids* **2015**, *105*, 84–91. [[CrossRef](#)]
59. Daro, N.; Vaudel, T.; Findouli, L.; Marre, S.; Aymonier, C. One-step synthesis of spin crossover nanoparticles using flow chemistry and supercritical CO₂. *Chem. A Eur. J.* **2020**, *26*, 16286–16290. [[CrossRef](#)]
60. Tomasko, D.L.; Burley, A.; Feng, L.; Yeh, S.K.; Miyazono, K.; Nirmal-Kuma, S.; Kusaka, I.; Koelling, K. Development of CO₂ for polymer foam applications. *J. Supercrit. Fluids* **2009**, *47*, 493–499. [[CrossRef](#)]
61. Suresh Kumar, T.V.; Sankar, K.U.; Divakar, S. Synthesis of thymol glycosides under SCCO₂ conditions using amyloglucosidase from *Rhizopus* mold. *J. Food Sci. Technol.* **2013**, *50*, 803–808. [[CrossRef](#)]
62. Holmes, J.D.; Lyons, D.M.; Ziegler, K.J. Supercritical fluid synthesis of metal and semiconductor nanomaterials. *Chem. A Eur. J.* **2003**, *9*, 2144–2150. [[CrossRef](#)] [[PubMed](#)]
63. Savage, P.E.; Li, R.; Santini, J.T. Methane to methanol in supercritical water. *J. Supercrit. Fluids* **1994**, *7*, 135–144. [[CrossRef](#)]
64. Dixon, C.N.; Abraham, M.A. Conversion of methane to methanol by catalytic supercritical water oxidation. *J. Supercrit. Fluids* **1992**, *5*, 269–273. [[CrossRef](#)]
65. Motonobu, G. Chemical recycling of plastics using sub- and supercritical fluids. *J. Supercrit. Fluids* **2009**, *47*, 500–507.
66. Lilca, W.D.; Sunggyu, L. Kinetics and mechanisms of styrene monomer recovery from waste polystyrene by supercritical water partial oxidation. *Adv. Environ. Res.* **2001**, *6*, 9–16. [[CrossRef](#)]
67. Yesodharan, S. Supercritical water oxidation: An environmentally safe method for the disposal of organic wastes. *Curr. Sci.* **2002**, *82*, 1112–1122.
68. Schmieder, H. Supercritical water oxidation: State of the art. *Chem. Eng. Technol.* **1999**, *2*, 903–908. [[CrossRef](#)]
69. White, A.; Burns, D.; Christensen, T.W. Effective terminal sterilization using supercritical carbon dioxide. *J. Biotech.* **2006**, *123*, 504–515. [[CrossRef](#)]
70. Cario, A.; Aubert, G.; Aymonier, C. Supercritical CO₂-based process to clean and sterilize FFP2 facial masks, Supercritical CO₂-based process to clean and sterilize FFP2 facial masks. In Proceedings of the 13th International Symposium on Supercritical Fluids, International Society for the Advancement of Supercritical Fluids, Montréal, QC, Canada, 15–18 May 2022.
71. Prasad, S.K.; Sangwai, J.S.; Byun, H.S. A review of the supercritical CO₂ fluid applications for improved oil and gas production and associated carbon storage. *J. CO₂ Util.* **2023**, *72*, 102479. [[CrossRef](#)]

72. Lackner, K. A guide to CO₂ sequestration. *Science* **2003**, *300*, 1677–1678. [CrossRef] [PubMed]
73. Taylor, T.T. Supercritical fluid chromatography for the 21st century. *J. Supercrit. Fluids* **2009**, *47*, 566–573. [CrossRef]
74. Fallahsohi, H. Energy analysis of the heat pump operating with supercritical CO₂ driven by thermal compression. *Am. J. Eng. Res.* **2023**, *12*, 61–74.
75. Xie, Y.; Sun, G.; Lun, L.; Su, H. Thermodynamic analysis of CO₂ supercritical two-stage compression refrigeration cycle. In Proceedings of the International Refrigeration and Air Conditioning Conference, Purdue, West Lafayette, IN, USA, 14–17 July 2008. Available online: <https://docs.lib.purdue.edu/cgi/viewcontent.cgi?article=1903&context=iracc> (accessed on 4 September 2024).
76. Cansell, F.; Aymonier, C.; Loppinet-Serani, A. Review on materials science and supercritical fluids. *Curr. Opin. Solid State Mater. Sci.* **2003**, *7*, 331–340. [CrossRef]
77. Simeski, F.; Ihme, M. Supercritical fluids behave as complex networks. *Nat. Commun.* **2023**, *14*, 1996. [CrossRef]
78. Burke, J. Solubility Parameters: Theory and Application—Part 2: The Hildebrand Solubility Parameter. 1984. Available online: <https://cool.culturalheritage.org/coolaic/sg/bpg/annual/v03/bp03-04.html> (accessed on 27 October 2024).
79. Doane-Weideman, D.; Liescheski, P.B. Chapter 5, Analytical supercritical fluid extraction for food applications. In *Oil Extraction and Analysis*, 1st ed.; Luthria, D.L., Ed.; AOCS Publishing: New York, NY, USA, 2004; pp. 40–69.
80. Giddings, J.C.; Myers, M.N.; McLaren, L.; Keller, R.A. High pressure gas chromatography of nonvolatile species. *Science* **1968**, *162*, 67–73. [CrossRef]
81. Rai, N.; Wagner, A.J.; Ross, R.B.; Siepmann, J.I. Application of the force field for predicting the hildebrand solubility parameters of organic solvents and monomer units. *J. Chem. Theory Comput.* **2008**, *4*, 136–144. [CrossRef]
82. Mathieu, D. Pencil and paper estimation of hansen solubility parameters. *ACS Omega* **2018**, *3*, 17049–17056. [CrossRef]
83. Lemmon, E.W.; Bell, I.H.; McLinden, M.O. *Reference Fluid Thermodynamic and Transport Properties (REFPROP), NIST Standard Reference Database 23, Version 10.0*; National Institute of Standards and Technology: Boulder, CO, USA, 2018.
84. Talreja, M.; Kusaka, I.; Tomasko, D.L. Fluid phase equilibria, analyzing surface tension in higher alkanes and their CO₂ mixtures. *Fluid Phase Equilibria* **2012**, *319*, 67–76. [CrossRef]
85. Zeppieri, S.; Rodriguez, J.; Lopez de Ramos, A.L. Interfacial Tension of Alkane + Water Systems. *J. Chem. Eng. Data* **2001**, *46*, 1086–1088. [CrossRef]
86. Rezk, M.G.; Foroozesh, J.; Abdulrahmand, A.; Gholinezhad, J. CO₂ Diffusion and Dispersion in Porous Media: Review of advances in experimental measurements and mathematical models. *J. Energy Fuels* **2022**, *36*, 133–155. [CrossRef]
87. Takahashi, S.; Hong, M. Diffusion coefficients of gases at high pressures—The CO₂–CH₄ system. *J. Chem. Eng. Jpn.* **1982**, *15*, 57–59. [CrossRef]
88. Santos, C.I.; Ribeiro, A.C.; Shevtsova, V. Binary diffusion coefficients for short chain alcohols in supercritical carbon dioxide—Experimental and predictive correlations. *Molecules* **2023**, *28*, 782. [CrossRef]
89. Guevara-Carrion, G.; Janzen, T.; Muñoz-Muñoz, Y.M.; Vrabec, J. Mutual diffusion of binary liquid mixtures containing methanol, ethanol, acetone, benzene, cyclohexane, toluene, and carbon tetrachloride. *J. Chem. Phys.* **2016**, *144*, 124501. [CrossRef] [PubMed]
90. Bandura, A.; Lvov, S. The ionization constant of water over wide ranges of temperature and density. *J. Phys. Chem. Ref. Data* **2006**, *35*, 15–30. [CrossRef]
91. Shcherbakov, V.V.; Artemkina, Y.M.; Akimova, I.A.; Artemkina, I.M. Dielectric characteristics, electrical conductivity and solvation of ions in electrolyte solutions. *Materials* **2021**, *14*, 5617. [CrossRef]
92. Olah, G.A.; Sury-Prakash, G.K.S.; Molnar, A.; Sommer, J. *Superacid Chemistry*; John Wiley & Son: Hoboken, NJ, USA, 2009; p. 36.
93. Bennett, E.L.; Calisir, I.; Yang, X.; Huang, Y.; Xiao, J. Correlation of dielectric properties with structure and H-bonding for liquids. *J. Phys. Chem. C* **2023**, *127*, 18669–18677. [CrossRef]
94. Uematsu, M.; Franck, E.U. Static dielectric constant of water and steam. *J. Phys. Chem. Ref. Data* **1980**, *9*, 1291–1306. [CrossRef]
95. Yoon, M.J.; In, J.H.; Lee, H.C.; Lee, L.H. Comparison of YAG: Eu phosphor synthesized by supercritical water and solid-state methods in a batch reactor. *Korean J. Chem. Eng.* **2006**, *23*, 842–884. [CrossRef]
96. Rai, U.S.; Singh, L.; Mandal, K.D.; Singh, N.B. An Overview on Recent Developments in the Synthesis, Characterization and Properties of High Dielectric Constant Calcium Copper Titanate Nano-Particles. *Nanosci. Technol.* **2014**, *1*, 1–17.
97. Drake, B.D.; Smith, R.L. Measurement of static dielectric constants of supercritical fluid solvents and cosolvents: Carbon Dioxide and argon, carbon dioxide, and methanol at 323 K and pressures to 25 MPa. *J. Supercrit. Fluids* **1990**, *3*, 162–168. [CrossRef]
98. Berna, A.; Chafer, A.; Monton, J.B. High-pressure solubility data of the system resveratrol (3) + ethanol (2) + CO₂ (1). *J. Supercrit. Fluids* **2001**, *19*, 133–139. [CrossRef]
99. Arichi, H.; Kimura, Y.; Okuda, H.; Baba, K.; Kozawa, M.; Arichi, S. Studies on Saitellariae radix. VI. Effects of flavonone compounds on lipid peroxidation in rat liver. *Chem. Pharm. Bull.* **1982**, *10*, 218–220.
100. Jang, M.; Cai, L.; Udecani, G.O.; Slowing, K.V.; Thomas, C.F.; Beecher, C.W.; Fong, H.H.; Farnsworth, N.R.; Kinghorn, A.D.; Mehta, R.G.; et al. Cancer chemopreventive activity of resveratrol, a natural product derived from grapes. *Science* **1997**, *275*, 218–220. [CrossRef] [PubMed]
101. Vestergaard, M.; Ingme, H. Antibacterial and antifungal properties of resveratrol. *Int. J. Antimicrob. Agents* **2019**, *53*, 716–723. [CrossRef]
102. USEPA Pollution Prevention Act. 1990. Available online: <https://www.epa.gov/p2/pollution-prevention-act-1990#:~:text=The%20Congress%20hereby%20declares%20it,be%20prevented%20or%20recycled%20should> (accessed on 8 August 2024).

103. Beckman, E.J. Supercritical and near-critical CO₂ in green chemical synthesis and processing. *J. Supercrit. Fluids* **2004**, *28*, 121–191. [CrossRef]
104. Keith, A.; Consani, K.A.; Smith, R.D. Observations on the solubility of surfactants and related molecules in carbon dioxide at 50 °C. *J. Supercrit. Fluids* **1990**, *3*, 51–65.
105. Li, K.; Xu, Z. Decomposition of high-impact polystyrene resin in e-waste by supercritical water oxidation process with debromination of decabromodiphenyl ethane and recovery of antimony trioxide simultaneously, *J Hazard Mater.* **2021**, *402*, 123684–402.
106. Ruamchat, T.; Hayashi, R.; Ngamprasertsith, S.; Oshima, Y. A novel on-site system for the treatment of pharmaceutical laboratory wastewater by supercritical water oxidation. *Environ. Sci.* **2006**, *13*, 297–304.
107. Peterson, A.A.; Vogel, F.; Lachance, R.P.; Fröling, M.; Antal, J.M.J.; Tester, J.W. Thermochemical biofuel production in hydrothermal media: A review of sub- and supercritical water technologies. *Energy Environ. Sci.* **2008**, *1*, 32–65. [CrossRef]
108. Che, W.T.; Jin, K.; Linda-Wang, N.W. Use of supercritical water for the liquefaction of polypropylene into oil. *ACS Sustain. Chem. Eng.* **2019**, *7*, 3749–3758.
109. Okolie, J.A.; Rana, R.; Nanda, S.; Dalai, A.K.; Kozinski, J.A. Supercritical water gasification of biomass: A state-of-the-art review of process parameters, reaction mechanisms and catalysis. *Sustain. Energy Fuels* **2019**, *3*, 578–598. [CrossRef]
110. Byrd, A.J.; Pant, K.K.; Gupta, R.B. Hydrogen production from glycerol by reforming in supercritical water over Ru/Al₂O₃ catalyst. *Fuel* **2008**, *87*, 2956–2960. [CrossRef]
111. Tzima, S.; Georgiopoulou, I.; Louli, V.; Magoulas, K. Recent Advances in Supercritical CO₂ extraction of pigments, lipids and bioactive compounds from microalgae. *Molecules* **2023**, *28*, 1410. [CrossRef]
112. Uwineza, P.A.; Waskiewicz, A. Recent advances in supercritical fluid extraction of natural bioactive compounds from natural plant materials. *Molecules* **2020**, *25*, 3847. [CrossRef]
113. NATEX Database. Available online: <https://www.natex.at/about-us/project-references/> (accessed on 8 August 2024).
114. Ngamprasertsith, S.; Menwa, J.; Sawangkeaw, R. Caryophyllene oxide extraction from lemon basil (*Ocimum citriodorum* Vis.) straw by hydrodistillation and supercritical CO₂. *J. Supercrit. Fluids* **2018**, *138*, 1–6. [CrossRef]
115. Mladenovic, M.Z.; Huang, O.; Wang, B.; Ginestet, A.; Desbiaux, D.; Baldovini, N. Chemical investigation on the volatile part of the CO₂ supercritical fluid extract of infected *Aquilaria sinensis* (Chinese Agarwood). *Molecules* **2024**, *29*, 2297. [CrossRef]
116. Delgado-García, Y.I.; Luna-Suárez, S.; López-Malo, A.; Morales-Camacho, J.I. Effect of supercritical carbon dioxide on physico-chemical and techno-functional properties of amaranth flour. *Chem. Eng. Process.* **2022**, *178*, 109031. [CrossRef]
117. Sakdasri, W.; Ngamprasertsith, S.; Sooksai, S.; Noitang, S.; Sukaead, W.; Sawangkeaw, R. Defatted fiber produced from lemon Basil (*Ocimum citriodorum* Vis.) seed with supercritical CO₂: Economic analysis. *Ind. Crops Prod.* **2019**, *135*, 188–195. [CrossRef]
118. Albarelli, J.Q.; Santos, D.T.; Cocero, M.J.; Meireles, M.A.A. Economic analysis of an integrated annatto seeds-sugarcane biorefinery using supercritical CO₂ extraction as a first step. *Materials* **2016**, *9*, 494. [CrossRef]
119. Cárdenas-Toro, F.P.; Meza-Coaquira, J.H.; Nakama-Hokamura, G.K.; Zobot, G.L. Obtaining bixin- and tocotrienol-rich extracts from peruvian annatto seeds using supercritical CO₂ extraction: Experimental and economic evaluation. *Foods* **2024**, *13*, 1549. [CrossRef] [PubMed]
120. Vardanega, R.; Nogueira, G.C.; Nascimento, C.D.O.; Faria-Machado, A.F.; Meireles, M.A.A. Selective extraction of bioactive compounds from annatto seeds by sequential supercritical CO₂ process. *J. Supercrit. Fluids* **2019**, *150*, 122–127. [CrossRef]
121. Massironi, A.; Di Fonzo, A.; Bassanini, I.; Ferrandi, E.E.; Marzorati, S.; Monti, D.; Verotta, L. Selective supercritical CO₂ extraction and biocatalytic valorization of *Cucurbita pepo* L. industrial residuals. *Molecules* **2022**, *27*, 4783. [CrossRef] [PubMed]
122. Albakry, Z.; Karrar, E.; Mohamed Ahmed, I.A.; Ali, A.A.; Al-Maqtari, Q.A.; Zhang, H.; Wu, G.; Wang, X. A comparative study of black cumin seed (*Nigella sativa* L.) oils extracted with supercritical fluids and conventional extraction methods. *J. Food Meas. Charact.* **2023**, *17*, 2429–2441. [CrossRef]
123. Sakdasri, W.; Sakulkittiyut, B.; Ngamprasertsith, S.; Supang, W.; Sawangkeaw, R. Effects of temperature and pressure on volatile compounds of black cumin seeds (*Nigella sativa* L.) oil extracted by supercritical carbon dioxide. *J. Am. Oil Chem. Soc.* **2024**, *1–9*. [CrossRef]
124. Díaz-Reinoso, B.; Moure, A.; Domínguez, H. Ethanol-Modified Supercritical CO₂ Extraction of chestnut burs antioxidants. *Chem. Eng. Process.* **2020**, *156*, 108092. [CrossRef]
125. Benito-Román, O.; Varona, S.; Sanz, M.T.; Beltrán, S. Valorization of rice bran: Modified supercritical CO₂ extraction of bioactive compounds. *J. Ind. Eng. Chem.* **2019**, *80*, 273–282. [CrossRef]
126. Picchioni, F. Supercritical carbon dioxide and polymers: An interplay of science and technology. *Polym. Int.* **2014**, *63*, 1394–1399. [CrossRef]
127. Kiran, E. Supercritical fluids and polymers—The year in review—2014. *J. Supercrit. Fluids* **2016**, *110*, 126–153. [CrossRef]
128. Pina-Martinez, A.; Privat, R.; Jaubert, J.N.; Peng, D.Y. Updated version of the generalized Soave α -function for the Redlich-Kwong and Peng-Robinson EoS. *Fluid Phase Equilibria* **2018**, *485*, 264–269. [CrossRef]
129. Pina-Martinez, A.; Privat, R.; Lasala, S.; Soave, G.; Jaubert, J.N. Search for the optimal expression of the volumetric dependence of the attractive contribution in cubic EoS. *Fluid Phase Equilibria* **2020**, *522*, 112750. [CrossRef]
130. DeFelice, J.; Lipson, J.E.G. Polymer miscibility in supercritical carbon dioxide: Free volume as a driving force. *Macromolecules* **2014**, *47*, 5643–5654. [CrossRef]

131. Behera, U.S.; Prasad, S.K.; Baskaran, D.; Byun, H.-S. Phase behavior of biodegradable poly(L-lactic acid) in supercritical solvents and cosolvents. *J. CO₂ Util.* **2024**, *79*, 102658. [[CrossRef](#)]
132. Zhang, K.; Wang, Y.; Jiang, J.; Wang, X.; Hou, J.; Sun, S.; Li, Q. Fabrication of highly interconnected porous poly(ϵ -caprolactone) scaffolds with supercritical CO₂ foaming and polymer leaching. *J. Mater. Sci.* **2018**, *54*, 5112–5126. [[CrossRef](#)]
133. Alekseev, E.S.; Alentiev, A.Y.; Belova, A.S.; Bogdan, V.I.; Bogdan, T.V.; Bystrova, A.V.; Gafarova, E.R.; Golubeva, E.N.; Grebenik, E.A.; Gromov, O.I.; et al. Supercritical fluids in chemistry. *Russ. Chem. Rev.* **2020**, *89*, 1337–1427. [[CrossRef](#)]
134. Jennings, J.; Beija, M.; Kennon, J.T.; Willcock, H.; O'Reilly, R.K.; Rimmer, S.; Howdle, S.M. Advantages of block copolymer synthesis by RAFT-controlled dispersion polymerization in supercritical carbon dioxide. *Macromolecules* **2013**, *46*, 6843–6851. [[CrossRef](#)]
135. Tsai, W.-C.; Wang, Y. Progress of supercritical fluid technology in polymerization and its applications in biomedical engineering. *Prog. Polym. Sci.* **2019**, *98*, 101161. [[CrossRef](#)]
136. Chafidz, A.; Jauhary, T.; Kaavessina, M.; Sumarno, S.; Latief, F.H. Formation of fine particles using supercritical fluid (SCF) process: Short review. *Commun. Sci. Technol.* **2018**, *3*, 57–63. [[CrossRef](#)]
137. Ha, E.-S.; Kang, H.-T.; Park, H.; Kim, S.; Kim, M.-S. Advanced technology using supercritical fluid for particle production in pharmaceutical continuous manufacturing. *J. Pharm. Investig.* **2022**, *53*, 249–267. [[CrossRef](#)]
138. Islam, T.; Al Ragib, A.; Ferdosh, S.; Uddin, A.B.M.H.; Haque Akanda, M.J.; Mia, M.A.R.; Reddy Prasad, D.M.; Karamuzzaman, B.Y.; Islam Sarker, M.Z. Development of nanoparticles for pharmaceutical preparations using supercritical techniques. *Chem. Eng. Commun.* **2022**, *209*, 1642–1663. [[CrossRef](#)]
139. Campardelli, R.; Baldino, L.; Reverchon, E. Supercritical fluids applications in nanomedicine. *J. Supercrit. Fluids* **2015**, *101*, 193–214. [[CrossRef](#)]
140. Franco, P.; De Marco, I. Supercritical antisolvent process for pharmaceutical applications: A review. *Processes* **2020**, *8*, 938. [[CrossRef](#)]
141. Gangapurwala, G.; Vollrath, A.; De San Luis, A.; Schubert, U.S. PLA/PLGA-Based drug delivery systems produced with supercritical CO₂—A green future for particle formulation? *Pharmaceutics* **2020**, *12*, 1118. [[CrossRef](#)]
142. Kankala, R.K.; Zhang, Y.S.; Wang, S.B.; Lee, C.H.; Chen, A.Z. Supercritical fluid technology: An emphasis on drug delivery and related biomedical applications. *Adv. Healthc. Mater.* **2017**, *6*, 1700433. [[CrossRef](#)] [[PubMed](#)]
143. Davies, O.R.; Lewis, A.L.; Whitaker, M.J.; Tai, H.; Shakesheff, K.M.; Howdle, S.M. Applications of supercritical CO₂ in the fabrication of polymer systems for drug delivery and tissue engineering. *Adv. Drug Deliv. Rev.* **2008**, *60*, 373–387. [[CrossRef](#)] [[PubMed](#)]
144. Simonov, A.S.; Kharitonova, E.P.; Fedosov, D.A.; Kolozhvari, B.A.; Gallyamov, M.O. How does processing in supercritical carbon dioxide influence the Nafion film properties? *Colloid Polym. Sci.* **2021**, *299*, 1863–1875. [[CrossRef](#)]
145. Kazaryan, P.S.; Agalakova, M.A.; Kharitonova, E.P.; Gallyamov, M.O.; Kondratenko, M.S. Reducing the contact angle hysteresis of thin polymer films by oil impregnation in supercritical carbon dioxide. *Prog. Org. Coat.* **2021**, *154*, 106202. [[CrossRef](#)]
146. Starannikova, L.E.; Alentiev, A.Y.; Nikiforov, R.Y.; Ponomarev, I.I.; Blagodatskikh, I.V.; Nikolaev, A.Y.; Shantarovich, V.P.; Yampolskii, Y.P. Effects of different treatments of films of PIM-1 on its gas permeation parameters and free volume. *Polymer* **2021**, *212*, 123271. [[CrossRef](#)]
147. Machmudah, S.; Wahyudiono, K.H.; Goto, M. 5. Supercritical fluid-assisted electrospinning. In *Green Electrospinning*; De Gruyter: Berlin, Germany, 2019; pp. 99–128.
148. Di Maio, E.; Kiran, E. Foaming of polymers with supercritical fluids and perspectives on the current knowledge gaps and challenges. *J. Supercrit. Fluids* **2018**, *134*, 157–166. [[CrossRef](#)]
149. Sarver, J.A.; Kiran, E. Foaming of polymers with carbon dioxide—The year-in-review—2019. *J. Supercrit. Fluids* **2021**, *173*, 105166. [[CrossRef](#)]
150. Gonçalves, L.F.F.F.; Reis, R.L.; Fernandes, E.M. Forefront research of foaming strategies on biodegradable polymers and their composites by thermal or melt-based processing technologies: Advances and perspectives. *Polymers* **2024**, *16*, 1286. [[CrossRef](#)]
151. Zhou, Y.; Tian, Y.; Peng, X. Applications and Challenges of Supercritical Foaming Technology. *Polymers* **2023**, *15*, 402. [[CrossRef](#)] [[PubMed](#)]
152. Reignier, J.; Huneault, M.A. Preparation of interconnected poly(ϵ -caprolactone) porous scaffolds by a combination of polymer and salt particulate leaching. *Polymer* **2006**, *47*, 4703–4717. [[CrossRef](#)]
153. Xin, X.; Liu, Q.-Q.; Chen, C.-X.; Guan, Y.-X.; Yao, S.-J. Fabrication of bimodal porous PLGA scaffolds by supercritical CO₂ foaming/particle leaching technique. *J. Appl. Polym. Sci.* **2016**, *133*, 43644. [[CrossRef](#)]
154. Salerno, A.; Zeppetelli, S.; Di Maio, E.; Iannace, S.; Netti, P.A. Architecture and properties of bi-modal porous scaffolds for bone regeneration prepared via supercritical CO₂ foaming and porogen leaching combined process. *J. Supercrit. Fluids* **2012**, *67*, 114–122. [[CrossRef](#)]
155. Carrascosa, F.; García, M.T.; Ramos, M.J.; García-Vargas, J.M.; Rodríguez, J.F.; Gracia, I. Enhancing polymeric bone scaffolds mechanical characteristics using supercritical CO₂ foaming and reinforcing agents. *J. Taiwan Inst. Chem. Eng.* **2024**, *162*, 105619. [[CrossRef](#)]
156. Salerno, A.; Leonardi, A.B.; Pedram, P.; Di Maio, E.; Fanovich, M.A.; Netti, P.A. Tuning the three-dimensional architecture of supercritical CO₂ foamed PCL scaffolds by a novel mould patterning approach. *Mater. Sci. Eng. C.* **2020**, *109*, 110518. [[CrossRef](#)]

157. Varma, A.; Ghosh, S. Supercritical carbon dioxide: A glimpse from the modern era of green chemistry. In *Advanced Nanotechnology and Application of Supercritical Fluids*; Springer: Cham, Switzerland, 2020; pp. 75–123.
158. Afraz, M.T.; Xu, X.; Adil, M.; Manzoor, M.F.; Zeng, X.-A.; Han, Z.; Aadil, R.M. Subcritical and supercritical fluids to valorize industrial fruit and vegetable waste. *Foods* **2023**, *12*, 2417. [\[CrossRef\]](#)
159. Al Khawli, F.; Pateiro, M.; Domínguez, R.; Lorenzo, J.M.; Gullón, P.; Kousoulaki, K.; Ferrer, E.; Berrada, H.; Barba, F.J. Innovative green technologies of intensification for valorization of seafood and their by-products. *Mar. Drugs* **2019**, *17*, 689. [\[CrossRef\]](#)
160. Restrepo-Serna, D.L.; Cardona Alzate, C.A. Economic pre-feasibility of supercritical fluid extraction of antioxidants from fruit residues. *Sustain. Chem. Pharm.* **2022**, *25*, 100600. [\[CrossRef\]](#)
161. Kitrytė, V.; Narkevičiūtė, A.; Tamkutė, L.; Syrpas, M.; Pukalskienė, M.; Venskutonis, P.R. Consecutive high-pressure and enzyme assisted fractionation of blackberry (*Rubus fruticosus* L.) pomace into functional ingredients: Process optimization and product characterization. *Food Chem.* **2020**, *312*, 126072. [\[CrossRef\]](#)
162. Nilmat, K.; Ngamprasertsith, S.; Sakdasri, W.; Karnchanatat, A.; Sawangkeaw, R. Sequential process to valorization of rambutan seed waste by supercritical CO₂-ethanol and subcritical water extractions. *Chem. Eng. Trans.* **2024**; *accepted for publishing*.
163. Nilmat, K.; Hunsub, P.; Ngamprasertsith, S.; Sakdasri, W.; Karnchanatat, A.; Sawangkeaw, R. Effects of defatting pretreatment on polysaccharide extraction from rambutan seeds using subcritical water: Optimization using the desirability approach. *Foods* **2024**, *13*, 1967. [\[CrossRef\]](#) [\[PubMed\]](#)
164. De Marco, I.; Riemma, S.; Iannone, R. Life cycle assessment of supercritical CO₂ extraction of caffeine from coffee beans. *J. Supercrit. Fluids* **2018**, *133*, 393–400. [\[CrossRef\]](#)
165. Hunsub, P.; Ngamprasertsith, S.; Prichapan, N.; Sakdasri, W.; Karnchanatat, A.; Sawangkeaw, R. Life cycle assessment of spray drying encapsulation on crude peptides produced from defective green coffee beans. *Clean Technol. Environ. Policy* **2024**, in press. [\[CrossRef\]](#)
166. Caldeira, C.; Vlysidis, A.; Fiore, G.; De Laurentiis, V.; Vignali, G.; Sala, S. Sustainability of food waste biorefinery: A review on valorisation pathways, techno-economic constraints, and environmental assessment. *Bioresour. Technol.* **2020**, *312*, 123575. [\[CrossRef\]](#)
167. Gwee, Y.L.; Yusup, S.; Tan, R.R.; Yiin, C.L. Techno-economic and life-cycle assessment of volatile oil extracted from *Aquilaria sinensis* using supercritical carbon dioxide. *J. CO₂ Util.* **2020**, *38*, 158–167. [\[CrossRef\]](#)
168. Bermejo, D.V.; Ibáñez, E.; Reglero, G.; Fornari, T. Effect of cosolvents (ethyl lactate, ethyl acetate and ethanol) on the supercritical CO₂ extraction of caffeine from green tea. *J. Supercrit. Fluids* **2016**, *107*, 507–512. [\[CrossRef\]](#)
169. Salerno, A.; Fanovich, M.A.; Pascual, C.D. The effect of ethyl-lactate and ethyl-acetate plasticizers on PCL and PCL–HA composites foamed with supercritical CO₂. *J. Supercrit. Fluids* **2014**, *95*, 394–406. [\[CrossRef\]](#)
170. Knez, Ž.; Markočič, E.; Leitgeb, M.; Primožič, M.; Knez Hrnič, M.; Škerget, M. Industrial applications of supercritical fluids: A review. *Energy* **2014**, *77*, 235–243. [\[CrossRef\]](#)
171. Knez, Ž. Enzymatic reactions in subcritical and supercritical fluids. *J. Supercrit. Fluids* **2018**, *134*, 133–140. [\[CrossRef\]](#)
172. Osman, A.I.; Qasim, U.; Jamil, F.; Al-Muhtaseb, A.a.H.; Jrai, A.A.; Al-Riyami, M.; Al-Maawali, S.; Al-Haj, L.; Al-Hinai, A.; Al-Abri, M.; et al. Bioethanol and biodiesel: Bibliometric mapping, policies and future needs. *Renew. Sustain. Energy Rev.* **2021**, *152*, 111677. [\[CrossRef\]](#)
173. Yusuf, N.N.A.N.; Kamarudin, S.K.; Yaakub, Z. Overview on the current trends in biodiesel production. *Energy Convers. Manag.* **2011**, *52*, 2741–2751. [\[CrossRef\]](#)
174. Ngamprasertsith, S.; Sawangkeaw, R. Transesterification in supercritical conditions. In *Biodiesel*; Margarita, S., Gisela, M., Eds.; IntechOpen: Rijeka, Croatia, 2011; p. Ch. 12.175.
175. Muhammad Niza, N.; Tan, K.; Lee, K.T.; Ahmad, Z. Influence of impurities on biodiesel production from *Jatropha curcas* L. by supercritical methyl acetate process. *J. Supercrit. Fluids* **2013**, *79*, 73–75. [\[CrossRef\]](#)
176. Lee, J.-S.; Saka, S. Biodiesel production by heterogeneous catalysts and supercritical technologies. *Bioresour. Technol.* **2010**, *101*, 7191–7200. [\[CrossRef\]](#)
177. Lukić, I.; Kesic, Z.; Zdujić, M.; Skala, D. Solid acids as catalysts for biodiesel synthesis. In *Heterogeneous Catalysts*; Nova Science Publishers, Inc.: New York, NY, USA, 2016; pp. 21–136.
178. Makarevicene, V.; Sendzikiene, E. Noncatalytic biodiesel synthesis under supercritical conditions. *Processes* **2021**, *9*, 138. [\[CrossRef\]](#)
179. Sreedhar, I.; Kishan, Y.K. Process standardization and kinetics of ethanol driven biodiesel production by transesterification of ricebran oil. *Int. J. Ind. Chem.* **2016**, *7*, 121–129. [\[CrossRef\]](#)
180. Casas, A.; Pérez, Á.; Ramos, M.J. Purification of methyl acetate/water mixtures from chemical interesterification of vegetable oils by pervaporation. *Energies* **2021**, *14*, 775. [\[CrossRef\]](#)
181. Komintarachat, C.; Sawangkeaw, R.; Ngamprasertsith, S. Continuous production of palm biofuel under supercritical ethyl acetate. *Energy Convers. Manag.* **2015**, *93*, 332–338. [\[CrossRef\]](#)
182. Saka, S.; Kusdiana, D. Biodiesel fuel from rapeseed oil as prepared in supercritical methanol. *Fuel* **2001**, *80*, 225–231. [\[CrossRef\]](#)
183. Sakdasri, W.; Sawangkeaw, R.; Ngamprasertsith, S. Continuous production of biofuel from refined and used palm olein oil with supercritical methanol at a low molar ratio. *Energy Convers. Manag.* **2015**, *103*, 934–942. [\[CrossRef\]](#)
184. Rade, L.L.; Arvelos, S.; de Souza Barrozo, M.A.; Romanielo, L.L.; Watanabe, E.O.; Hori, C.E. Evaluation of the use of degummed soybean oil and supercritical ethanol for non-catalytic biodiesel production. *J. Supercrit. Fluids* **2015**, *105*, 21–28. [\[CrossRef\]](#)

185. Lamba, N.; Modak, J.M.; Madras, G. Fatty acid methyl esters synthesis from non-edible vegetable oils using supercritical methanol and methyl tert-butyl ether. *Energy Convers. Manag.* **2017**, *138*, 77–83. [CrossRef]
186. Román-Figueroa, C.; Olivares-Carrillo, P.; Paneque, M.; Palacios-Nereo, F.J.; Quesada-Medina, J. High-yield production of biodiesel by non-catalytic supercritical methanol transesterification of crude castor oil (*Ricinus communis*). *Energy* **2016**, *107*, 165–171. [CrossRef]
187. Lamba, N.; Gupta, K.; Modak, J.M.; Madras, G. Biodiesel synthesis from Calophyllum inophyllum oil with different supercritical fluids. *Bioresour. Technol.* **2017**, *241*, 767–774. [CrossRef]
188. Nan, Y.; Liu, J.; Lin, R.; Tavlarides, L.L. Production of biodiesel from microalgae oil (*Chlorella protothecoides*) by non-catalytic transesterification in supercritical methanol and ethanol: Process optimization. *J. Supercrit. Fluids* **2015**, *97*, 174–182. [CrossRef]
189. Supang, W.; Ngamprasertsith, S.; Sakdasri, W.; Sawangkeaw, R. Biodiesel production from spent coffee grounds by using ethanolic extraction and supercritical transesterification. *BioEnergy Res.* **2024**. [CrossRef]
190. Monteiro, M.; Luis, C.; Pinheiro, R.; Batalha, M.; César, A. Glycerol from biodiesel production: Technological paths for sustainability. *Renew. Sustain. Energy Rev.* **2018**, *88*, 109–122. [CrossRef]
191. Esan, A.O.; Olabemiwo, O.M.; Smith, S.M.; Ganesan, S. A concise review on alternative route of biodiesel production via interesterification of different feedstocks. *Int. J. Energy Res.* **2021**, *45*, 12614–12637. [CrossRef]
192. Sakdasri, W.; Komintarachat, C.; Sawangkeaw, R.; Ngamprasertsith, S. A review of supercritical technologies for lipid-based biofuels production: The glycerol-free processes. *Eng. J.* **2021**, *25*, 1–14. [CrossRef]
193. Saka, S.; Isayama, Y. A new process for catalyst-free production of biodiesel using supercritical methyl acetate. *Fuel* **2009**, *88*, 1307–1313. [CrossRef]
194. Zare, A.; Nabi, M.N.; Bodisco, T.A.; Hossain, F.M.; Rahman, M.H.; Ristovski, Z.D.; Brown, R.J. The effect of triacetin as a fuel additive to waste cooking biodiesel on engine performance and exhaust emissions. *Fuel* **2016**, *182*, 640–649. [CrossRef]
195. Casas, A.; Ruiz, J.R.; Ramos, M.J.; Pérez, Á. Effects of triacetin on biodiesel quality. *Energy Fuels* **2010**, *24*, 4481–4489. [CrossRef]
196. Goembira, F.; Matsuura, K.; Saka, S. Biodiesel production from rapeseed oil by various supercritical carboxylate esters. *Fuel* **2012**, *97*, 373–378. [CrossRef]
197. de Mello, B.T.F.; Portillo Trentini, C.; Postau, N.; da Silva, C. Sequential process for obtaining methyl esters and triacetin from crambe oil using pressurized methyl acetate. *Ind. Crops Prod.* **2020**, *147*, 112233. [CrossRef]
198. Supang, W.; Ngamprasertsith, S.; Sakdasri, W.; Sawangkeaw, R. Ethyl acetate as extracting solvent and reactant for producing biodiesel from spent coffee grounds: A catalyst- and glycerol-free process. *J. Supercrit. Fluids* **2022**, *186*, 105586. [CrossRef]
199. Farobie, O.; Matsumura, Y. A comparative study of biodiesel production using methanol, ethanol, and tert-butyl methyl ether (MTBE) under supercritical conditions. *Bioresour. Technol.* **2015**, *191*, 306–311. [CrossRef] [PubMed]
200. Ngamprasertsith, S.; Laetoheem, C.-e.; Sawangkeaw, R. Continuous production of biodiesel in supercritical ethanol: A comparative study between refined and used palm olein oils as feedstocks. *J. Braz. Chem. Soc.* **2014**, *25*, 1746–1753. [CrossRef]
201. Ridwan, I.; Katsuragawa, N.; Tamura, K. Process optimization, reaction kinetics, and thermodynamics studies of water addition on supercritical methyl acetate for continuous biodiesel production. *J. Supercrit. Fluids* **2020**, *166*, 105038. [CrossRef]
202. Sakdasri, W.; Ngamprasertsith, S.; Daengsanun, S.; Sawangkeaw, R. Lipid-based biofuel synthesized from palm-olein oil by supercritical ethyl acetate in fixed-bed reactor. *Energy Convers. Manag.* **2019**, *182*, 215–223. [CrossRef]
203. Campanelli, P.; Banchemo, M.; Manna, L. Synthesis of biodiesel from edible, non-edible and waste cooking oils via supercritical methyl acetate transesterification. *Fuel* **2010**, *89*, 3675–3682. [CrossRef]
204. Singh, C.S.; Kumar, N.; Gautam, R. Supercritical transesterification route for biodiesel production: Effect of parameters on yield and future perspectives. *Environ. Prog. Sustain. Energy* **2021**, *40*, e13685. [CrossRef]
205. Sawangkeaw, R.; Teeravitud, S.; Bunyakiat, K.; Ngamprasertsith, S. Biofuel production from palm oil with supercritical alcohols: Effects of the alcohol to oil molar ratios on the biofuel chemical composition and properties. *Bioresour. Technol.* **2011**, *102*, 10704–10710. [CrossRef] [PubMed]
206. de Jesus, A.A.; de Santana Souza, D.F.; de Oliveira, J.A.; de Deus, M.S.; da Silva, M.G.; Franceschi, E.; da Silva Egues, S.M.; Dariva, C. Mathematical modeling and experimental esterification at supercritical conditions for biodiesel production in a tubular reactor. *Energy Convers. Manag.* **2018**, *171*, 1697–1703. [CrossRef]
207. Günay, M.E.; Türker, L.; Tapan, N.A. Significant parameters and technological advancements in biodiesel production systems. *Fuel* **2019**, *250*, 27–41. [CrossRef]
208. Turro, N.J. Molecular structure as a blueprint for supramolecular structure chemistry in confined spaces. *Proc. Natl. Acad. Sci. USA* **2005**, *102*, 10766–10770. [CrossRef]
209. Kiwaroun, C.; Tubtimdee, C.; Piumsombon, P. LCA studies comparing biodiesel synthesized by conventional and supercritical methanol methods. *J. Clean. Prod.* **2009**, *17*, 143–153. [CrossRef]
210. Tan, K.T.; Lee, K.T.; Mohamed, A.R. Prospects of non-catalytic supercritical methyl acetate process in biodiesel production. *Fuel Process. Technol.* **2011**, *92*, 1905–1909. [CrossRef]
211. Akkarawatkhosith, N.; Kaewchada, A.; Jaree, A. Enhancement of continuous supercritical biodiesel production: Influence of co-solvent types. *Energy Procedia* **2019**, *156*, 48–52. [CrossRef]
212. Han, H.; Cao, W.; Zhang, J. Preparation of biodiesel from soybean oil using supercritical methanol and CO₂ as co-solvent. *Process Biochem.* **2005**, *40*, 3148–3151. [CrossRef]

213. Sendzikiene, E.; Makareviciene, V. Catalytic biodiesel synthesis under supercritical conditions. *Mendeleev Commun.* **2021**, *31*, 442–450. [CrossRef]
214. Hoekman, S.K.; Broch, A.; Robbins, C.; Cenicerros, E.; Natarajan, M. Review of biodiesel composition, properties, and specifications. *Renew. Sustain. Energy Rev.* **2012**, *16*, 143–169. [CrossRef]
215. Minami, E.; Saka, S. Kinetics of hydrolysis and methyl esterification for biodiesel production in two-step supercritical methanol process. *Fuel* **2006**, *85*, 2479–2483. [CrossRef]
216. Yusuf, N.N.A.N.; Kamarudin, S.K. Techno-economic analysis of biodiesel production from *Jatropha curcas* via a supercritical methanol process. *Energy Conv. Manag.* **2013**, *75*, 710–717. [CrossRef]
217. Martinovic, F.L.; Kiss, F.E.; Micic, R.D.; Simikić, M.Đ.; Tomić, M.D. Comparative techno-economic analysis of single-step and two-step biodiesel production with supercritical methanol based on process simulation. *Chem. Eng. Res. Des.* **2018**, *132*, 751–765. [CrossRef]
218. Sakdasri, W.; Sawangkeaw, R.; Ngamprasertsith, S. Techno-economic analysis of biodiesel production from palm oil with supercritical methanol at a low molar ratio. *Energy* **2018**, *152*, 144–153. [CrossRef]
219. Gutiérrez Ortiz, F.J.; de Santa-Ana, P. Techno-economic assessment of an energy self-sufficient process to produce biodiesel under supercritical conditions. *J. Supercrit. Fluids* **2017**, *128*, 349–358. [CrossRef]
220. Tipsri, T.; Lersbamrungsuk, V. Techno-economic analysis of biodiesel production from waste cooking oil using supercritical and subcritical processes. *Science. Eng. Health Stud.* **2019**, *13*, 153–162.
221. Moliere, M. The fuel flexibility of gas turbines: A review and retrospective outlook. *Energies* **2023**, *16*, 3962. [CrossRef]
222. Gülen, S.C.; Curtis, M. Gas turbine's role in energy transition. *J. Eng. Gas Turbines Power* **2024**, *146*, 101008. [CrossRef]
223. Rochelle, D.; Najafi, H. A review of the effect of biodiesel on gas turbine emissions and performance. *Renew. Sustain. Energy Rev.* **2019**, *105*, 129–137. [CrossRef]
224. Moliere, M.; Panarotto, E.; Aboujaib, M.; Bisseaud, J.; Campbell, A.; Citeno, J.; Maire, P.-A.; Ducrest, L. Gas turbines in alternative fuel applications: Biodiesel field test. In Proceedings of the ASME Turbo Expo 2007: Power for Land, Sea, and Air, Montréal, QC, Canada, 14–17 May 2007.
225. Glaude, P.A.; Fournier, R.; Bounaceur, R.; Molière, M. Adiabatic flame temperature from biofuels and fossil fuels and derived effect on NOx emissions. *Fuel Process. Technol.* **2010**, *91*, 229–235. [CrossRef]
226. Altaher, M.A.; Andrews, G.E.; Li, H. Study of biodiesel emissions and carbon mitigation in gas turbine combustor. *Am. J. Eng. Res.* **2014**, *3*, 290–298.
227. Gupta, K.; Sidiqi, A.; Sarviya, R. Evaluation of soya bio-diesel as a gas turbine fuel. *Iran. J. Energy Environ.* **2010**, *1*, 205–210.
228. Teleman, Y. Rankine Cycles: Modeling and Control, Thesis. Available online: <https://lup.lub.lu.se/student-papers/search/publication/8522986> (accessed on 19 August 2024).
229. Marzouk, O.A. Subcritical and supercritical Rankine steam cycles, under elevated temperatures up to 900 °C and absolute pressures up to 400 bara. *Adv. Mech. Eng.* **2024**, *16*, 1–18. [CrossRef]
230. Once-Through Boilers, Technical Brochure Published by Mitsubishi Power. Available online: <https://power.mhi.com/products/boilers/lineup/once-through> (accessed on 15 August 2024).
231. Patel, S. The World-Class Coal Power Efficiency of Rheinhafen-Dampfkraftwerk Block 8. 1 August 2019. Available online: <https://www.powermag.com/the-world-class-coal-power-efficiency-of-rheinhafen-dampfkraftwerk-block-8/> (accessed on 19 August 2024).
232. Zhang, Z.; Zhou, R.; Ge, X.; Zhang, J.; Wu, X. Perspectives for 700 °C ultra-supercritical power generation: Thermal safety of high-temperature heating surfaces. *Energy* **2020**, *190*, 116411. [CrossRef]
233. Brun, K.; Friedman, P.; Dennis, R. *Fundamentals and Applications of Supercritical Carbon Dioxide (sCO₂) Based Power Cycles*; Woodhead Pub.: Duxford, UK, 2017.
234. Romero, M.; Gonzalez-Aguilar, J. Solar thermal CSP technology. *WIREs Energy Environ.* **2014**, *3*, 42–59. [CrossRef]
235. NREL Brochure. Available online: <https://www.nrel.gov/docs/fy17osti/67464.pdf> (accessed on 19 August 2024).
236. SOLARSCO2OL EU H2020 Project. Available online: <https://www.solarsco2ol.eu/> (accessed on 19 August 2024).
237. Molière, M.; Privat, R.; Jaubert, J.-N.; Geiger, F. Supercritical CO₂ power technology: Strengths but challenges. *Energies* **2024**, *17*, 1129. [CrossRef]
238. USDOE Brochure, Clean Coal and Natural Gas Power Systems. Available online: <https://www.energy.gov/supercritical-co2-tech-team> (accessed on 11 August 2024).
239. Stepanek, J.; Syblik, J.; Entler, S. Axial sCO₂ high-performance turbines parametric design. *Energy Convers. Manag.* **2022**, *274*, 116418. [CrossRef]
240. McClung, A.; Brun, K.; Delimont, J. Comparison of supercritical CO cycles for oxycombustion. In Proceedings of the ASME Turbo Expo 2015, Montréal, QC, Canada, 15–19 June 2015. paper GT2015.
241. Patel, S. Power (Magazine), 8 Rivers Unveils 560 MW of Allam Cycle Gas-Fired Projects for Colorado, Illinois. 15 April 2021. Available online: <https://www.powermag.com/8-rivers-unveils-560-mw-of-allam-cycle-gas-fired-projects-for-colorado-illinois/> (accessed on 27 October 2024).
242. Patel, S. Power (Magazine), Breakthrough: NET Power's Allam Cycle Test Facility Delivers First Power to ERCOT Grid. 18 November 2021. Available online: <https://www.powermag.com/breakthrough-net-powers-allam-cycle-test-facility-delivers-first-power-to-ercot-grid/> (accessed on 19 August 2024).

243. World Nuclear Organization. Available online: <https://world-nuclear.org/information-library/current-and-future-generation/cooling-power-plants#:~:text=These%20use%20supercritical%20water%20around,plants%20are%20operating%20world-wide> (accessed on 7 October 2024).
244. International Energy Agency. Access to Electricity. Available online: <https://www.iea.org/reports/sdg7-data-and-projections/access-to-electricity> (accessed on 11 August 2024).
245. Irman, N.; Abd Latif, N.H.; Brosse, N.; Gambier, F.; Svamani, F.; Hussin, M.H. Preparation and characterization of formaldehyde-free wood adhesive from mangrove bark tannin. *Int. J. Adhes. Adhes.* **2022**, *114*, 103094. [CrossRef]
246. Bendeif, S.; Kadi, K.; Arhab, R.; Ziegler-Devin, I.; Brosse, N.; Addad, D. HPAEC-PAD, biochemical characterization, and evaluation of the antioxidants activities of polysaccharides extracted from Olive Mill Wastewater of two endemic varieties of Khenchela region, Algeria. *Bioact. Carbohydr. Diet. Fibre* **2023**, *30*, 100363. [CrossRef]
247. Autor, E.; Cornejo, A.; Bimbela, F.; Maisterra, M.; Gandía, L.M.; Martínez-Merino, V. Extraction of phenolic compounds from *Populus Salicaceae* Bark. *Biomolecules* **2022**, *12*, 539. [CrossRef]
248. Bermudez Aponte, N.A.; Meille, V. Use of biosourced molecules as liquid organic hydrogen carriers (LOHC) and for circular storage. *Reactions* **2024**, *5*, 195–212. [CrossRef]
249. Ribeiro, N.; Soares, G.C.; Santos-Rosales, V.; Concheiro, A.; Alvarez-Lorenzo, C.; García-González, C.A.; Oliveira, A. A new era for sterilization based on supercritical CO₂ technology. *J. Biomed. Mater. Res. B Appl. Biomater.* **2019**, *108*, 399–428. [CrossRef] [PubMed]
250. Warambourg, V.; Mouahid, A.; Crampon, C.; Galinier, A.; Claeys-Bruno, M.; Badens, E. Supercritical CO₂ sterilization under low temperature and pressure conditions. *J. Supercrit. Fluids* **2023**, *203*, 106084. [CrossRef]
251. Hattori, H. Nonaqueous Cleaning Challenges for Preventing Damage to Fragile Nanostructures. In *Developments in Surface Contamination and Cleaning: Methods for Surface Cleaning*; Kohli, R., Mittal, K.L., Eds.; Elsevier Inc.: Amsterdam, The Netherlands, 2017; Volume 9, pp. 1–25.
252. Li, Y.; Zhang, L.; Tian, Q.; Xu, Q. Supercritical CO₂-assisted fabrication of advanced two-dimensional materials and their heterostructure. *Curr. Opin. Green Sustain. Chem.* **2020**, *28*, 100424. [CrossRef]
253. Liu, H.; Chen, B.Q.; Pan, Y.J.; Fu, C.P.; Kankala, R.K.; Wang, S.B.; Chen, A.Z. Role of supercritical carbon dioxide (scCO₂) in fabrication of inorganic-based materials: A green and unique route. *Sci. Technol. Adv. Mater.* **2021**, *22*, 696. [CrossRef]
254. Lee, H.B.; Chen, K.L.; Su, J.W.; Lee, C.Y. The use of surfactants and supercritical CO₂ assisted processes in the electroless nickel plating of printed circuit board with blind via. *Mater. Chem. Phys.* **2020**, *241*, 122418. [CrossRef]
255. Reverchon, E. Supercritical antisolvent precipitation of micro- and nanoparticles. *J. Supercrit. Fluids* **1999**, *15*, 1–21. [CrossRef]
256. Vorobei, A.M.; Parenago, O.O. Using Supercritical Fluid Technologies to Prepare Micro- and Nanoparticles. *Russ. J. Phys. Chem.* **2021**, *95*, 407–417. [CrossRef]
257. Rosa, M.T.; Alvarez, V.H.; Albarelli, J.Q.; Santo, D.T.; Meireles, M.A.; Saldana, M.D.A. Supercritical anti-solvent process as an alternative technology for vitamin complex encapsulation using zein as wall material: Technical-economic evaluation. *J. Supercrit. Fluids* **2020**, *159*, 104499. [CrossRef]
258. Wu, F.; Liu, X.; Qu, G. High value-added resource utilization of solid waste: Review of prospects for supercritical CO₂ extraction of valuable metals. *J. Clean. Prod.* **2022**, *372*, 133813. [CrossRef]
259. Ruiu, A.; Li, W.J.; Senila, M.; Bouilhac, C.; Foix, D.; Bauer-Siebenlist, B.; Seauveau-Pirouley, K.; Jänisch, T.; Böringer, S.; Lacroix-Desmazes, P. Recovery of precious metals: A promising process using supercritical carbon dioxide and CO₂-soluble complexing polymers for palladium extraction from supported catalysts. *Molecules* **2023**, *28*, 6342. [CrossRef] [PubMed]
260. Grumett, P. Precious metal recovery from spent catalysts. *Platinum Metals Rev.* **2003**, *47*, 163–166.
261. Shimada, T.; Ogumo, S.; Ishihara, N.; Sawada, K.; Kosaka, Y.; Yukihide, M. A study on the technique of spent fuel reprocessing with supercritical fluid direct extraction method (Super-DIREX method). *J. Nucl. Sci. Technol.* **2002**, *39*, 757–760. [CrossRef]
262. Sugiyama, W.; Yamamura, T.; Park, K.C.; Tomiyasu, H.; Shiokawa, Y.; Okada, H.; Sujita, Y. An extreme disposition method for low-level radioactive wastes using supercritical water. *Prog. Nucl. Energy* **2005**, *47*, 448–453. [CrossRef]

Disclaimer/Publisher’s Note: The statements, opinions and data contained in all publications are solely those of the individual author(s) and contributor(s) and not of MDPI and/or the editor(s). MDPI and/or the editor(s) disclaim responsibility for any injury to people or property resulting from any ideas, methods, instructions or products referred to in the content.